ADVERTIMENT. La consulta d'aquesta tesi queda condicionada a l'acceptació de les següents condicions d'ús: La difusió d'aquesta tesi per mitjà del servei TDX (www.tesisenxarxa.net) ha estat autoritzada pels titulars dels drets de propietat intel·lectual únicament per a usos privats emmarcats en activitats d'investigació i docència. No s'autoritza la seva reproducció amb finalitats de lucre ni la seva difusió i posada a disposició des d'un lloc aliè al servei TDX. No s'autoritza la presentació del seu contingut en una finestra o marc aliè a TDX (framing). Aquesta reserva de drets afecta tant al resum de presentació de la tesi com als seus continguts. En la utilització o cita de parts de la tesi és obligat indicar el nom de la persona autora.

ADVERTENCIA. La consulta de esta tesis queda condicionada a la aceptación de las siguientes condiciones de uso: La difusión de esta tesis por medio del servicio TDR (www.tesisenred.net) ha sido autorizada por los titulares de los derechos de propiedad intelectual únicamente para usos privados enmarcados en actividades de investigación y docencia. No se autoriza su reproducción con finalidades de lucro ni su difusión y puesta a disposición desde un sitio ajeno al servicio TDR. No se autoriza la presentación de su contenido en una ventana o marco ajeno a TDR (framing). Esta reserva de derechos afecta tanto al resumen de presentación de la tesis como a sus contenidos. En la utilización o cita de partes de la tesis es obligado indicar el nombre de la persona autora.

WARNING. On having consulted this thesis you're accepting the following use conditions: Spreading this thesis by the TDX (www.tesisenxarxa.net) service has been authorized by the titular of the intellectual property rights only for private uses placed in investigation and teaching activities. Reproduction with lucrative aims is not authorized neither its spreading and availability from a site foreign to the TDX service. Introducing its content in a window or frame foreign to the TDX service is not authorized (framing). This rights affect to the presentation summary of the thesis as well as to its contents. In the using or citation of parts of the thesis it's obliged to indicate the name of the author

Philosophy Doctor Thesis

Optical Communications Group
Signal Theory and Communications Department

OPTIMIZATION OF EMERGING EXTENDED FTTH WDM/TDM PONS AND FINANCIAL OVERALL ASSESSMENT

Author

Sotiria Chatzi

Advisors

José A. Lázaro Villa
Ioannis Tomkos

Thesis presented in fulfilment of doctorate program of the
Signal Theory
& Communications department
Technical University of Catalonia

July 2013

The work described in this thesis was performed at the Signal Theory and Communications department of the Universitat Politècnica de Catalunya / BarcelonaTech. It was supported by the European Comission through the FP7 Projects SARDANA, EURO-FOS and BONE.

Sotiria Chatzi
Optimization of Emerging Extended FTTH WDM/TDM PONs and Financial Overall Assessment
Subject Headings: Optical fiber communication

Copyright © 2013 by Sotiria Chatzi

All rights reserved. No part of this publication may be reproduced, stored in a retrieval system, or transmitted in any form or by any means without the prior written consent of the author.

Printed in Barcelona, Spain.

ISBN:
Reg: B.

To my grandfather,

who taught me how to read, write and play cards, before I was 4

Abstract

Fiber-To-The-Home (FTTH) has experienced a boost in the last years which came as a consequence to the continuous technological evolution in hardware as well as in software, which in their turn have drove the evolution of internet applications. Numerous optical fiber network implementations have been realized worldwide. Several architectures and technologies have been tested in real life scenarios and many more have been designed in university labs and telecommunication companies. The point has now been reached, where one refers to next-generation networks.

At the end of the day the most critical factor in optical networks, is their cost, their effectiveness and the counterbalance among the two elements. A thorough inquiry has been performed on both aspects of Fiber-To-The-x (FTTx) and optical networks in general. Topics on their performance in combination with their cost and financial assessment have been covered for many different infrastructures and technologies, focusing mainly on the Passive Optical Networks (PONs).

Hybrid Wavelength Division Multiplexing / Time Division Multiplexing PONs, have been studied scientifically so as to expand their limits. This has been realized by applying elaborate design, in–line remote amplification, use of alternative as well as extended band for the signal transmission, dispersion compensation and signal equalization and with the help of numerous studies.

Table of Contents

Chapter I – Introduction

Chapter II – State of the art

Chapter III – Techno-economics

Chapter IV – SARDANA and challenges of long reach and enhanced PONs

Chapter V – In-line amplification

Chapter VI – Alternative band operation of a WDM/TDM PON

Chapter VII – Extended band operation of a WDM/TDM PON

Chapter VIII – Dispersion compensation in optical networks

Chapter IX – Combination of in-line amplification / extended band use / equalization use for WDM/TDM PONs

Chapter X – Conclusions

Chapter I
Introduction

Internet has changed radically in the last few years. In this sense, web browsing has been replaced nowadays by video streaming. Multimedia services, such as high definition cloud gaming, continue to drive the need for more bandwidth. Nielsen's law predicts that the increase of a high end user connection speed, is up 50% annually. In other words, a need for 20Mbps today will be translated into a need of 152Mbps by 2016 and future research is targeting to 400Gb/s. It is evident, that high speed broadband is critical for the future networked reality. The question that remains to be answered, is how access networks can lead us to the digital world.

As far as the current generation of access technologies is concerned, there are two options for increasing the connection speed. The first one, is maximizing the use of the existing copper infrastructure and the second one is installing a new fiber plant. In case of copper use, in order to achieve a large bandwidth delivered to the end customer, the copper loop has to shorten, thus fiber has to extend deeper into the network. This leads to networks consisting of fiber fed Very-high-bit-rate digital subscriber line 2 (VDSL2) nodes.

Ultimately, fiber is expected to connect all users. Fiber-to-the-Home (FTTH) is one of the largest and fastest rising infrastructures in developed countries, promising to constitute the pillars on which a vision of future digitized society will be based and materialized. The reason for that, is the set of promising applications that such an infrastructure can provide, which range from luxurious delivery of digital visual and audio streaming and on-line teleconferences, to e-health for the elderly and people living in remote areas, as well as e-learning and e-government for people having difficulties moving from their house, or just wanting to reduce commuting. Internet of people, internet of things, internet of intelligence and internet of services constitute the internet of the future which will need to be based on a ubiquitous, high-capacity network. Fiber-to-the-Home development requires constantly evolving technologies that deliver the maximum possible bandwidth, to the maximum possible distance and to the ultimate number of end users, with the most cost effective way and with the lowest possible operational cost. Therefore, the design of a network that can cover simultaneously all those needs could represent an innovative solution on Fiber-to-the-Home.

Throughout the years, since the beginning of fiber networks, many solutions have been proposed as the most appropriate ones. The debate on the most efficient

technology for Fiber to the Home networks is the most long lasting one and the richest in arguments. This debate is usually followed by another one, on the most adequate architecture to be used to serve the needs of each area. Usually, the architecture is combined with the technology to be used, in the sense that each technology is better served by a specific architecture. For example, point-to-multipoint (P2MP) or star architectures, can serve both passive and active technologies, while point-to-point (P2P) architectures are mostly used in active networks. The most frequently installed technologies are: the passive optical networks (PON) standardized from the International Telecommunications Union (ITU-T), under the umbrella of the initials G.98x, like Asynchronous Transfer Mode (ATM) PON (APON), broadband PON (BPON), Gigabit PON (GPON) and nowadays 10G-PON (XG-PON) and additionally, the PONs standardized by IEEE, like Ethernet PON (EPON) and Gigabit EPON (G-EPON). On the other hand, many operators worldwide have chosen the simple solution of Active Ethernet optical network, deployed in P2P architecture, or, in some cases, deployed in a P2MP topology, also known as Active star. Wavelength division multiplexing (WDM) and wavelength division multiplexing/time division multiplexing (WDM/TDM) PON, two emerging technologies, appear to be the descendants of the aforementioned technologies.

There is a large record of studies on the financial assessment on each of these solutions and part of this study has been the estimation of several costs related with FTTH infrastructures. In all previously mentioned networks, the maturity of the equipment could provide a relative cost advantage when compared with the WDM/TDM PON under development. Nevertheless, the savings this new technology promises to bring, can be perceived when one takes under consideration the number of wavelengths served with the same feeder fiber, as well as the number of customers served per wavelength. Furthermore, this technology promises to expand the physical reach of already standardized optical network technologies, thus reducing the active equipment cost per unit of length.

1.1 Motivation

Already designed and tested WDM/TDM PONs can demonstrate their cost and general efficiency, with their prolonged limits in terms of users served and physical reach. Nevertheless, an assiduous study in terms of economic and technical aspects of the FTTH networks available, has shown that the most cost effective solution is the one of WDM/TDM PON. Its limits and the expansion of those limits can, on the one hand, ensure the viability of such a network among the existing and incumbent technologies, and on the other, ensure its future sustainability for many years. This last quality, along with compatibility with existing infrastructures, is both desirable and important for new technologies of optical networks.

The existing WDM/TDM networks promise to deliver symmetrical several hundred Mbit/s, spread along distances up to 100km to more than 1000 users. This study has been based on a network in which a WDM ring is used for the transport of the large amount of downstream and upstream information, with the use of several wavelengths and TDM trees that multiplex in the time domain, data, which reach from several end users. Several λs, deriving from corresponding operators, share a common infrastructure [1]. Along the WDM ring, passive remote nodes (RN) which implement cascadable 2-to-1 fiber optical add and drop functions, are distributing different wavelengths to each of the access trees. Remote amplification is introduced at the RN by means of erbium doped fiber (EDFs) to compensate add/drop losses, while optical pump for the remote amplification is provided by pumping lasers located at the central office (CO), also providing extra Raman gain along the ring. The optical network units (ONUs) are

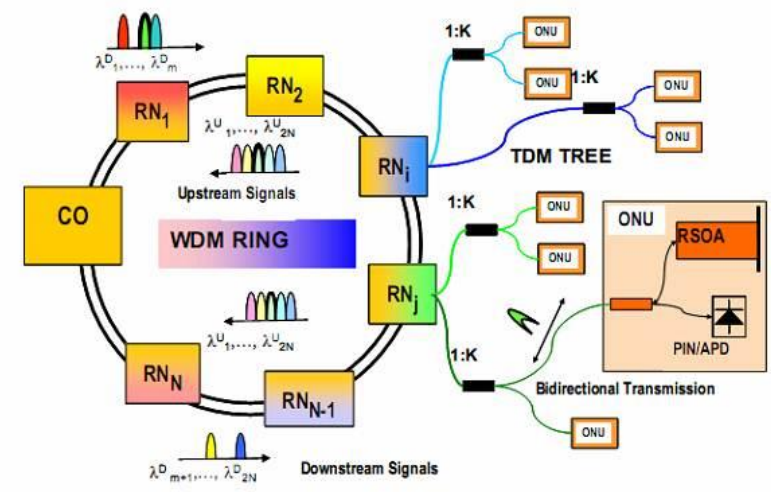

Fig. 1.1 SARDANA: Scalable Advanced Ring-based Dense Access Network Architecture and its main technical and design characteristics (www.ict-sardana.eu)

usually based in reflective devices -in the network examined: reflective semiconductor optical amplifiers (RSOAs)-, operating on the principle of re-modulating. They use either the downstream signal itself, or a dedicated continuous wave (CW) signal fed by the optical line terminal. This network design is called Scalable Advanced Ring-based passive Dense Access Network Architecture (SARDANA) and can be seen in Fig 1.1.
It's a network that can offer many possibilities, but can also be expanded and enhanced. Some of the challenges this specific design is facing are namely:

i. Limited pump power

The supply of pump power, in the form of compact standard laser modules, used to amplify the signals, either with remotely pumped erbium-doped fiber amplifiers or by utilizing the Raman effect, is concentrated and localized in the CO. Due to security regulations and due to capital and operational expenditure (CAPEX and OPEX) considerations, the provided to the network pump power is limited.

Furthermore, the fiber non-linear effects as well as the fact that the sources are shared, induce extra limitations to the value of the pump power that could conditionally be used. The pump power requirements regarding remote erbium doped amplification and Raman amplification though, are very important physical parameters of the network, affecting not only its limits of reach and number of users, but also the wavelength plan.

ii. Limited bandwidth which translates into serving a limited number of users

The signal power, as in respect to the pump power, is up-limited by non-linear effects. The non-linear effects depend on the frequency allocation, creating a need for careful assignation of the working wavelengths. This limitation, which is originally a power limitation, creates an interdependent bandwidth limitation. Furthermore, transmission bandwidth is critical in PONs at 10GBit/s to maintain a low cost implementation. The use of an alternative/extended set of wavelengths is a suggested solution to this limitation.

iii. Chromatic dispersion (CD) limiting the reach or/and increasing the need for higher OSNR

The chromatic dispersion at 10GBit/s is a limiting transmission factor especially in cases there is induced chirp from the transmitter. CD reduces both the bit-error-rate (BER) performance and the range of optimal receiver (Rx) and transmitter (Tx) bandwidth. In contradiction to the aforementioned idea of extending the transmission wavelength, in links affected by chromatic dispersion, too high Rx-bandwidth and Tx bandwidth are leading to extra penalties. The use of dispersion compensation and signal equalization can reduce the effect of CD.

iv. Signal distortion due to transmission in long distance

The transmission of the signal can be overwhelmed by the noise conducted along the fiber, as well as thermal noise. Rayleigh back scattering, fiber imperfections as well as dispersion and attenuation of the signal, cause the need for elaborated optical amplification.

1.2 Objectives

Two are the main objectives of this thesis. The first is the techno-economic evaluation of several technologies and topologies used in FTTH infrastructures, as well as an assessment of the WDM/TDM PON in this framework. The second is the expansion of limits in terms of reach and number of users in a WDM/TDM passive network. This study aims at examining several approaches in order to achieve this expansion. In this effort the main limitations, mentioned earlier were addressed by:

- Means of smart design to try to expand the limits of either reach or number of customers served, or both
- The use of an alternative band as well as of the combination of the normal with the alternative one to expand the capacity of customers served.
- The use of remotely pumped EDFs, who are in line with the several WDM λs, to provide adequate amplification to the total number of the signals so as to reach the desired point.

- Raman amplification, which has been used as an auxiliary mechanism to remotely pumped EDFs to amplify the signal.
- Dispersion compensation, as a way to improve the quality of the signal.
- Electronic equalization, as a technique to refine the signal.
- Finally all of the aforementioned methods were used in combination, for maximizing the performance of the network

1.3 Thesis overview

This thesis, covers two general concepts. The first is the techno-economic evaluation of all FTTH technologies and architectures and the assessment of WDM/TDM PON among them. In this effort, a newly emerged design, based on the principles of WDM/TDM, named Scalable Advanced Ring-based Dense Access Network Architecture, has been used as a reference. The second, is the expansion of next generation WDM/TDM PON designs and the focus is transferred from the financial to the technological and operational characteristics of the optical access network, as well as the experimental study performed in order to prolong their boundaries. Once more, the prototype of SARDANA has been used. The thesis is organised as follows.

In the second chapter, an overview of existing optical access networks takes place, asides of the existing infrastructures and the already deployed Fiber-to-the-X (FTTx) networks worldwide. FTTx penetration in the form of numbers of users per country is given. The status of research regarding techno-economics of optical networks, as well as of the research on WDM/TDM PONs is described. On the third chapter the existing technologies for extended PONs are presented, along with the latest designs and technologies used for WDM/TDM PONs. Furthermore a techno-economic evaluation of existing FTTx infrastructures in terms of outside plant, likewise in terms of active equipment takes place. On the fourth chapter, a presentation of SARDANA is realised, along with the challenges of long reach-enhanced PONs. This is the initial model, on which both the estimation of CAPEX for WDM/TDM infrastructures, as well as the first ideas on expansion of WDM/TDM PONs have been based.

On the fifth chapter, an initial approach on the problem of restricted pump power is being addressed, by means of network design, in terms of wavelength allocation. Additionally, the solution of using remotely pumped EDFs in line with the WDM signals is being examined, as well as, some aspects of the operation of EDFs. On the sixth chapter, the idea of using an alternative band of transmission, more specifically the L-band instead of the C-band, in combination with in-line amplification of the signals using remotely pumped EDFs is investigated.

On the seventh chapter, the use of an extended band of transmission, namely the window covering both C+L bands is considered, so as to increase the number of end users served, as well as to cover the possible need of alternative operators to be served easily by the same infrastructure in the future. Additionally, on the same chapter, the Raman effect as a means of amplification of the signal is studied. This effort has been in co-operation with the Instituto de Telecomunicações (IT).

Chapter eight, is focused on the effects of transmitter-induced chirp and signal dispersion on transmission in long distances, as well as a study on the effect of the ER of the signal in dispersion. In addition, the behaviour of dispersion compensation and electronic equalization on distorted signals is presented, aiming at determining the possible limits of a realistic transmission link.

In chapter nine, the combination of the solutions suggested in previous chapters is examined, as well as the ultimate reach of the network when it operates. Finally, on the last chapter we present in summarizing all the knowledge that has been acquired throughout this study, the conclusions we have ended up at and some recommendations for future research.

Chapter II
State of the art

This chapter covers the present situation regarding the subjects dealt within this thesis. As the main research subject of the study is FTTH, initially, the penetration of this technology in Europe and worldwide is presented. Following, aspects of the techno-economic studies made on the FTTx infrastructures and the corresponding technologies are exposed. Next, an overview of the current state of research on WDM/TDM PONs is given.

2.1 Optical networks worldwide

FTTx is spreading very swiftly in all continents, in several forms, with the use of different topologies and different technologies. According to the latest registration (2011) of FTTH Council, more than 75 million users worldwide are connected with fiber optic connections to the home [2]. From those connections, 60 million are used in Asia, 10 million in United States of America (USA), 5.5 million in Europe and 0.5 million in United Arabic Emirates (UAE). Data released from the FTTH Council, rank the countries with the highest penetration worldwide as can be seen in Fig.2.1.

In terms of infrastructure, as far as Europe is concerned, there are approximately 28 million homes passed and an average take up rate of 18.4% [2]. Russia though, according to the latest reports [3], has added 2.2 million new FTTH subscribers in the second half of 2012 to reach a grand total of 7.5 million fiber-connected homes. Moreover, French government has announced that it will invest 20 billion Euros into ultra-fast broadband infrastructure, with a special focus on future-proof fiber, in the coming years [4].

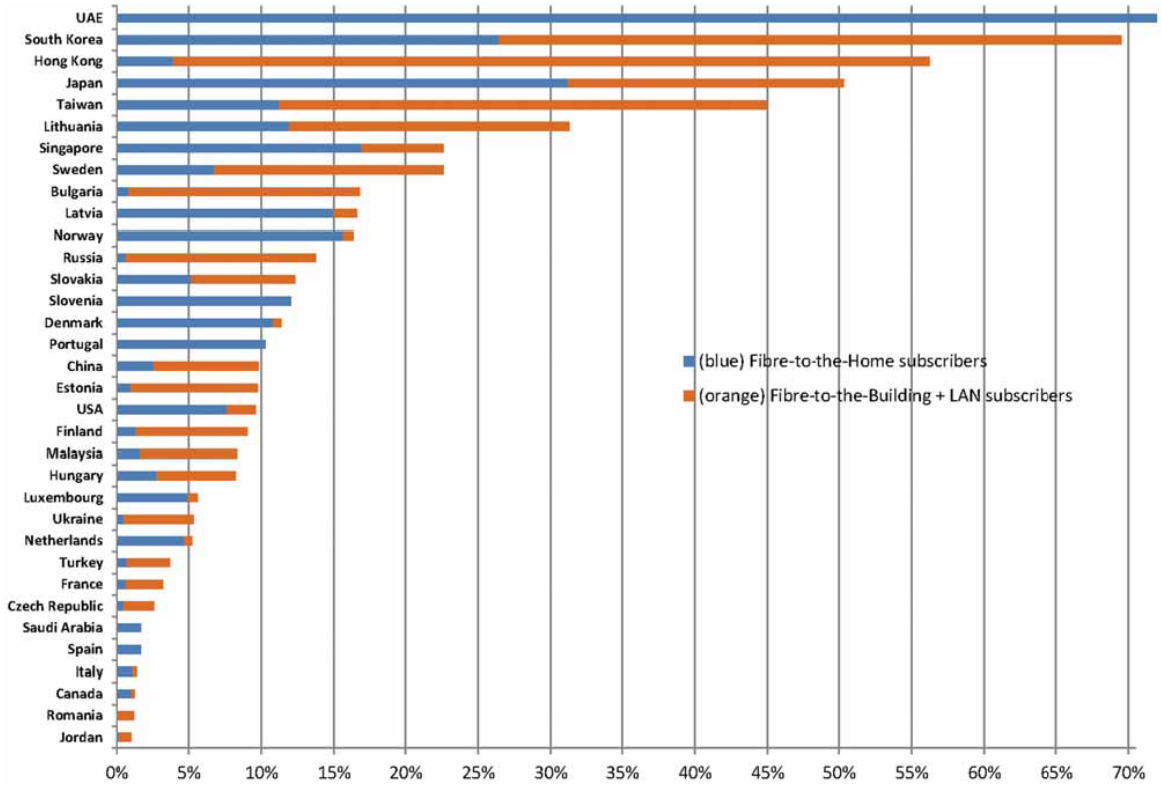

Fig. 2.1 Market Penetration of FTTH - Ranked by Country
(Press conference FTTH Council Europe 15/2/2012)

2.2 Techno-economics

During recent years, an increasing number of research papers, besides the consultancies' reports, have been composed within national and international collaborative projects, aiming to contribute to this broadband debate, regarding the cost and the efficiency of each FTTx solution, which has started as early as in the late 80's. Models have been developed, for the estimation of the several costs involved in the implementation of an optical network.

In fact, there are published guidelines and instructions for creating a techno-economic model [5]. European telecom operator combined these guidelines with a thorough and detailed financial evaluation of several scenarios of deployment, based though, only on current technologies, not covering future ones, such as WDM/TDM PONs [5]. Furthermore, automated network planning tools have been implemented, which helped in techno-economic research [6]. But, these tools have been used for the comparison of FTTx and FTTH architectures that both use commercially available technologies [6]. Since the subject of the infrastructure cost has been a matter of great concern for most of the local authorities in technologically evolved countries, studies have been performed, that concern each country/area locally and individually. Therefore, most of the investigations are focused on specific regional needs. For example, there are deployment studies that focus on the geographical characteristics of a particular area,

while there are others that focus on the preferred technological choices of the country's strongest telecom market players.

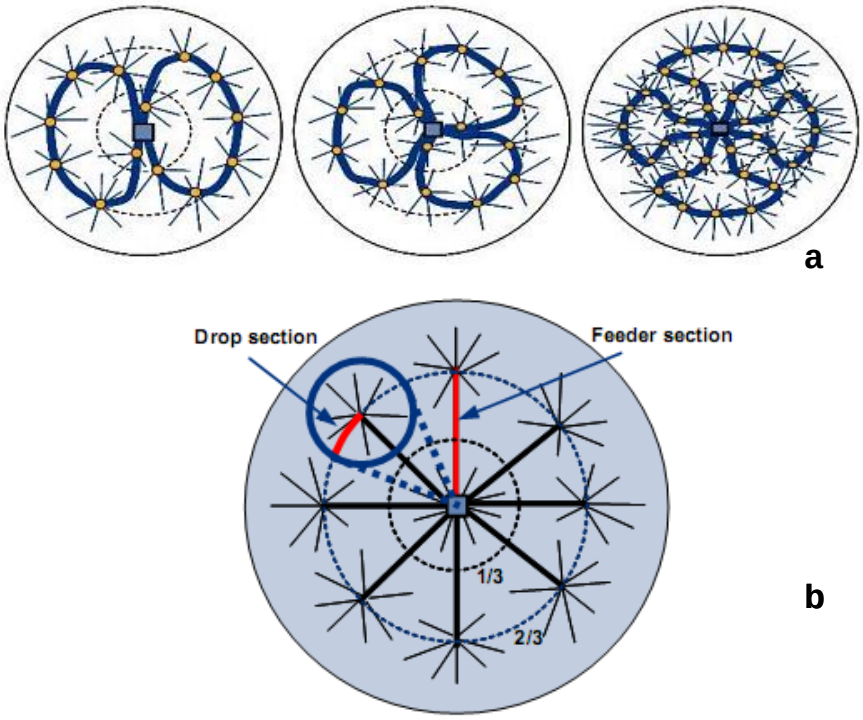

Fig. 2.2 Examples of geometric models used for techno-economic calculations of: a) GPON, b) P2P, fiber distribution [6]

Therefore, there are studies comparing FTTH deployments with Fiber-To-The-Curb/Very-high-bit rate digital subscriber line (FTTC/VDSL) as in [6]. The network design (geometric) models used to calculate the necessary equipment to deploy the several different infrastructures are based on mathematic norms, and algorithms. These models, that use in addition correction factors [7], give an approximation of the required optical fiber length and consequently of the total material needed for the implementation of the network. Three examples of these models appear in Fig 2.2 and Fig 2.3.

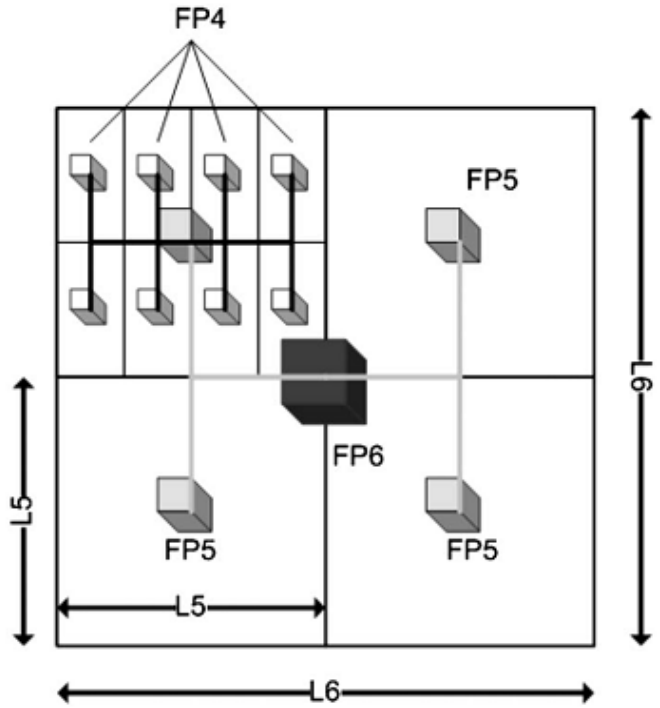

Fig. 2.3 Geometric model for techno-economic evaluation of FTTC/VDSL and FTTH Roll-Out [7]

A subject that concerned researchers, is the cost of transition from an FTTx infrastructure to FTTH, or to another version of FTTx [8], but, once more, only commercialized technologies such as GPON and Active Optical Networks (AONs) have been examined. Likewise, disputes have arisen regarding the prevalence of PONs and AONs [8]. The study in [8] focuses, as can be seen in Fig.2.4, on the two FTTH-AON architectures, namely Active star and Home run. As far as PONs are concerned WDM and TDM technologies were investigated. Once more, the hybrid solution of WDM/TDM PON was not included in the study.

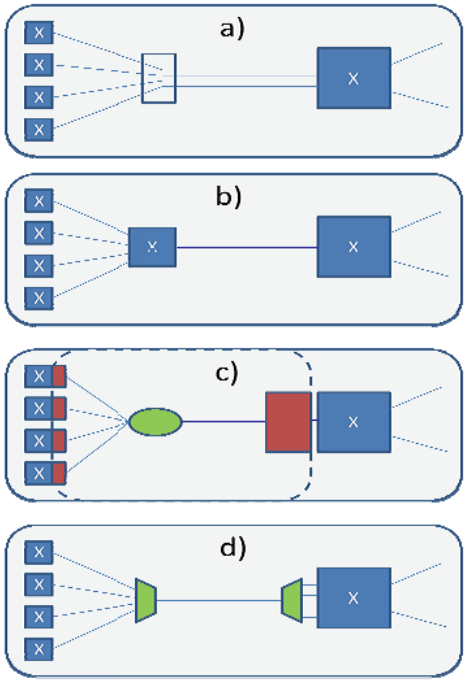

Fig. 2.4 a)AON homerun, b)AON active star, c) TDM PON, d) WDM PON. Comparison of Active star and home run AONs with TDM and WDM PONs [8]

The number of the techno-economic evaluations seen in publications is as high as the number of possible combinations of the FTTx infrastructures with all the technologies used for an optical access network. There is big literature regarding the assessment of GPON in contrast with Ethernet Point to Point (EP2P) as well as Active star deployments [9]. One of these comparative studies weighs WDM PONs against TDM PONs [10], giving some interesting results regarding the required infrastructure and the cost difference between Greenfield and Brownfield scenarios, yet again without presenting any actual network technology, but on the contrary, basing the results on a theoretical abstract design. As technology progresses, research focuses in new optical network implementations. For example, we have seen the comparison of two similar hybrid WDM/TDM PONs appearing in [11]. The study has taken into consideration two flavours of WDM/TDM PONs, whose main difference is localized in the ONU. The results of this techno-economic comparison have been extracted for two scenarios, one of an urban and one of a rural area correspondingly and can be seen on Fig 2.5. The comparison has been performed for two similar PONs, not taking into consideration older technologies and how the WDM/TDM PON can offer a financially distinctive choice when compared with existing and deployed technologies.

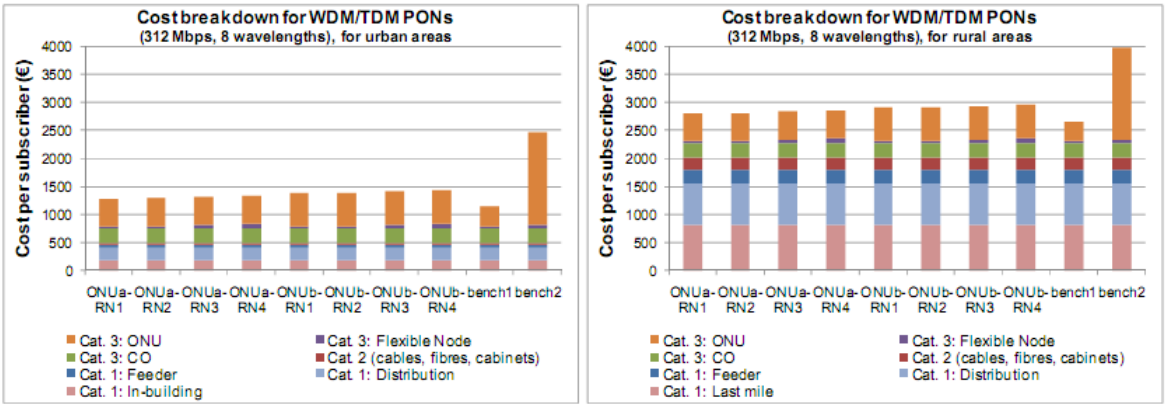

Fig. 2.5 Cost breakdown for the cost per subscriber for different hybrid WDM/TDM PON technologies [11]

As can be observed, scientific research has been focused on the composition of different elements of this multidimensional study, aiming to derive with the most effective FTTx/FTTH architecture and technology. In this thesis, several techno-economic comparisons among various existing, emerging and future technologies and infrastructures are presented, in an effort to combine all of these elements. The reason for this was the need to explore the entire cost of different optical access networks and estimate whether the new technologies provide indeed a significant cost reduction. The hypothesis was proven correct, therefore, the estimation of the cost difference among the several infrastructures, followed. Hybrid WDM/TDM PON was found to be the most cost effective solution, nevertheless a complete study on current – commercialized architectures and technologies has been realised as well, in order to have a definite and integral result. This realisation on the cost-effectiveness of the WDM/TDM PON led us to study the ways this technology could be expanded compared to the existing implementations.

2.3 WDM/TDM PON

Quite a few studies on WDM/TDM PONs have been performed and are at the moment taking place by researchers worldwide. Research projects currently proceeding or recently completed are presented below.

The project PIEMAN (Photonic Integrated Extended Metro and Access Network) [12] is a 6th Framework Program (FP) Specific Targeted Research Project (STReP) that focussed on the development of colourless electro-optical devices of the ONT for WDM/TDM PONs, with bandwidth up to 10 Gbit/s downstream and upstream. This technology can thus be available also at this level. Since this project is mostly a network element - development initiative, it does not focus on network design, therefore does not contribute to network design and optimization.

MUSE (Multi Service Access Everywhere) [13] is a 6FP Information Society Technologies project whose scope is multi-layered on several wired access techniques. Optical access technologies under study here, are a coarse wavelength division multiplexing (CWDM) resilient ring system and a hybrid fibre radio solution, suited to feed Worldwide Interoperability for Microwave Access (WiMAX) base stations. The subject of Dense Wavelength Division Multiplexing (DWDM) has not been addressed, while the focus is mostly on the end-to-end inter-domain compatibility using Internet Protocol (IP) Ethernet technologies and the Media Access Control (MAC) protocol that was developed as an evolution of the Full Service Access Network (FSAN) GPON system.

The project HARMONICS (Hybrid Access Re-configurable Multi-wavelength Optical Networks for IP-based Communication Services) [14] is a hybrid access network, combining an optical feeder network with multiple access technologies. It is a WDM PON and the studies performed in the framework of this project were mainly metro and MAC oriented. HARMONICS used electric switching and fixed lasers and did not reach to the end-user, therefore it consists of a service-metropolitan area network (MAN) solution. It integrated different traffics and proposed the use of a combined WDM/TDM solution, implemented in the MAN ring, with FTTC possible extension. Therefore, the point of FTTH WDM/TDM PON that is the main research subject of this work, has not been raised.

Project SUCCESS-HPON (Stanford University aCCESS Hybrid WDM/TDM Passive Optical Network - A Next Generation Optical Access Architecture for Smooth Migration from TDM-PON to WDM-PON) (Stanford University) [15], in Fig 2.6 ,proposes complex ONUs with tuneable sources and active RNs. It is a general architecture of next generation hybrid WDM/TDM optical access architecture. SUCCESS-HPON is well developed on the MAC domain but can present limited physical layer experiments.

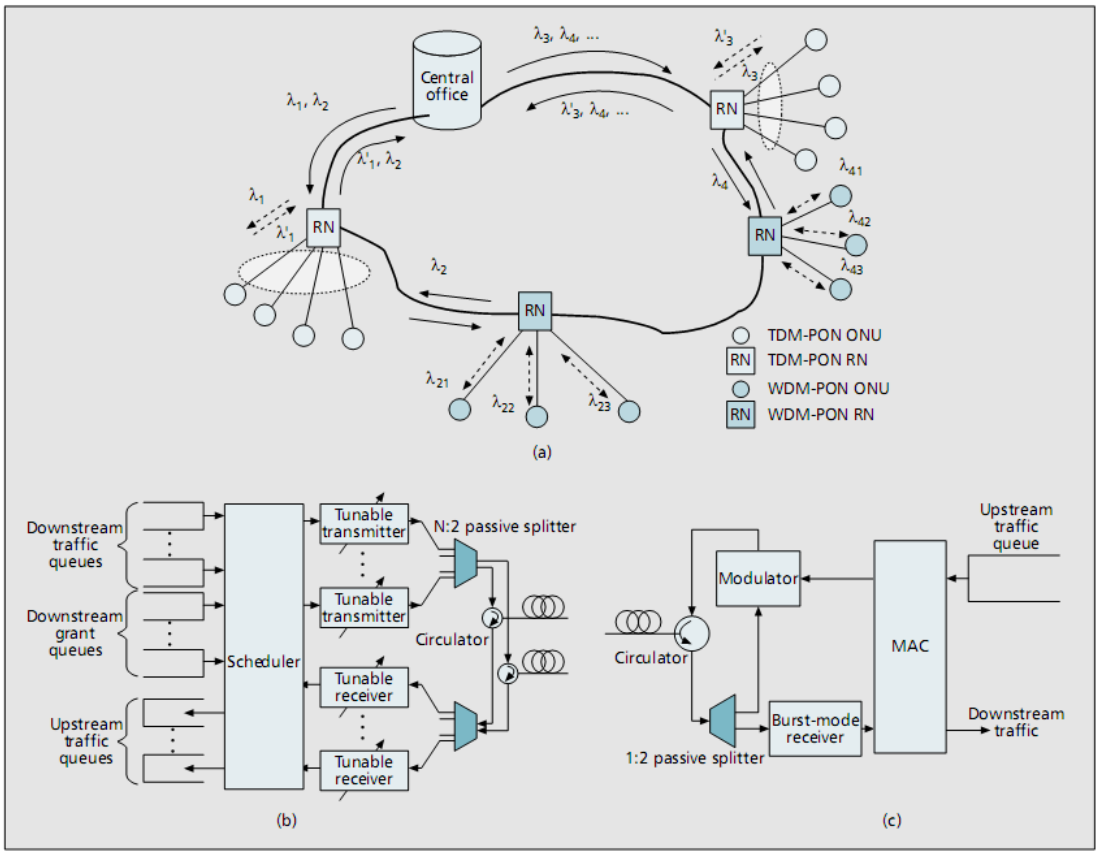

Fig. 2.6. SUCCESS-HPON: a) overall architecture, b) OLT block diagram, and c) WDM-PON ONU block diagram [15]

Other projects carried out in the past, like PRISMA, TOBASCO, PLANET, SUPERPON, etc, also used hybrid transmission media and/or active devices (like switches, O/E converters, optical amplifiers) along the PON. The main research line followed by these projects is not in accordance to the study represented in this thesis, as the network examined herein is a fully passive solution.

ePhoton/One IST Network of Excellence [16], included specific joint activities in topics like next-generation PONs, impairment monitoring and electronic compensation. It has focused of CWDM in contradiction with the studies represented here, who have been focusing on DWDM technology.

As far as single research institutes, or collaborations among them or among industry and academic institutions is concerned, there is a number of efforts taking or have been taken place worldwide. Most of them are presented below.

Shangai University has focused on the development of a hybrid WDM/TDM PON. Their efforts are concentrated towards the development of a new WDM/TDM PON design based on a dual fiber ring with access-tree topology, which utilizes a reconfigurable optical add-drop multiplexer based on wavelength blocker technology. Furthermore, they have focused on the design of a self seeding Fabry-Perot (FP) fiber laser at the ONU [17]. Huazhong University of science and technology in China has focused on the development of a long reach WDM/TDM PON. This network is based on the use of RSOAs as well as the use of optical add drop multiplexers (OADMs) [18]. Korea Telecom in co-operation with Chungnam National University have focused their

efforts towards the development of a new WDM/TDM PON design based on a dual fiber ring with access-tree topology, which utilizes a reconfigurable optical add drop multiplexer. The design has used RSOAs and remotely pumped EDFAs in combination with 32 WDM channels and 16 TDM channels per wavelength [19, 20].

KTH in co-operation with Ericsson and Zhejiang University researched the transition from TDM to WDM/TDM PON [21]. They have suggested a protection scheme that would serve as the intermediate step for the smooth migration from TDM PON to WDM/TDM PON. The feasibility of such a project in terms of cost has been investigated as well [22].

Korea Advanced Institute of Science and Technology (KAIST) with Samsung electronics have researched a WDM/TDM PON that can serve up to 128 users. This is achieved by cascading 1X16 arrayed waveguide grating (AWG) and 1X8 splitters. The use of a single FP-Laser Diode (LD) has been considered, with an amplified spontaneous emission (ASE) injection. Multipath transmission mechanism from optical line terminal (OLT) in optical wireless converged network architecture has also been investigated [23]. Korea and Bangladesh have introduced a similar design in the form of a self restored tree type WDM/TDM PON. The network is implemented with the use -in this case also- of a 1X16 AWG in the OLT and 1X4 Band Splitting Wavelength Division Multiplexing (BSWDM) filters both in the OLT as well as in the first stage RNs. In the second stage RN, a pair of 1:16 passive splitter is used so that TDM-PON de-multiplexes and multiplexes signals at channel level respectively [24].

COBRA institute, Eidhoven and Genexis have created a WDM/TDM PON network entitled: "Dynamically reconfigurable Broadband Photonics (BBPhotonics) network". The configuration is served by an OLT that transmits 8 data-and-continuous wavelengths (CW) wavelength pairs. The CW are transmitted by the OLT for use in the upstream modulation. The CO, where the OLT lies, is connected through a Standard Single Mode Fiber (SSMF) ring with 4RNs. Each RN with the use of a reconfigurable OADM serves 16 reflective optical network units (ONUs). In this framework experiments over 27km were performed, demonstrating simultaneous up and downstream traffic at 10Gb/s per channel. [25].

NTT Access Network Service Systems laboratories in Japan have performed a study on the existing WDM/TDM PON technologies and suggest two different solutions for the way the future research could evolve. NTT's interest in present and future results of academic research in the WDM/TDM PON technology proclaim an interest on behalf of the operator to use such a technology for future network implementations [26]. They suggest a WDM/TDM system based on their developed technologies. Furthermore, studies have been performed for the use of a dynamic wavelength and bandwidth allocation (DBWA) algorithm so as to use, as efficiently as possible, the available bandwidth resources and to tune them in correspondence with the users' requests. The DWBA operation has been tested with 40Gb/s tunable laser.

ETRI in Korea along with National ICT of Australia and the University of Melbourne suggest a multiwavelength PON (MW) as a useful antecedent of

WDM/TDM PON which will allow a smooth migration from the existing systems to the aforementioned future one [27] The MW PON consists of a remote AWG used as a channel multiplex, a remote splitter and a group of circulators in the RN and small splitters near the ONUs. The seed light is composed of multiple wavelengths rather than a single one. A RSOA is used as a colorless upstream transmitter and a low-cost channel filter is integrated into the RSOA-based transmitter the receiver of the MW PON. ETRI in co-operation with Korea University of science and technology have suggested a protection structure for WDM/TDM PONs. Moreover they have suggested a WDM/TDM PON that operates with tunable laser diodes and considers RSOAs for uplink transmitters [28]. Finally ETRI in cooperation with Korea Telecom have deployed the first commercial WDM//TDM PON in which one feeder fiber can support 512users. The system uses RSOAs in the ONUs and 16X1.25 Gb/s colorless gigabit WDM/PON and a legacy TDM/PON with optical-electrical-optical converters [29]. KDDI R&D Laboratories in Japan propose a ring based WDM/TDM PON implemented with the use of an injection-locked Fabry-Perot LD and a wavelength converter [30].

The institute for Infocomm research in Singapore has proposed a WDM/TDM PON with dynamic virtual PON capabilities, 10Gb/s downstream and 1.25Gb/s upstream. Furthermore, they have suggested the use of DPSK in the downlink and OOK in the uplink operating in the same bandwidth as before [31]. NUST, National University of Science & Technology in Pakistan proposes a WDM/TDM PON architecture based on EPON technology [32]. Corning has performed an experimental study on a 11.1Gb/s WDM/TDM system that supports 8 channels in 100km and 1:128 wavelength split ratio, with the use of EDFA in the experimental set up [33].

As far as WDM/TDM PON research on the MAC layer is concerned, National Taipei University of Technology in Taiwan has studied a delay sensitive multicast mechanism for downstream traffic in WDM/TDM PON [34]. University of California has developed an algorithm for efficient bandwidth usage, using a behaviour-aware user-assignment approach, based on the daily usage profiles [35].

Obviously, there is a large interest worldwide about this new technology and the support it is receiving, is an index that it will be the new technology to be used in FTTx and more specifically FTTH deployments. This, as well as the cost reduction we have estimated that the new technology will bring along, was the driver for the research on the expansion of the limits of a WDM/TDM PON as mentioned already.

Chapter III
Techno-economics

In this chapter, we expose the financial drivers behind the initiation of this study on the extension of limits of a WDM/TDM PON. In this framework, different architectures of FTTH and the technologies used to implement them are analyzed, in their cost and performance aspects. A study of the outside plant (OSP) cost as a function of household (HH) densities for all FTTH architectures and technologies such as GPON, EP2P, WDM/TDM PON, as well as a comparison on the aforementioned cost of each, is presented. In addition, a complete study on the overall cost of three access-metro network architectures has been performed. The estimation includes the OSP cost, as well as the active equipment cost of three optical networks, namely, metro network & GPON in the access part, metro network & EP2P in the access part and finally an access-metro WDM/TDM PON architecture. Moreover, a first attempt is being made on the cost estimation of future architectures that will host large splitting ratio PONs. This attempt serves like a preamble on the future work that needs to be done on FTTH techno-economics.

The 3rd chapter is organized in four parts. In the first, the drivers and the general reasons behind the research on FTTH networks are presented, whereas on the second, the motivation behind this specific study along with the tools used, are developed. Furthermore, in the second, the basic characteristics of the FTTx networks are exposed, followed by a description of the technologies that can be used for the deployment of FTTH architectures. In the third, a presentation of the actual-real life implementation of an optical access network, in terms of equipment and installation, is taking place, while on the fourth we are explaining the methodology followed, for the estimation of the cost in each case. On the final part, the findings and results are presented, along with some conclusions.

3.1 Drivers and requirements behind FTTH research

Communication services offered to customers have been fast developed in the last decades. End users are no longer interested only in voice telephony, broadcast television and radio; they are also increasingly asking for always-on fast Internet communication, fast peer-to-peer file transfer, high definition multimedia, on-line gaming, etc. Since the

access part of a network is the one that usually generates the bottleneck, an efficient access network is required for the delivering of these high bandwidth applications.

Existing copper-based technologies can cover present needs but are not future proof due to their limited performance in terms of reach and bandwidth [36]. This is the main reason that has motivated operators to either deploy optical access networks as Fiber-To-The-Node (FTTN), Fiber-To-The-Curb (FTTC), Fiber-To-The-Buiding (FTTB) along with the existing copper cable network and gradually transit to FTTH, or, move at once towards the deployment of a FTTH network and providing higher bandwidth.

The increase of high bandwidth applications, coupled with the need for decrease of the investment levels for next generation networks deployments, has led incumbent operators to deploy various forms of optical access networks and different kinds of FTTx architectures and technologies. Some of the main players of the broadband market in Europe, in order to cover the need for cost efficiency, have adopted PON technology, while the need for future proof and simple solutions, has lead others to the adoption of P2P architectures, usually combined with active technology. In most European countries though, the prevailing status in optical access networks is that of a combination of P2P and P2MP architectures deployed from different operators, as well as a combination of active and passive technologies. Still, the majority of the European customers are being served with internet connections provided by the technology of Asymmetric Digital Subscriber Line (ADSL), ADSL2 and VDSL in combination with fibre reaching a central aggregation point like FTTC or FTTN. Furthermore, new DSL technologies, such as Fast Access to Subscriber Terminals (G.Fast) and Vectoring VDSL, seem to gain ground lately in telecom equipment makers and operators preferences. Nevertheless, a lot of cities have already deployed FTTB (as in Swedish municipalities or in Lithuania) and FTTH networks; the technologies used for FTTH are Gigabit-Passive-Optical-Network (GPON) technology (Orange, Telefonica) or active P2P (Amsterdam municipality, alternative providers in Poland and France).

It is evident that fiber infrastructures constitute the present and the future of land telecommunications. Therefore, thorough research has been performed for the cost efficiency and the performance of optical access networks. Several studies have been implemented on the comparison between GPON and EP2P [37]. Ever since the idea of using fiber to the access part of the networks has emerged, numerous comparisons were published both for the cost [38] and the performance [39] of the several types of access networks. Investigations have also been made for next generation extended PONs [40] and their cost [41]. Some of them are based in the evaluation of the OSP cost while some others estimate the cost of the necessary active components [42] or both [43]. Nevertheless, in this thesis, a complete study of OSP cost as a function of household (HH) densities for all FTTH architectures and technologies and comparison on the aforementioned cost of all the FTTx architectures –namely: FTTN, FTTC, FTTB, FTTH-P2P, FTTH-GPON, FTTH-Active star, and FTTH-WDM/TDM PON as well as of some high splitting ratio solutions- is performed and presented. The cost difference

of several FTTx deployments and the cost comparison between four different FTTH architectures is shown. It is clear, that the difference between Fiber to the Node, to the Curb and to the Building is a rather significant one and that among the technologies examined, the WDM/TDM PON is the most cost effective. Finally, as far as PONs are concerned, it is shown that the increase of the splitting ratio leads, as expected, to a cost improvement due to the smaller number of fibres used. Yet, this is not as significant, as the ducts and trenches sizes that are used in current FTTH deployments, do not allow for the maximum benefit to be achieved. However, another important finding is that the cost savings in high splitting ratio PONs are not increasing linearly with the splitting ratio.

3.2 Motivation of this study and tools

As seen and reviewed so far, at present, there is a global tendency to migration towards FTTx architectures. Numerous examples of research publications have dealt with the subject of the most sufficient financially and future-proof solution. The reason for our techno-economic comparison was the need to explore the cost of different optical access networks and estimate whether the new technologies indeed provide a significant cost reduction. With this study, we try to compensate for the gap in the literature as far as a techno-economic evaluation of an emerging technology is concerned. What we believe has been missing is an objective approach to the implementation of a network, avoiding approximations and correction factors, but based on an real life deployment method. The results of this research proved that the presumption we made initially regarding the most cost efficient network was correct, therefore, we proceeded to the estimation of the cost difference among the several infrastructures. Hybrid WDM/TDM PON was found to be the less costly solution, nevertheless, in order to have a definite and integral result, a complete study on commercialized architectures and technologies has been realised as well.

The tools that have been used so far, have been abstract in their way of calculations and have either covered only a part of the costs involved with such an investment, or they have focused on already established and commercially available technologies. What this thesis is focused on, is a realistic and complete approach to the cost estimation of FTTx and FTTH networks, including, all parameters that comprise an optical fiber network. Both, existing - commercialized protocols used to deliver high bandwidth to end-users, as well as, new promising and non-standardized, yet complete protocols, have been taken into account. Moreover, a first glance on the cost of future high spitting ratio PONs, whose technology has not yet been fully developed, has been ventured.

The model used, which is described in subsection 3.4.2 and 3.4.3 is designed in great detail, based on instructions given from a construction company and is using very tangible parameterization in order to reach the numerical results presented. The several components needed to create an optical fiber network are presented, as well as their cost. Details have been given on the actual deployment procedure and on the model design. The architectures dealt with, are explained in detail and so are the technologies. In the case of the newly developed technology (WDM/TDM PON) network, the necessary

adjustments and extrapolations in time have been performed so as to achieve objective results. The model created can be used as it is for a real greenfield deployment, calculating the exact quantity of all elements needed and their exact placement on an area, estimating in detail the cost of the final network, according to the chosen technology and architecture. The study has been performed for the area of Athens and concerns both scarcely and densely populated urban areas. Nevertheless, the model can be used in rural areas as well. From the results presented one can clearly discern that WDM/TDM PON technology is the less expensive.

3.3 FTTx architectures and technologies used in FTTH

Several implementations of optical based access networks have been suggested. Numerous types exist in terms of technologies as well as in terms of architectures used. Each choice serves different needs and covers different requirements. The prevailing architectures for FTTH access networks are P2P or P2MP / Star architectures (Fig. 3.1.) [38]. In the P2P (or Home Run) architecture, each fiber is dedicated to each end-user (Fig. 3.1a) which is being translated into significantly high cost, even in the level of infrastructure implementation. In P2MP architectures (Fig. 3.1b and 3.1c) the feeder fiber is shared among many end-users according to the technology used.

Furthermore hybrid fiber-copper solutions have been suggested. Those are low cost solutions for current deployments such as FTTB, FTTC and FTTN. FTTN is defined as a fiber and copper local loop architecture for delivering broadband Internet to subscribers. With FTTN, fiber is installed only to copper local loop aggregation points known as feeder distribution interfaces (FDIs). FTTC is similar to FTTN with the difference that the street cabinet is much closer to the user's premises (typically within 300 meters). FTTB is defined as the architecture in which the final connection to the subscriber's premises is a communication medium other than fiber. The fiber cable is terminated on the premises for carrying communications for a single building with potentially multiple subscribers. FTTH is defined as a communications architecture in which the final connection to the subscriber's premises is optical fiber. The fiber cable is terminated at the subscriber's premise for carrying communications to a single end – user.

Two main categories of technologies are being used for the implementation of FTTH [38]. Those are namely PONs and AONs. AONs and PONs can be implemented in P2MP infrastructures, while P2P architectures are mostly based on Ethernet protocols. The P2P or Home Run architecture has a dedicated fiber or pair of fibers connecting the Central office with the end user. The P2MP in the case of AON is also referred to as Active star and has a powered device in the field, such as a switch or router [44]. The PONs have several implementations which will be analytically described.

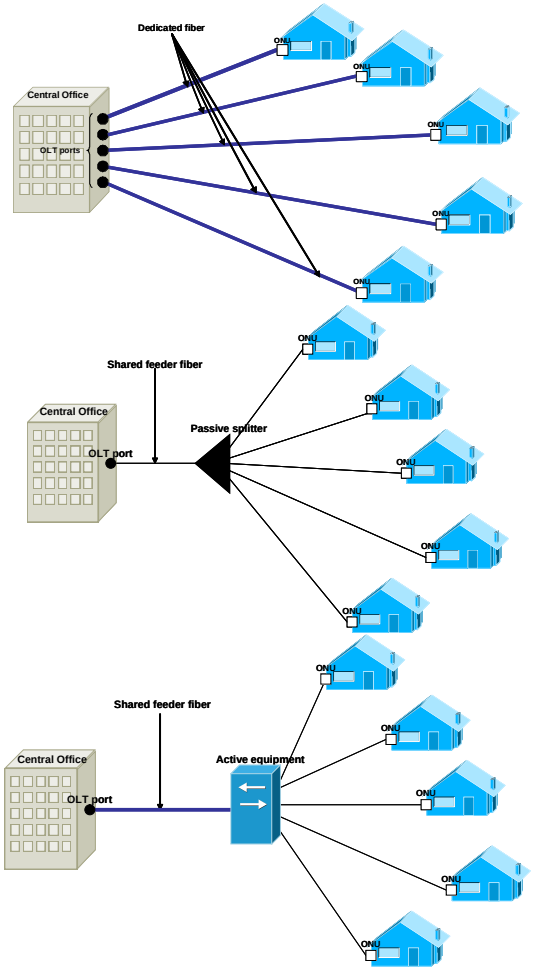

Fig. 3.1. FTTH in a) P2P - Home run architecture, b) Passive optical network - P2MP (passive star) architecture, c) P2MP - Active star architecture [38]

3.3.1 Time division Multiplexing (TDM) PONs

For TDM-PON, a single wavelength is being broadcasted as downstream and another is used in the upstream. A passive power splitter is used as the remote terminal. Each ONU signals are multiplexed in the time domain. ONUs see their own data through the address labels embedded in the signal. The splitting ratio varies from 16-128.

Different versions of already standardized PONs are BPON [45], GPON [46], EPON [47], 10G-EPON [48] and 10G-PON [49]. GPON is the prevailing technology in PONs nowadays especially in Europe. Due to the restrictions in bandwidth and reach presented in TDM PON standards up to now, the next reasonable step forward is the use of WDM in combination with TDM. In fact, hybrid WDM/TDM PON is an intermediate stage in PON deployment between currently deployed TDM PON and the future WDM PON [50].

3.3.2 GPON

Gigabit-capable Passive Optical Networks (GPON) are standardised by ITU-T under the family of recommendations G.984 [46]. The combinations of up/downstream speeds are several, but when referring to the bandwidths delivered to the end customer considered in this study only two can be considered:
1.2Gbit/s up, 2.4 Gbit/s down
2.4 Gbit/s up, 2.4 Gbit/s down.

The term physical reach is used to determine the maximum physical distance between ONU and OLT. Two options are defined for the physical reach: 10km and 20 km. In this investigation only the option of 10km is considered. The reason for this, is that it is assumed that 10km is the maximum distance over which Fabry Perot Laser diode can be used in the ONU for high bit rates

The splitting ratio considered is 1:16. The bit rate offered is thus, 156Mb/s. This bit rate is set as the reference bit rate, to which the performance and the overall cost of each optical access network technology will be evaluated. In other words, all deployments and technologies examined here should be able to offer a service of 156Mb/s to each end user. Considering this as the final target, we study the planning of the network and the components needed in order to achieve it, which will eventually give the overall cost.
There are several types of duplex GPON systems. Namely:
Type A: Consists of double optical fibers before and after the splitter for reliability. The ONUs and OLTs are singular.
Type B: Consists of double OLTs and double optical fibers between the OLTs and the optical splitter.
Type C: Consists of double number of OLTs, double fibers as well as double number of ONUs.
Type D: It consists of the evolution of the three previous types in terms of reliability. It allows the mixing of duplicated and non-duplicated ONUs [46].

We have investigated Type A – Fiber duplex system, since this topology and its operation has similar performance characteristics in terms of reliability, with the other three FTTH networks. More specifically the haul between the OLT and the end user equipment can be recovered in the case of a fiber cut in all cases.

3.3.3 Hybrid Wavelength Division Multiplexing / Time Division Multiplexing (TDM) PON

In this architecture several single λ sources or a multi-wavelength source emit a number of wavelengths which are routed throughout the access network. With several techniques the WDM signals are de-multiplexed into a number of individual λ channels. Each of these channels, with the use of power splitters and TDM technology, serves a number of subscribers according to the splitting ratio.

The WDM/TDM PON investigated in this study is based on the Scalable Advanced Ring-based Dense Architecture (SARDANA) [51]. SARDANA is engineered to incorporate functionalities of metropolitan networks and furthermore its size and limits make it an access-metro convergence solution. It is an architecture that aims at enhancing the performance of PONs, by implementing a scalable access WDM/TDM PON. It is based on a WDM ring for the transport of downstream and upstream information and TDM trees. In the CO a stack of lasers is used to serve with different λs the different tree network segments on a TDM basis. Placed on the ring, passive RN perform optical add and drop functions. With the use of filters, two wavelengths drop at each RN. Each of the two dropped wavelengths is driven to independent TDM PONs. It is a flexible network, whose characteristics in terms of maximum distance, number of wavelengths and splitting ratio can change according to the needs of the area that has to be served. Nevertheless its design characteristics and attributes are thoroughly described in the next chapter of the thesis. In this chapter, since we examine an urban deployment scenario, we consider 32 wavelengths, 1:64 splitting ratio, 20km ring length, feeder length –starting at the RN and ending at the splitter- up to 2.9 km and distribution along with drop length equal to 0.1km. The number of end users per ring is therefore set to 2048.

3.3.4 Ethernet Point to Point (EP2P)

In a point to point network each user is connected by a dedicated fiber to the CO. A router acts as central element, while the access switches transport the IP packets to the end user. The customer premises equipment (CPE) translates the IP traffic into application signals like Internet or telephony. As the network is scaled to more users, the routing function is distributed over an array of interconnected routers. Eventually, the routing function can be partitioned into two levels: a lower level with distribution routers and a higher level with interconnection routers. The distribution routers distribute the IP traffic to the various access switches, while the interconnection routers enable the interconnection to the service providers [52].The distribution of IP traffic via the Ethernet/IP network is based on standards. In this study the Fast Ethernet standard is considered. Fast Ethernet defines a version of Ethernet with a nominal data rate of 100 Mb/s. 100 Megabit Ethernet100BASE-BX [53] is a version of Fast Ethernet over a single strand of optical fiber. Single-mode fiber is used, along with a special multiplexer which splits the signal into transmit and receive wavelengths. Distances from the switch can be 10, 20 or 40 km. In this work we have considered 20km.

3.3.5 Active Star

A Star architecture (also known as a Double Star) is an attempt to reduce the total

amount of fiber deployed and hence lower costs by introducing feeder fiber sharing. In a star architecture, a remote node is deployed between the CO and the subscriber's premises. Each OLT port and the feeder fiber between the CO and the remote node is shared by anywhere from four to a thousand homes (the split ratio) via dedicated distribution links from the remote node.

When the remote node contains active devices such as a multiplexer (or Ethernet switch), the architecture is referred to as an Active Star as the remote node needs to be powered. The Remote Node in the Active Star network has a multiplexer / demultiplexer. The remote node switches the signal in the electrical domain (to the intended recipient) and hence OEO conversions are necessary at the remote node. This central device, routes all messages between devices. Since the feeder bandwidth is shared among multiple end points, the maximum sustained capacity available to each home – both upstream and downstream – is less with an active star architecture than with Home Run fiber [38].

3.4 FTTH infrastructure cost considerations – components

3.4.1 Outside plant

One of the most important cost factors in the deployment of an optical network is the outside plant equipment. For the calculation of capital expenditure (CAPEX) per user, one must consider the actual deployment methods of a fiber network and the components needed to create the infrastructure. To describe an FTTH infrastructure network, it is essential to describe some of the basic equipment [54]. An FTTH network normally forms part of an existing access network, connecting a large number of end users back to a central point, the CO, or access node. Each CO contains the required active transmission equipment used to provide the applications and services over optical fiber to the subscriber. Explaining outwards from the CO towards the subscriber, the key FTTH Infrastructure Elements needed are:

Central Office or Access Node
Feeder Cabling
Primary Fiber Concentration points (PCP)
Distribution Cabling
Secondary Fiber Concentration points (SCP)
Drop Cabling
Internal Cabling (in-house cabling)

The most conventional method to install underground cable, involves the creation of a duct network to enable subsequent installation of cables by pulling, blowing or using floatation techniques. This network comprises of a combination of large main ducts that contain smaller subducts for individual cable installation Fig 3.2 b), (or in other cases large main ducts into which, cables are progressively pulled one

over the other as the network grows Fig 3.2 a)) and furthermore small sub-ducts for the installation of a single cable for the drop part of the network. The drop cables will contain only 1 or 2 fibers for the connecting circuitry and possibly additional fibers for backup. The drop cables are installed in special pavement trenches.

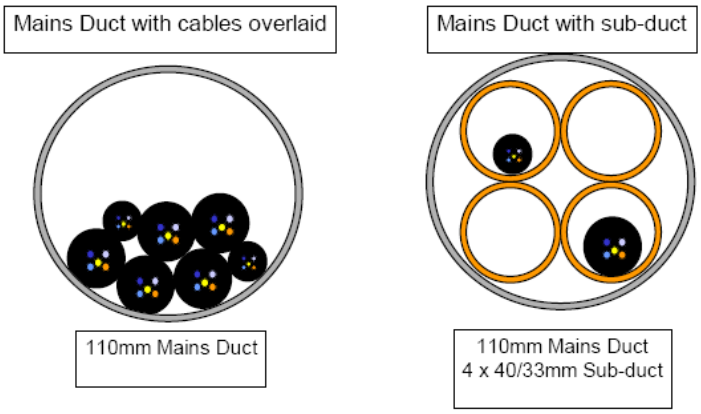

Fig. 3.2. a) section of duct with fiber cables, b) section of duct with subducts and fiber cables (www.emtelle.com)

Summarizing the installation method, for underground networks the drop cabling may be deployed within small ducts, within micro-ducts or by direct burial to achieve a single dig and installation solution. In this study we consider the use of microducts inside trenches. Additionally, we consider the blowing technique for installation of cables in the combined network comprising of ducts/subducts and we do not take into account in CAPEX calculations the inhouse cabling for it can take many forms or be absent whatsoever. Below we mention the necessary main elements of the network taken into account for the estimation of the total CAPEX.
Necessary main elements:

Trenches
Ducts and subducts
Fiber cables
Branching boxes
Splitters
Handholes – manholes
Y-branches

Feeder cables are large size optical cables, with a wide number of optical fibers. The number of feeder fibers in point to point active deployments equals the number of end users (total number of households in FTTH). In PONs it equals the total number of users divided by the splitting ratio. Thus the use of passive fiber splitting devices

positioned as close as possible to the end user, enables the use of smaller fiber count cables for the feeder part of the network, providing reduction of the costs.
The distribution fiber cables are used between the splitter or the branching boxes and the Y branches. These are usually cables consisting of a low number of fibers. This number depends on the deployment topology (usually based on the topology and density of the premises deployment in an area, for instance the distribution of streets in a rural location). Distribution cables are smaller in number of fibers, therefore in size, than the feeder cables in standardized PONs, AONs and P2P deployment.

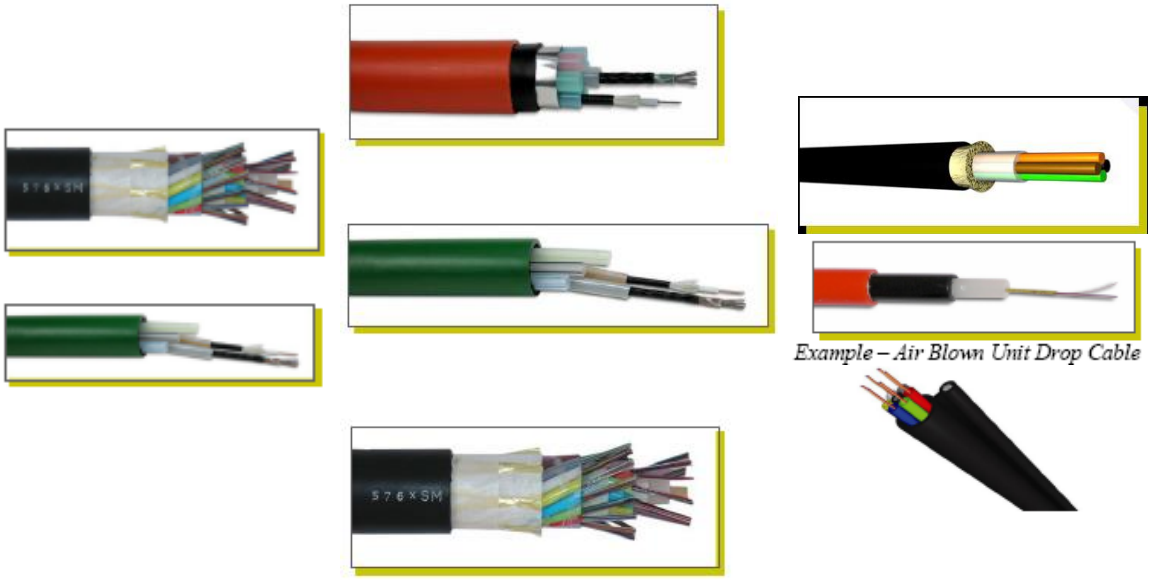

Fig. 3.3. a) feeder cables, b) distribution cables, c) drop cables (www.emtelle.com)

Drop cables lay between the drop terminals (Y-branches in this case) and ONUs. These are protected single or two fibers armored cables, one for each ONU. Each cable is terminated with a special protected connector that withstands environmental conditions. In Fig 3.3 feeder, distribution as well as drop cables are depicted.

3.4.2 Methodology of calculations (OSP)

For the calculations we have used parameters for typical deployment areas with different densities. The number of buildings, namely multi-dwelling units (MDUs) and single-dwelling units (SDUs), as well as the number of HH units are given or calculated. Then the mean distance among buildings is estimated which is referred to as Inter Building Spacing (IBS) [55]. IBS obviously depends on the HH/buildings density. A Y-branch is being used to separate the individual drop cables from the distribution ones. The splitters of PONs as well as the branching boxes of EP2P are placed inside handholes/manholes every several buildings. The switches, are placed inside cabinets in chosen crossroads. Those are the points where we have the transition from distribution to feeder fibers as seen in Fig 3.4 and Fig 3.5.

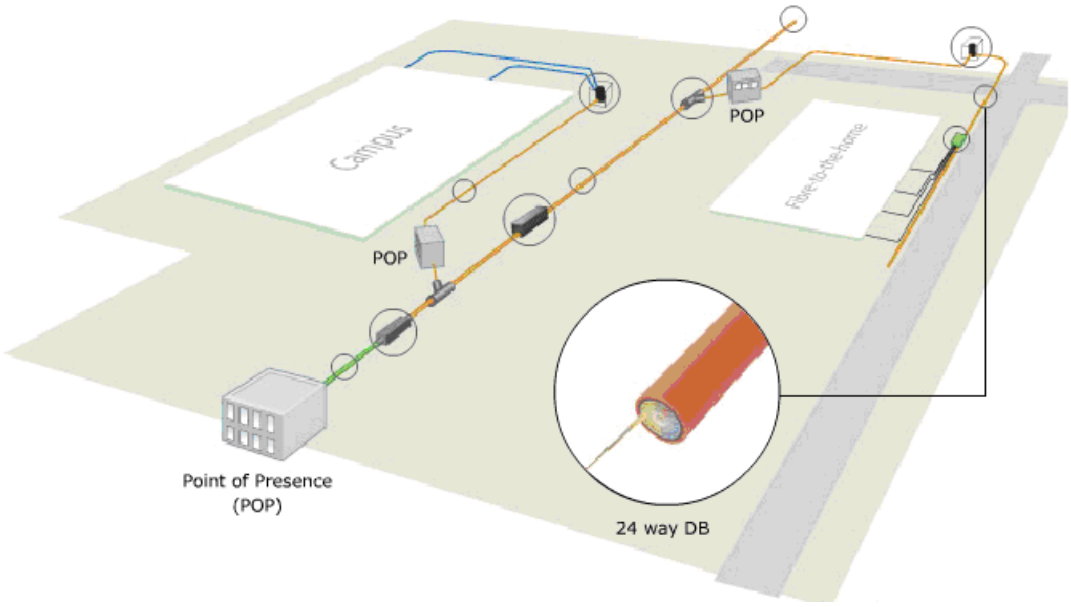

Fig. 3.4. POPs, feeder cabling, distribution cabling, drop cabling and ducts with subducts and fiber cables (www.emtelle.com)

The feeder fibers are launched from the OLTs in the COs which are housed in the points of presence (POPs). The CO is placed in the POP of the network which is a building that houses all active transmission equipment. There, all fiber terminations are managed and the interconnection between the optical fibers and the active equipment is facilitated. The main network cables entering the node terminate and run to the active equipment. The feeder cables also connect to the active equipment and run out of the building and into the FTTH network area. Inside the CO, separate cabinets and termination shelves may be considered for equipment and individual fiber management to simplify fiber circuit maintenance as well as avoid accidental interference to sensitive fiber circuits.

In the cases where the metro network is also considered (results, Fig 3.8.-3.11.) we consider that the metro network is deployed in special trenches with low fiber count cables. For the cases of GPON and WDM/TDM PON we consider that each CO/POP will serve up to 100.000 users, while for the case of EP2P this number is appointed to 20.000 due to fiber handling constraints at the CO. By dividing the total number of the users with 100.000 we reach to the final number of COs needed [56, 57].
For the calculation of OSP CAPEX per user, we consider:

The total length of the different types of trenches needed
The total length of the different types of ducts and sub-ducts needed
The total length of the different types of fiber cables needed
The total number of hand-holes / manholes & branch off closures needed
The total number of cabinets needed
The total number of y-branches needed

The total number of the splitters needed
The total cost all the aforementioned components
The total cost for the installation of the several components

To evaluate the actual cost benefits, we performed a detailed techno-economic calculation. For the estimation of the OSP CAPEX per user, for each FTTx network architecture, we have considered the actual deployment methods of a fiber network and

Table 3.1.

OUTSIDE PLANT MATERIAL & INSTALLATION COST

Description	Unit	$
HDPE duct – (24 micro tubes)	m	2.25
HDPE duct – (7 micro tubes)	m	2.2
HDPE duct – (2 micro tubes)	m	0.75
Manhole	each	500
Handhole	each	400
96 - fiber cable	m	2.8
72 - fiber cable	m	2.1
12 - fiber cable	m	1.1
8 - fiber cable	m	1.1
Microcable- 1f	m	0.3
Y-Branch unit	each	35
Trench I	m	25
Trench II	m	20
Microtrench I	m	16
Microtrench II	m	14
Pavement trench	m	35
HDPE duct in trench	m	0.55
Cable in subduct	m	0.45
Splicing	each	5

the components needed to create the infrastructure as described in *Outside Plant Equipment* section. To estimate the cost of the FTTN, FTTC and FTTB we assume that the FTTx network forms part of an existing access network, connecting a large number of end users to the CO. On the other hand for calculating the full CAPEX cost of the three technologies (EP2P, GPON, and WDM/TDM PON) we consider metro-access networks where EP2P and GPON form the access part, while on the WDM/TDM PON the metro with the access parts are converged. As far as the FTTH infrastructure is concerned, the cost of the OSP elements considered are namely: the metro and feeder cabling, the PCP, the distribution cabling, the SCP and the drop cabling [54]. The handholes or manholes that house the splitters, the branching boxes and the cabinets that contain the switches are considered as the PCP and the SCP are the Y-branches that help to disjoin the drop cables. Regarding the FTTx infrastructure, only the cost of the fiber network deployment is considered along of course with the necessary OSP additional material. Finally the cables installation, for the needs of the techno-economic study, has been considered to take place with the blowing technique which is one of the most cost effective ones. The cost estimations were based on individual components and

civil work costs, as shown in Table 3.1., and were provided by a construction and a telecom company.

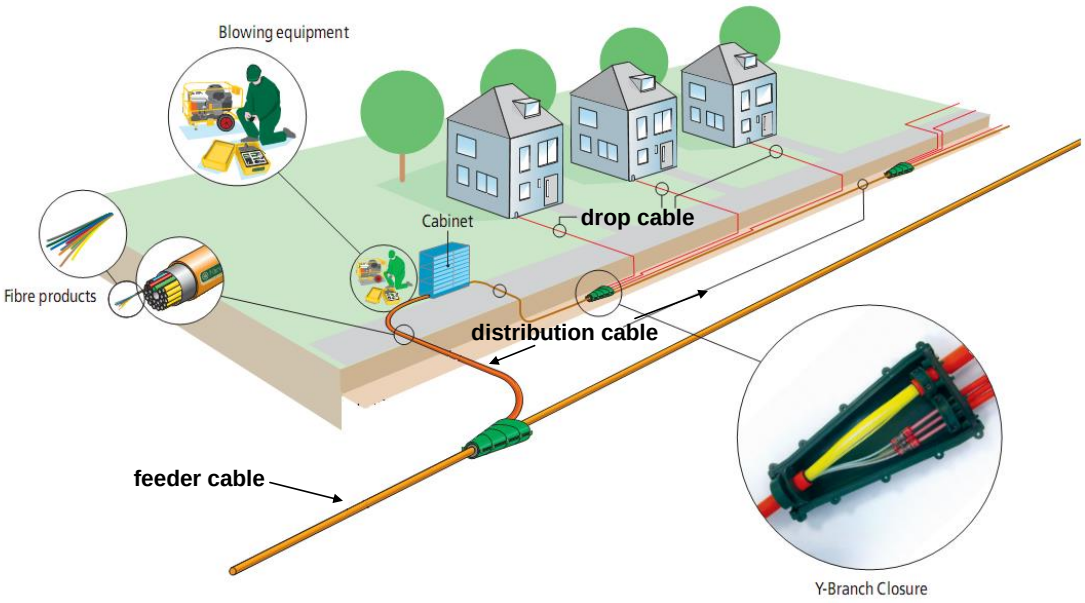

Fig. 3.5. POPs, feeder cabling, distribution cabling, drop cabling , y-branch closures and cabinets (www.emtelle.com)

The potential deployment area considered is a regular rectangular shaped typical residential area with a mixture of MDUs and SDUs and with a varying density of HH per km^2. The deployment considered, is based on the geographic model which can be seen in Fig. 3.5 and which has been used in several other studies [55-60]. The feeder part of the network is deployed in big trenches (trench I) with a capacity of 8 subducts, each containing 7 high fiber count cables, therefore 56 high-fiber-count cables, inside sub-ducts for easy installation and replacement. The trench II is a trench with capacity of 6 subducts each containing 24 low-fiber-count cables, which have not been used in this specific deployment. The use of this type of trench would be useful in scarcely populated areas and the model can be very easily modified and adapted to the use of trench II. Nevertheless, the use of this trench is not suggested in densely populated areas, where a larger number of users (subsequently – fibers) should be served by each trench. The distribution part of the network is parceled according to the density of the area into smaller ducts (microtrench I, II) varying from 96 low-fiber-count cables (microtrench I) capacity to 48 low-fiber-count cables (microtrench II). These are used between the splitter and the Y-branches. The drop part is implemented within a pavement trench with higher cost due to the high restoration cost, by microducts containing 1, 2, 8 or 12 fiber cables. For the estimation of CAPEX per user and as far as the OSP is concerned, we consider the total length of the different types of trenches, ducts, subducts and fiber cables, the total number of handholes/manholes, splitters and Y-branches needed, their total cost and the cost of their installation.

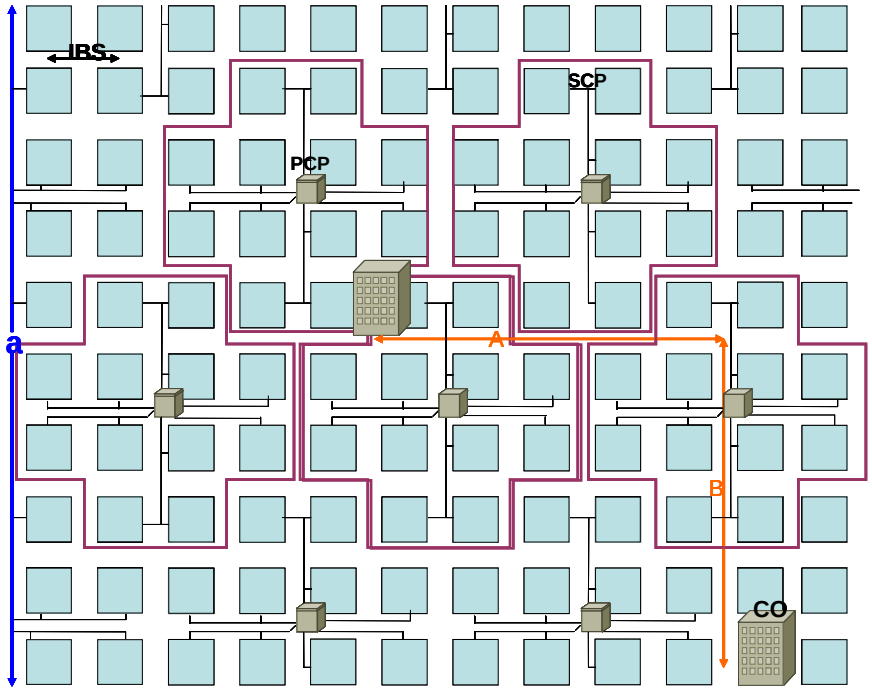

Fig. 3.6. Geographic model used for the calculation of the outside plant cost [60]

The IBS, thus the mean distance among buildings, appearing in Fig 3.6 is calculated by considering the area under investigation rectangular with a length α.

$$IBS = \sqrt{a\hat{}2 / |buildings|} \qquad \text{Eq. 3.1}$$

The PCPs are placed in crossroads. The choice of the crossroads depends on the building density and it is made on such a way that every street is served by a single duct. What appears as a double line in each street are the fibers serving the building, nevertheless all the cables are placed in a duct placed on one side of the street. Vertical lines are considered to serve the buildings on the opposite side. The distance among the COs (A+B) is set to two times the maximum reach of each technology.

$$A + B = 2 \times reach_{max} \qquad \text{Eq. 3.2}$$

3.4.3 Methodology of calculations (Active equipment)

The active equipment cost calculation includes the cost of the OLTs and their individual parts, the cost of the ONUs and their parts, as well as the cost of the routers and switches placed in the field for EP2P. For the case of WDM/TDM PON we include also the cost of the RNs –even though they don't include any active elements- which are new components introduced in this novel architecture. Every RN cost is shared by two PON trees, since two wavelengths are dropped/added in each one of them. The use of a single wavelength per tree is exploited by the reflective semiconductor optical amplifier in the

ONU, which reflects, amplifies and remodulates the signal, offering a low cost solution. Since the prices for the new components are not available, estimation was made, based on existing prices for the individual parts and the overall costs were extrapolated in time.

3.4.4 Results

The application of the techno-economic model/methodology for the various cases of FTTx architectures revealed the results presented in Fig 3.7 in terms of the OSP costs. In the case of FTTx, we do not consider that the same bandwidth is delivered to each end user. Further more, as mentioned already, only the estimation of the fiber infrastructure cost is taking place. The copper cables are considered to be already deployed (brownfield deployment); therefore their cost is not included in the calculations. It is shown that there is a significant cost difference among the different FTTx architectures which is due to the difference on the distance among the end point of the infrastructure and the customer. FTTN appears to be the cheapest solution, while FTTB the most costly one. This explains the fact that the incumbent operators are mainly deploying xDSL since they own the already deployed copper part of the network. Of course in FTTx cases examined, the cost savings are translated in degradation of the services offered due to the narrow bandwidth and high crosstalks.

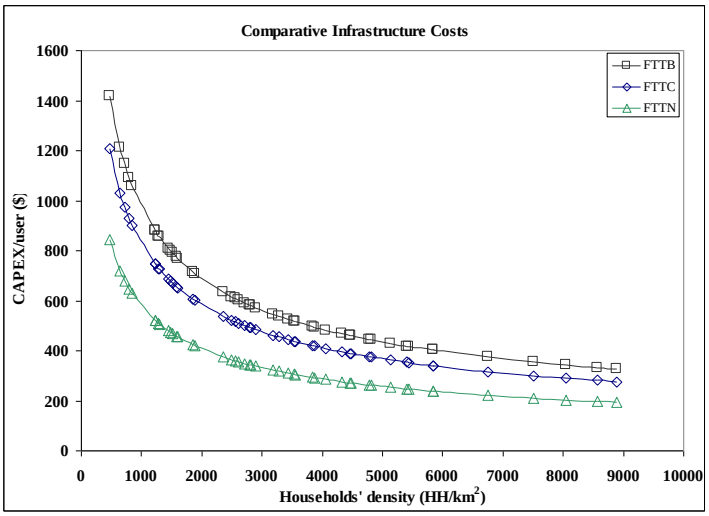

Fig. 3.7. Comparative OSP infrastructure costs for FTTx architectures, where X stands for Building, Curb and Node [60]

When EP2P, GPON and WDM/TDM PON are compared in terms of cost, the cost for both the OSP and the active equipment is estimated for each of the three architectures and the results are shown in Fig 3.8. and 3.9. respectively. The overall cost comparison is shown in Fig.3.10. As one can observe, there is a reduction in the range of 20% in CAPEX/user when the metro & GPON solution is compared to the metro & EP2P network, while there is a reduction in the range of 40% when WDM/TDM PON is compared to the last one. When WDM/TDM PON is compared to GPON the decrease is approximately 20%. All these results are shown in Fig.3.11. As can be observed the OSP cost is higher for EP2P which is expected due to its intrinsic characteristic of a dedicated fiber per customer. This leads to a higher number of cables, ducts and subducts as well as larger and more costly trenches. Furthermore it requires the use of more and larger COs which nevertheless are not included in the CAPEX estimation. The GPON CAPEX/user is larger than in the case of WDM/TDM PON, since a smaller maximum reach as well as a smaller splitting ratio is required in order to achieve the same bandwidth.

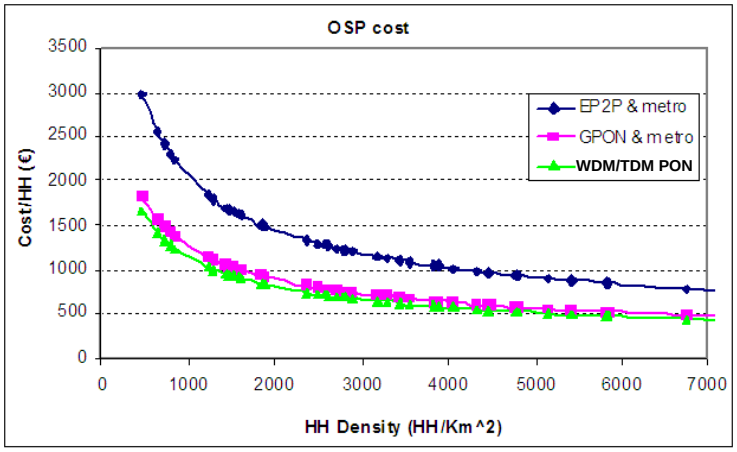

Fig. 3.8. OSP equipment CAPEX/user vs. HH density [59]

The active equipment per user is smaller in the case of EP2P, since there is an almost fixed ratio between the number of users a router and a switch can serve, therefore on the price corresponding to each user. Furthermore the cost of the active solution is as expected about 20% larger than the solution of PON. We observe, that the hybrid

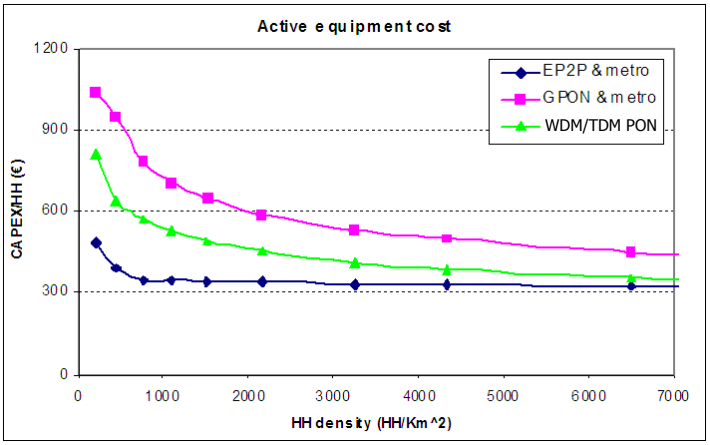

Fig. 3.9. Active equipment CAPEX/user vs. HH density [59]

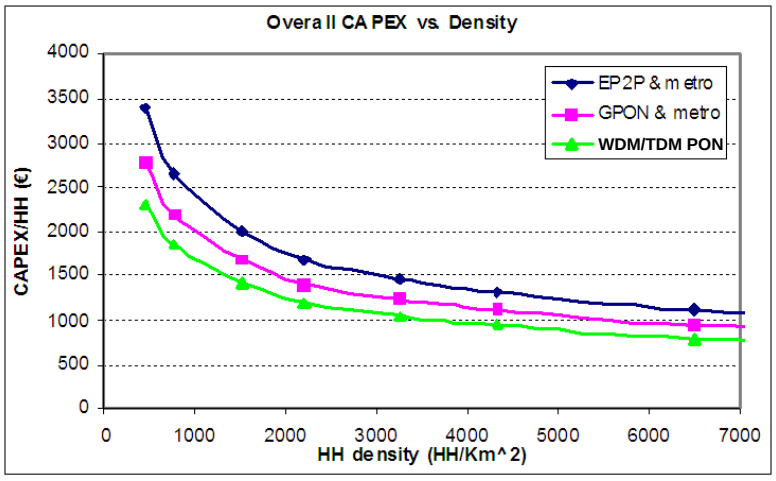

Fig. 3.10. Overall CAPEX/user vs. HH density [59]

solution of WDM/TDM PON that SARDANA offers in combination with the granularity and the design flexibility introduced, can provide a solution of €2300 for the lower density considered, which is 450 HH/km^2 and less for every other larger density. Moreover even though in this study it has not been considered, one should take into account that PONs are "green solutions" meaning they provide cost savings in OPEX.

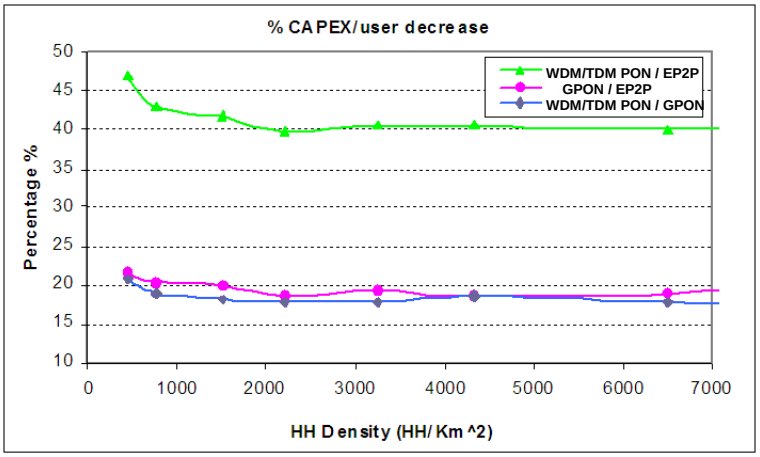

Fig. 3.11. Cost comparison vs. HH density [59]

Fig. 3.12 gives a perspective on the OSP cost difference among the different technologies used in FTTH architecture.

It is evident that the most cost saving technology in terms of OSP cost is the WDM/TDM PON. The reason for that is the efficient use of the fiber resources, in the largest part of the network. The feeder and the distribution part, is shared among a much larger number of end-users than in any other technology. The cost difference among the active star and GPON is due to the fact that the PCP (switch) in the case of Active star because of its ability to serve a higher number of end users, is placed much further from the customer than the equivalent (splitter) in the case of GPON, which is translated into larger length of distribution network, therefore larger quantity of material is needed in the first case. The reason of the cost efficiency of GPON over EP2P in terms of OSP is evident and consists of the larger number of fibers needed which translates to larger trenches needing larger ducts.

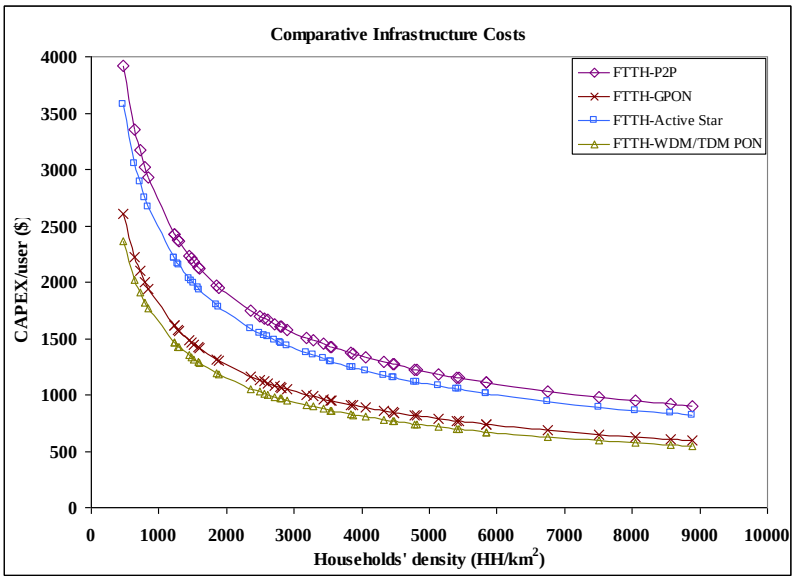

Fig. 3.12. Comparative OSP infrastructure costs for FTTH architectures with different technologies, namely EP2P, GPON, Active star and WDM/TDM PON [60]

Chapter IV
SARDANA and challenges of long reach and enhanced PONs

This chapter is focused on the presentation of SARDANA design. SARDANA as mentioned in chapter I stands for Scalable Advanced Ring-based Dense Access Network Architecture and it is an FP7 STREP project, implementing an elaborate design of a converged access-metro optical network. Its target is to enhance dense Passive Fibre-to-the-Home networks. After a short presentation of SARDANA and its most important aspects and components, we expose the basic challenges of long reach and enhanced PONs. Finally, we suggest a number of ways for overcoming these challenges, which have actually been the core of this thesis work.

4.1 SARDANA

Scalable Advanced Ring-based Dense Access Network Architecture is a WDM/TDM PON whose concept was conceived, in an effort to solve the problem of continuously increasing request for bandwidth, via an environmental friendly and cost effective way. It is considered an environmental friendly solution, since it is fully passive, and cost efficient, since it can reach 100km (in case of resiliency / fiber cut) while serving a large number of end users, with symmetric bandwidth of several hundred of Mbit/s per user. Additionally, the fact that it consists of a fully passive solution -in other words it uses no active equipment on the field- renders to it the advantage of low operational expenditures. This network combines the WDM and the TDM dimensions to expand traditional PON limits. It comprises of a scalable and extended access WDM/TDM PON, formed in a double fiber ring and secondary single fiber trees.

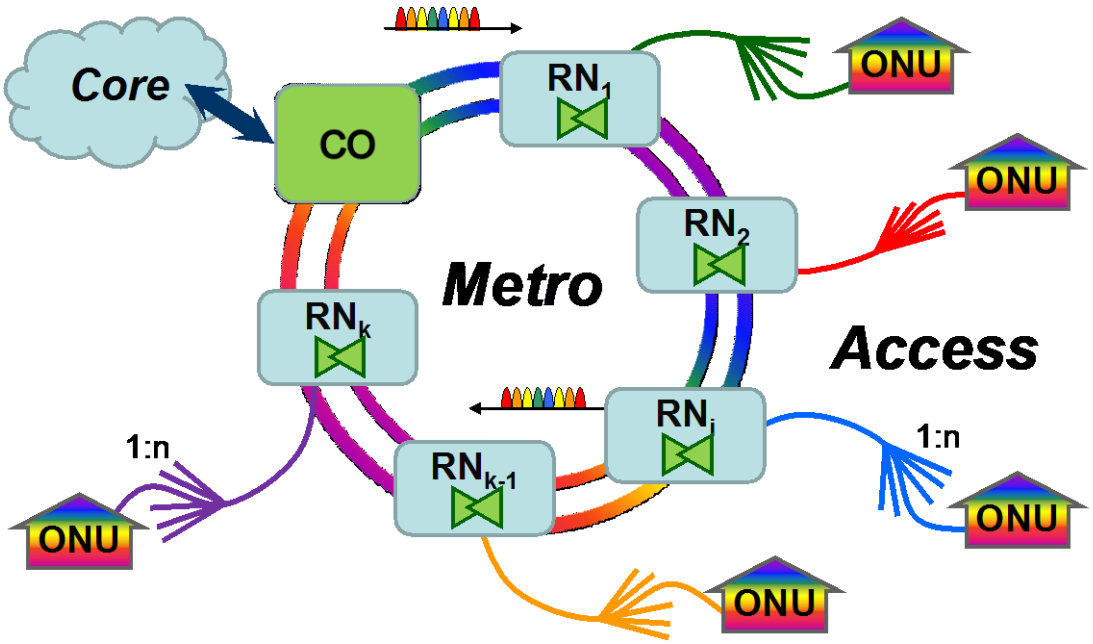

Fig. 4.1 SARDANA design

Its architecture is based on a double WDM ring for the transport of the large amount of downstream and upstream information (up to 1.2Tbit/s if using 64 wavelengths for 2000 users) and TDM trees, transmitting up to 3 wavelengths from corresponding operators, sharing a common infrastructure. The WDM ring is implemented by a double-fibre ring for resiliency and potentially reducing to a single-fibre ring after further evolution of user equipment. One ring is dedicated to the transmission of downstream signals and the other to the transmission of the upstream ones. The transmission of both down- and up-stream signals is bi-directional. The reason for this design is that in case of a fiber cut the network can be configured on the opposite direction. The ring carrying the upstream signals, is used for the transmission of another signal which is emitted from the OLT and counter propagates with the upstream signals, which originate from the ONUs. This signal is single wavelength and it is used as the optical pump for the EDFAs that are placed in the RN along the ring. Part of the signal is dropped at each RN to be used for the amplification of both upstream and downstream signals. On the other hand, the counter propagation of the optical pump with the upstream signals makes it possible to take advantage of the stimulated Raman scattering to amplify the upstream signals. Finally, the TDM trees are implemented with the use of single fiber.

The passive RNs that are placed along the WDM fiber ring, implement cascadable 2-to-1 fibre optical add and drop functions by means of athermal splitters and fixed filters that distribute different wavelengths to each of the access trees. The combination of splitters and filters selects two wavelengths and distributes them to two independent single fiber trees per RN [1]. The trees' splitting ratio can vary according to the needs of the network in terms of number of users. Proposed splitting ratios for an

urban deployment are 1:32, 1:64, 1:128, so the variation of served users is flexible, but its increase is achieved in expense of additional losses. Remote amplification is introduced at the RN by means of EDFs to compensate add/drop losses; optical pump for the remote amplification is provided by pumping lasers located at the CO, also providing extra Raman gain along the ring. RN evolves providing higher performances, and this is one of the subjects dealt with in this thesis.

Subsequently, two TDM trees are –usually- connected to each RN for PB optimization. The number of users served by the network is: $Users = 2RN * K$, where *K = 1/splitting ratio*. The athermal filters included in the RNs distribute different wavelengths to each of the TDM trees and EDFs provide the necessary gain to compensate link losses, with the use of remote pumping from lasers located at the CO. The RNs, with reduced footprint, do not require any environmentally-controlled location.

The CO (OLT) uses a stack of lasers to serve the different tree network segments on a TDM basis, using standard G/E-PON equipment adequately adapted to SARDANA. WDM is used for wavelength routing at the central ring, while TDM uses DBA techniques to have an optimum use of the bandwidth resource at the access trees. The CO centralizes the light generation for the whole network and its control both for down-stream and for up-stream transmissions. The laser providing the pump signal is collocated with the OLT [1]. The CO is used to house all the active components of the network and therefore SARDANA can be characterized as a fully passive architecture.

At the other end, the user equipment (ONU) is colourless and maximally simplified, implemented with an integrated reflective semiconductor device (RSOA+EAM) for up-stream remodulation, on the same fibre and on the same wavelength.

Common shared infrastructure and multi-operability are provided as well. On one hand, different operators can be serving different TDM tree, sharing the same ring and CO infrastructure. On the other hand, a higher level of multioperability can be also implemented at the TDM trees level. Service overlay from different operators at different wavelengths (Fig. 4.1) is also implemented by using evolved designs of RN, allowing to the users to select service provider by using pluggable filters at the input of their user's equipment (Fig. 4.1).

Overall this design focuses on long reach and increased end-user number, while providing high bit rate connectivity. In next generation passive optical networks, longer reach can be achieved with the use of some form of optical amplification. Amplification can of course be attained by the use of distributed EDFAs, but then the network can no longer be characterized as passive. In order to further reduce the cost of the network and simplify its operation, there is a need for optimization, both in the architecture and the technology used.

4.2 Main limitations in SARDANA and long reach-enhanced PONs

The phenomena that are most often met in research papers referring to long reach and enhanced PONs are namely: signal attenuation, chromatic dispersion and non linear effects. These are the main limitations in PONs nowadays and these are the problems which researchers are called to address.

According to the definition given, attenuation is reduction of the signal strength during transmission. Attenuation is an important consideration in the design of an optical communication system, since it plays a major role in determining the maximum transmission distance between a transmitter and a receiver or an in-line amplifier. The basic attenuation mechanisms in a fiber are absorption, scattering and radiative losses of the optical energy. Absorption is related to the fiber material, whereas scattering is associated both with the fiber material and with structural imperfections in the optical waveguide [61].

Chromatic dispersion is the term given to the phenomenon by which, different spectral components of a pulse travel at different velocities. It is considered an important linear distortion that affects the performance of optical systems leading to pulse spreading and the so-called inter symbol interference (ISI). Chromatic dispersion has two main components. The first one, material dispersion, appears due to the fact that the refractive index of silica is frequency dependent. Thus, different frequency components travel at different speeds in silica [62]. The second one, waveguide dispersion occurs because a single mode fiber confines only about 80% of the optical power to the core. Dispersion thus arises, since the 20% of the light propagating in the cladding, travels faster than the light confined to the core. The amount of waveguide dispersion depends on the fiber design, since the modal propagation constant β is a function of α/λ (the optical fiber dimension relative to the wavelength λ, here, α is the core radius).

As far as non-linear effects are concerned, they fall into two categories: non-parametric and parametric ones. The ones belonging to the first category, arise due to the interaction of light waves with photons (molecular vibrations) in the silica medium. The two main effects in this category are stimulated Brillouin scattering (SBS) and stimulated Raman scattering (SRS).

The second set of non linear effects arises due to the dependence of the refractive index on the intensity of the applied electric field, which in turn is proportional to the square of the field amplitude. The most important non linear effects in this category are self phase modulation (SPM) and four-wave mixing (FWM) [63].

4.3 Solutions on the main limitations of long reach/enhanced PONs

The suggested solutions for overcoming limitations in a fully passive optical network infrastructure are the results of a combination of two requirements. The first is to fight the challenges presenting themselves in optical networks due to natural phenomena, with the effective use of other phenomena, without the use of electro-optical conversion and the second to avoid the use of any active equipment whatsoever in the field. Nevertheless, electronic devices have been suggested for use in the ONU. Below we present four of these suggested solutions which will be further investigated in the next chapters of the thesis.

4.3.1 Amplification

In order to preserve the passiveness of an optical network, two solutions have been suggested, that are based purely on qualities of the material used in optical networks and to their interaction with light.

The first is amplification with the use of Erbium Doped Fibers. Er^{3+} as will be explained on the next chapter are risen with the help of optical pumping, in other words with the help of photons, from their ground state into excited states. This requires three energy levels. The top one to which the electron is elevated should lie energetically above the desired lasing level. After reaching its excited state, the electron must release some of its energy and drop to the desired lasing level. From this level, a signal photon can then trigger it into stimulated emission, whereby it releases its remaining energy in the form of a new photon with a wavelength identical to that of the signal photon. Since the pump photon must have a higher energy than the signal photon, the pump wavelength is shorter than the signal wavelength [64]. This attribute is successfully used in passive optical networks for amplification that avoids electro-optic conversion.

Raman amplification is based on a non-linear effect, the so-called stimulated Raman scattering, that in some cases, as for example WDM transmission, could be harmful for the quality of the signals, but could also be beneficial when used for providing amplification. In this case study SRS has been used as an amplification mechanism. The phenomena behind Raman amplification is that if two or more signals at different wavelengths are injected into a fiber, SRS causes power to be transferred from the lower-wavelength channels to the higher-wavelength channels. The energy of a photon at a wavelength λ is given by hc/λ, where h is Planck's constant. Thus a photon of lower λ has a higher energy. So the transfer of energy from a signal of lower wavelength to a signal of higher energy corresponds to emission of photons of lower energy caused by photons of higher energy [65]. Therefore in this case, with the use of an auxiliary wavelength (used also as pump signal for EDFAs) we use SRS to our benefit.

Since we want to preserve the full passiveness of the design, remote pumping has been introduced. Nevertheless, attenuation and dispersion degrade the efficacy of optical pump and of course, cost efficiency, safety regulations and non-linear effects do not allow for unlimited pump power use.

4.3.2 Compensation techniques

4.3.2.1 Dispersion compensation fibers

Chromatic dispersion can be effectively compensated by using optical techniques, which is only natural to expect, given that chromatic dispersion originates in the optical domain. Special chromatic dispersion compensating fibers (DCFs) have been developed that provide negative chromatic dispersion in the 1550nm wavelength range. Some of the typical values where DCFs can provide total chromatic dispersion are between -340 and -1360ps/nm and these modules are commercially available. DCFs can be used as pre-compensators when located after an optical amplifier and before the transmission fiber. They are characterised as post-compensators when they are placed after the transmission fiber and before the optical amplifier. Their characteristics are concentrated in plots called dispersion maps. More specifically in a dispersion map one can find the accumulated dispersion and the power level as functions of the distance along the fiber. Their use in the OLT, allows for a simultaneous dispersion pre-compensation of all the WDM signals.

4.3.2.2 Equalization

An optical system, such as a laser, fiber and photo detector constitute a channel over which the signal is being transmitted, if non linearities are ignored, the main distortion caused by this channel is the dispersion –induced broadening of the pulse. Dispersion is a linear effect, and hence the effect of the channel on the pulse, due to dispersion, can be modelled by the response of a filter with transfer function $H_D(f)$. Therefore, in principle, by using the inverse of this filter, say $H^{-1}{}_D(f)$as the equalization filter, this effect can be cancelled completely at the receiver. This is what an equalization filter is trying to accomplish. On the other hand, for conventional direct detection RXs, the linear distortion that is induced by CD in the optical domain is transformed into a nonlinear distortion in the electrical signal, which explains why only limited performance improvements can be achieved by using a linear baseband equalizer with only one baseband received signal. This also explains why nonlinear techniques, such as Non – linear Decision Feedback Equalization (DFE) and Maximum Likelihood Sequence Estimation (MLSD), are more effective in combating CD in direct detection RXs, [66-68].

A commonly used filter structure for equalization is shown in Fig. 4.3. This filter structure is called a transversal filter. It is essentially a tapped delay line: the signal is delayed by various amounts and added together with individual weights. The choice of the weights, together with the delays, determines the transfer function of the

equalization filter. The weights of the tapped delay line have to be adjusted to provide the best possible cancellation of the dispersion-induced pulse broadening.

Electronic equalization involves a significant amount of processing that is difficult to do at higher bit rates, such as 10 Gb/s. Nevertheless, we have used it quite successfully. Following we see some models of optical electronic equalizers in more detail.

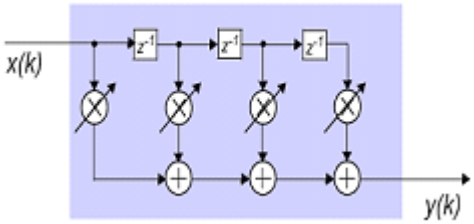

Fig. 4.3. Optical electronic equalizer (Feedback Forward Equalizer)

There are three main architectures for electrical channel equalizer (ECE). The most basic scheme is the feed-forward equalizer (FFE) (Fig. 4.3). In this set-up, a finite-impulse-response (FIR) filter is added to the transmission line after the optical-to-electrical conversion. The filter has several stages, each consisting of a delay element, a multiplier and an adder. After every delay element, an image of the non-delayed input is multiplied with a coefficient and added to the signal. The number of filter stages used and the coefficients chosen are crucial for effective dispersion cancellation. Automatic control of the filter coefficients is essential.

The filters can be designed based on prior information and kept fixed in the RX (the RX filter used after detection to suppress the out of band noise is a typical example), or they can be adaptive, and designed each time a connection is established, and are called adaptive regardless of the computation mechanism used for determining their coefficients, i.e., adaptively or not. When the distortion is time varying the coefficients need to be recomputed at given time intervals or continuously adapted to track the variations in the channel. The most common linear filter structure is the feed-forward (tapped-delay line) structure and can be implemented either in continuous or discrete time (Fig 4.4).

It produces, as mentioned already, an output equal to the sum of weighted combination of different delayed signals. The coefficients of the filter are computed by optimizing a suitably chosen metric. The minimum mean squared error (MMSE) and the least squares (LS) are the most commonly used two criteria. MMSE filter coefficients are given by the Wiener-Hopf equations and can be adaptively estimated using gradient optimization, and the LS weights, using recursive estimates of the input correlation matrix based on the zero-forcing (ZF) algorithm. Least Mean Squares (LMS) algorithm uses an instantaneous estimate of the statistics required for the gradient updates of the Wiener-Hopf solution, and is a simple and effective solution that has been successfully used in most adaptive filtering applications to date.

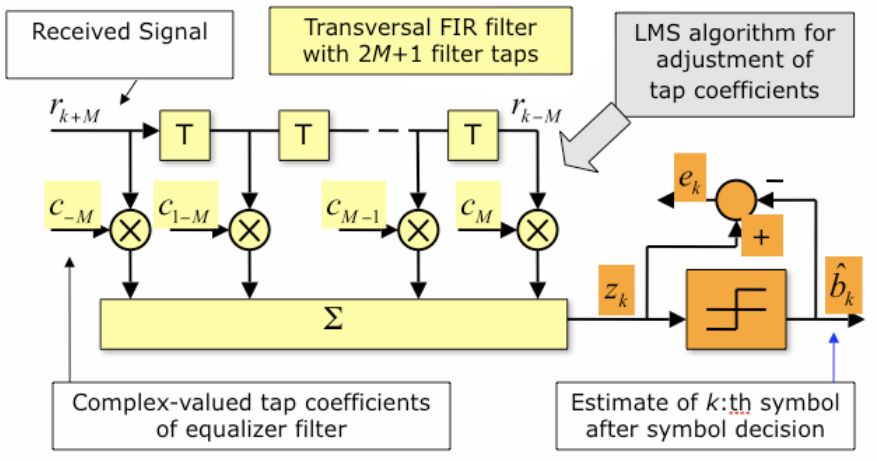

Fig. 4.4. Block diagram of the Decision- feedback equalizer (DFE) structure

A second approach is the decision-feedback equalizer (DFE) (Fig. 4.4, 4.5). This structure is an FFE with a second FIR filter added to form a feedback loop. Again, the coefficients of both filters require active control. Today's integration levels permit either FFE or DFE to be built into a clock-data recovery or demultiplexer chip with an extra power requirement of about 500 mW. The tap coefficients of the filter are calculated and are always adjusted in an adaptive operation according to an algorithm that runs in parallel with the purpose to minimize the error. The type of the algorithm and more significantly the way that this algorithm is optimized are particularly important in order to minimize the error and enhance the transmission properties of the system. The general operating modes of the adaptive equalizer include training and decision mode. During the training mode the algorithm adjusts to the channel characteristics and calculates the filter taps to compensate for the introduced impairments. In the decision mode, small variations in the taps allows for the compensation of the time varying effects of the channel. The most common algorithm that is used in order to calculate the taps is the LMS. The goal of that algorithm is to minimize the MSE between the desired equalizer output and the actual equalizer output. It is controlled by the error signal which is derived by the output of the equalizer with some other signal which is the replica of transmitted signal. The DFE version of the equalizer is a non- linear process that uses the same algorithm but it subtracts the interference by the already detected data offering advanced performance characteristics.

DFEs have long been used in digital communication systems. In channels with high ISI they outperform linear equalizers such as the ZF or MMSE equalizers. A DFE is a nonlinear equalizer that employs previous decisions to eliminate the ISI caused by previously detected symbols on the current symbol to be detected. A simple block diagram for a DFE is shown in Fig. 4.5.

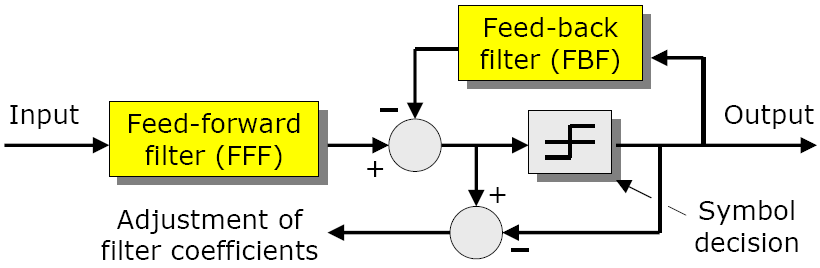

Fig. 4.5. Block diagram of the Decision Feedback Equalizer (DFE).

The DFE consists of two filters. The first filter is a feed-forward filter, identical in form to the linear equalizer described above. It is generally a fractionally spaced FIR filter, meaning that the tap spacing must be smaller than the symbol interval, with adjustable tap coefficients. Its input is the received filtered signal sampled at some rate that is a multiple of the symbol rate. The second filter is a feedback filter. It is implemented as an FIR filter with symbol-spaced taps having adjustable coefficients. Its input is the set of previously detected symbols. The output of the feedback filter is subtracted from the output of the feed-forward filter to form the input to the detector. The detector determines which of the possible transmitted symbols is closest in distance to the input signal. What makes the DFE nonlinear is the nonlinear characteristic of the detector that provides the input to the feedback filter. The tap coefficients of the feed-forward and feedback filters are selected to optimize some desired performance measure. For mathematical simplicity, the MSE criterion is usually applied, and a stochastic gradient algorithm is commonly used to implement an adaptive DFE.

The most sophisticated structure is the maximum-likelihood (sequence) detector (MLD/MLSD) (Fig. 4.6). This is effectively a digital signal processor that performs the necessary mathematical operations on the incoming data stream to reconstruct the transmitted signal. More specifically, an MLSE receiver compares a long section of the noisy received signal with all the possible waveforms of the same length that could be received and chooses the one that is “closer” to the received. The drawback of this method is that it needs the signal to be in digitized form at the input, which requires an analogue-to-digital converter running at full line rate and at a high resolution. MLSE estimates the channel and decides the most likely sequence sent at the transmitter based on the received signal. MLSE is a Viterbi decoder. It has two parts: channel estimation (ISI estimation) and decoding. Decoding complexity of MLSE is the same as the Viterbi decoders. Channel estimation can be thought as the encoder that encodes the original signal with the weighted neighboring bit values. Due to encoders' nature, the channel is assumed to be linear. If the channel is time varying, then the estimation should be able to track the changes. MLSE also requires soft decisions for decoding to maximize the gain. This is analogous to hard and soft decision Viterbi decoding performance difference. The effectiveness of MLSE in the compensation of the chromatic dispersion may extend into several hundred kilometre range, but at such long range, the complexity of the MLSE processor is very large. It is important to examine and optimize the effectiveness of MLSE equalization and provide techniques to reduce complexity without impacting performance.

As indicated already, digital equalizers based on MLSE are regarded as most efficient electronic equalization leading to lowest penalties (Fig 4.6). In difference to simple RXs, where each bit is decided immediately, in a MLSE the decision is

performed by calculating the transmitted bitstream with the highest probability. That means, that the probability for all bit combinations for the whole sequence is considered and the combination with highest probability is assumed as the transmitted bit combination. The overall probability of a transmitted bit combination is given by the product of all single bit probabilities. Instead of probability its logarithmic value is used and all separated logarithmic probabilities can be added, which is easier for hardware realization.

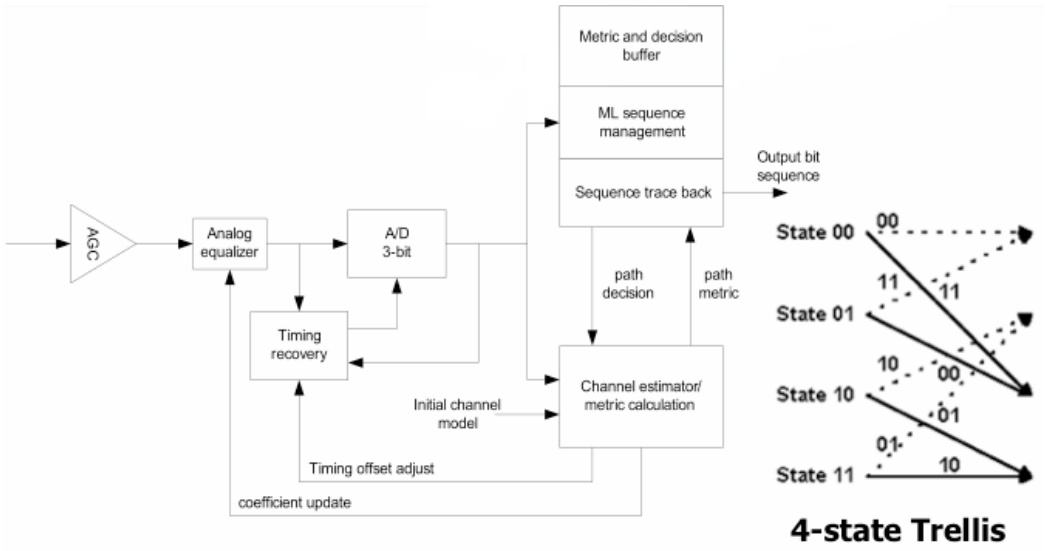

Fig. 4.6. Viterbi Equalizer based on MLSE

The signal distortion within an optical channel can be assumed as coding of signal, which is very similar to convolutional codes. The Viterbi algorithm was originally devised for decoding convolutional codes, and thus can be implemented as a realization of the MLSE.

The reason for the limited performance of electronic dispersion compensation (EDC) on CD mitigation in optical communication is due to the nonlinear characteristics of the absolute square operation of DD. In [69] a nonlinear electrical equalizer based on Volterra theory to mitigate this kind of nonlinear ISI is proposed. For illustration, the advanced equalization scheme or Nonlinear DF Equalizer setup is shown in Fig 4.7. The NL-DFE can be considered as the extension of a normal DFE including the nonlinear ISI mitigation. NL-DFE outperforms normal DFE and VE.

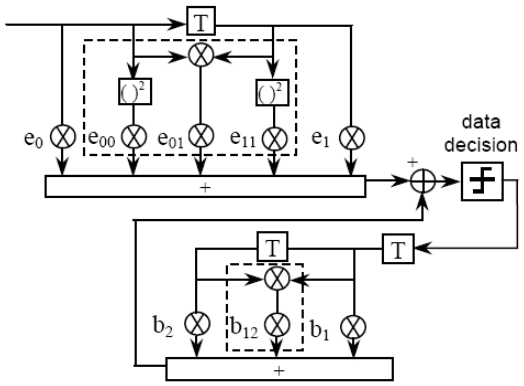

Fig. 4.7. Setup of NL-DFE: nonlinear part of setup marked with dashed boxes.

However, in this thesis the equalizers that will be used are FFE and DFE.

4.3.2.3 Reduced OLT power

The non linear effects cannot be faced at their root, so the best suggested solution is the decrease of the output power at the OLT. In the case of the aforementioned design, the decrease of the power also applies for the optical pump which in this case creates a constraint on the amplification possible in each RN, proportional to the distance of the RN from the OLT. Moreover, safety regulations do not allow for use of power above a certain threshold.

Chapter V
In line amplification

In this chapter we present a design of a WDM/TDM PON with remotely pumped EDFs to be used for amplification. The theoretical background on Erbium Doped fibers is described, as well as their use in signal amplification. Next, we examine the wavelength dependency of the gain in erbium doped amplifiers, which proves to be a very important factor in the design of the aforementioned WDM/TDM PON. Subsequently a theoretical approach of the in-line amplification takes place. Continuing, we expose the effect of noise figure in Optical Signal to Noise Ratio (OSNR) when a number of cascaded RNs placed in-line with the transmission path of the signal and the one subsequent to the other is used, as amplification approach to a WDM/TDM PON. Some design issues on in-line amplification are exposed with more important the wavelength allocation of the network; and finally, the simulation results of a special WDM/TDM PON operating with the help of in-line amplification are presented commented and evaluated.

5.1 Erbium Doped Fiber Amplifiers

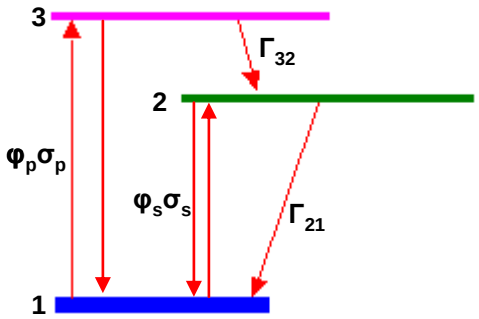

Fig. 5.1. The three level system used for the amplifier model [71]

5.1.1 Basics

The most usual way to model the physics of an Erbium Doped Fiber Amplifier is to use a three-level atomic system. Therefore we consider a three level system as depicted in Fig. 5.1.

As one can see the ground state is depicted as 1, the intermediate state into which energy is pumped is labelled 3 and state 2 is the basic excited state. If state 2 has

a long lifetime (which as will be proven consequently is a characteristic of a good amplifier) it is referred to as metastable level. State 2 is the upper level of the amplifying transition and state 1 is the lower level. The populations of levels 1, 2 and 3 are named N_1, N_2 and N_3 correspondingly. In order to have amplification we need to have population inversion among states 1 and 2 and of course since state 1 is the ground state the number of the excited photons (belonging to state 2) need to be at least half in number of the total population of erbium ions. That means we need a rather high threshold pump power for achieving amplification.

Let us consider that the transmission of light in a fiber is a one dimensional problem and that the pump and signal intensities as well as the erbium distribution are constant in the transverse dimensions over an effective cross-sectional area of the fiber.
The incident light intensity flux at the frequency corresponding to the 1 to 3 transition is denoted by φ_p and corresponds to the pump. The incident flux at the frequency corresponding to the 1 to 2 transition is denoted by φ_s and corresponds to the signal field. There are numerous reasons that cause change in population for each level, such as absorption of photons from the incident light field and spontaneous and stimulated emission. We denote as Γ_{32} the transition probability from level 3 to level 2, which is mostly non-radiative and Γ_{21} the transition probability from level 2 to level 1 which in the case of Er^{3+} is mostly due to radiative transitions. We denote the absorption cross section for the 1 to 3 transition by σ_p and the emission cross section for the 2 to 1 transition by σ_s.
The rate equations for the population changes are written as:

$$\frac{dN_3}{dt} = -\Gamma_{32}N_3 + (N_1 - N_3)\varphi_P\sigma_P \qquad \text{Eq. 5.1}$$

$$\frac{dN_2}{dt} = -\Gamma_{21}N_2 + \Gamma_{32}N_3 - (N_2 - N_1)\varphi_S\sigma_S \qquad \text{Eq. 5.2}$$

$$\frac{dN_1}{dt} = \Gamma_{21}N_2 - (N_1 - N_3)\phi_P\sigma_P + (N_2 - N_1)\phi_S\sigma_S \qquad \text{Eq. 5.3}$$

In a steady state situation, the time derivatives will all be zero

$$\frac{dN_1}{dt} = \frac{dN_2}{dt} = \frac{dN_3}{dt} = 0 \qquad \text{Eq. 5.4}$$

and the total population N is given by

$$N = N_1 + N_2 + N_3 \qquad \text{Eq. 5.5}$$

Using equation 5.1 we can write the population of level 3 as

$$N_3 = \frac{1}{1 + \Gamma_{32} / \phi_p \sigma_p} N_1 \qquad \text{Eq. 5.6}$$

When Γ_{32} is large compared to the effective pump rate into level 3, $\varphi_p\sigma_p$, N_3 is very close to zero, so that the population is mostly in levels 1 and 2. Substituting N_3 in equation 2 with the use of equation 5.6 we obtain:

$$N_2 = \frac{\left(\phi_p \sigma_p / \Gamma_{32} \right) + \phi_s \sigma_s}{\Gamma_{21} + \phi_s \sigma_s} N_1 \qquad \text{Eq. 5.7}$$

We then use equation 5.5 to derive the populations N_1 and N_2 and the population inversion $N_2 - N_1$:

$$N_2 - N_1 = \frac{\varphi_p \sigma_p - \Gamma_{21}}{\Gamma_{21} + 2\varphi_s \sigma_s + 2\varphi_p \sigma_p} N \qquad \text{Eq. 5.8}$$

The condition for population inversion, and thus for gain on the 2 to 1 transition, is that $N_2 \geq N_1$. The threshold corresponds to $N_1 = N_2$ and results in the following expression for the pump flux required:

$$\varphi_{th} = \frac{\Gamma_{21}}{\sigma_p} = \frac{1}{\tau_2 \sigma_p} \qquad \text{Eq. 5.9}$$

In a situation where the signal intensity is very small and the decay rate is Γ_{32} is large compared to the transition rate induced by the pump field, $\varphi_p\sigma_p$, we can thus write the population inversion as:

$$\frac{N_2 - N_1}{N} = \frac{\varphi'_p - 1}{\varphi'_p + 1} \qquad \text{Eq. 5.10}$$

Where

$$\varphi'_p = \frac{\varphi_p}{\varphi_{th}} \qquad \text{Eq. 5.11}$$

The plot of equation 10 can be shown in Fig. 5.2. Below the pump threshold the inversion is negative; above the pump threshold it is positive. When the inversion is negative, there are more absorptive transitions then emissive transitions at the signal

wavelength, and the signal sees negative gain, i.e. attenuation. Conversely when the inversion is positive, the signal experiences positive gain as it traverses the excited medium.

The pump intensity, in units of energy per unit area per unit time, is expressed as $I_p = h\nu_p.\varphi_p$. The threshold pump intensity is then given very simply by the expression:

$$I_{th} = \frac{h\nu_p \Gamma_{21}}{\sigma_p} = \frac{h\nu_p}{\sigma_p \tau_2} \qquad \text{Eq. 5.12}$$

This equation is intuitively easy to understand. The higher σ_p is, the higher the probability that a pump photon is absorbed, which lowers the number of pump photons necessary to guarantee that enough are absorbed to reach threshold. In addition, the

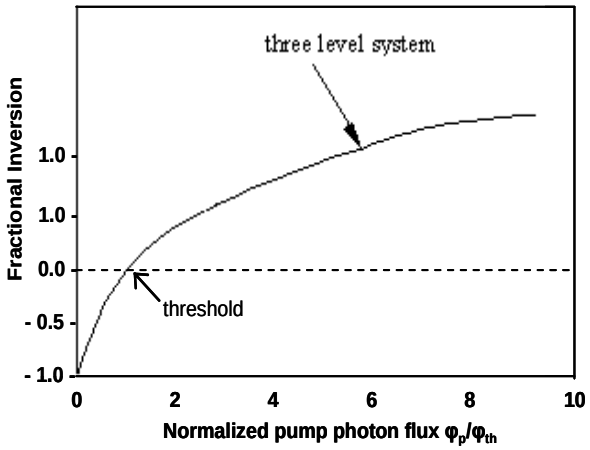

Fig. 5.2. Fractional population inversion $(N_2\text{-}N_1)/N$ in a three level system [71]

longer τ_2 is, the longer the energy stays in the reservoir formed by level 2, and as a result less pump photons are needed per unit time to keep energy in level 2. The conditions for low pump threshold are thus easily summarized as:

- High absorption cross section
- Long lifetime of the metastable level

For a given pump power , to obtain the maximum amount of gain for a given erbium concentration in the fiber core, the fiber length should be increased to the point at which the pump power becomes equal to the intrinsic pump threshold. For axial points z, along the length of the fiber, prior to that point the gain is positive, after that point the gain is negative, and so the fiber should be terminated at the point where the pump power has decreased to the threshold level. This determines the optimal length of the fiber.

We now consider N, N_1, N_2, N_3 as densities of population in unit of number of ions per unit volume. Two light fields travel through the medium, interacting with the ions, and have intensities I_s (signal field) and I_p (pump field). The photon fluxes are given by:

$$\varphi_s = \frac{I_s}{h\nu_s} \qquad \text{Eq. 5.13}$$

and

$$\varphi_p = \frac{\mathrm{I}_p}{h\nu_p} \qquad \text{Eq. 5.14}$$

The propagation of the signal when treated along a single direction z (the axis of the fiber) is a one dimensional problem, which is a simplification of the three-dimensional character of the erbium ion distribution in the fiber core and of the light modes.
The light field intensities are derived from the light field powers by the following simplified relationship:

$$\mathrm{I}(z) = \frac{P(z)\Gamma}{\mathrm{A}_{eff}} \qquad \text{Eq. 5.15}$$

Where Γ is the overlap factor, representing the overlap between the erbium ions and the mode of the light field, and A_{eff} is the effective cross-sectional area of the distribution of erbium ions. Expression 5.15 states that the intensity of the field at a point z will be taken to its cross-sectional average, computed as the amount of the power travelling through the erbium –doped region of the fiber, divided by its cross-sectional area. Assuming in the following discussion that both pump and signal beans are propagating in the same direction, i.e., a co-propagating configuration as opposed to a counter-propagating, the following take place. The fields will be attenuated or amplified after an infinitesimal length dz by the combined effects of absorption arising from ions in their ground state (N_1) and stimulated emission from ions in the excited state (N_2 and N_3).

$$\frac{d\varphi_s}{dz} = (N_2 - N_1)\sigma_s\varphi_s \qquad \text{Eq. 5.16}$$

$$\frac{d\varphi_p}{dz} = (N_3 - N_1)\sigma_p\varphi_p \qquad \text{Eq. 5.17}$$

This leads after some calculations, to the following equation for the signal intensity growth or decay:

$$\frac{dI_s}{dz} = \frac{\frac{\sigma_p I_p}{h\nu_p} - \Gamma_{21}}{\Gamma_{21} + 2\frac{\sigma_s I_s}{h\nu_s} + \frac{\sigma_p I_p}{h\nu_p}}\sigma_s I_s N \qquad \text{Eq. 5.18}$$

We can write an equation for the attenuation of the pump intensity as

$$\frac{dI_p}{dz} = -\frac{\Gamma_{21} + \frac{\sigma_s I_s}{h\nu_s}}{\Gamma_{21} + 2\frac{\sigma_s I_s}{h\nu_s} + \frac{\sigma_p I_p}{h\nu_p}}\sigma_p I_p N \qquad \text{Eq. 5.19}$$

From equation 5.18, it is clear that the condition for gain for the signal field is that

$$I_p \geq I_{th} = \frac{h\nu_p}{\sigma_p \tau_2} \qquad \text{Eq. 5.20}$$

where we again used $\Gamma_{21}=1/\tau_2$ and I_{th} is the pump threshold intensity for gain at the signal wavelength. This is equivalent to the condition derived above for population inversion. We can write the equations in a somewhat simpler fashion by defining the intensities in units of the pump threshold. These normalised intensities are given by

$$I'_p = \frac{I_p}{I_{th}} \qquad \text{Eq. 5.21}$$

and

$$I'_s = \frac{I_s}{I_{th}} \qquad \text{Eq. 5.22}$$

We further define the quantity η as

$$\eta = \frac{h\nu_p}{h\nu_s}\frac{\sigma_s}{\sigma_p} \qquad \text{Eq. 5.23}$$

and the saturation intensity $I_{sat}(z)$ as

$$I_{sat}(z) = \frac{1 + I'_p(z)}{2\eta} \qquad \text{Eq. 5.24}$$

We can write the propagation equations for the normalized intensities as

$$\frac{dI'_s(z)}{dz} = \frac{1}{1 + I'_s(z)/I_{sat}(z)}\left(\frac{I'_p(z)-1}{I'_p(z)+1}\right)\sigma_s I'(z) N \qquad \text{Eq. 5.25}$$

and for the pump

$$\frac{dI'_p(z)}{dz} = \frac{1+\eta I'_s(z)}{1+2\eta I'_s(z)+I'_p(z)}\sigma_p I'_p(z) N \qquad \text{Eq. 5.26}$$

Equations 5.25 and 5.26 determine the behaviour of erbium-doped fiber amplifiers, at the simplest level. The signal propagation equation will lead to gain only if $I_p \geq I_{th}$. This is the expected threshold condition. When the pump intensity is less than the threshold, the signal is attenuated; when it is larger the signal is amplified. Under the conditions of small signal gain, where $I'_s << I_{sat}$ (this condition is satisfied when the signal is weak and the pump is strong) and assuming for simplicity that the pump is constant as a function of z (the fiber in uniformly inverted), the signal propagation equation is easily integrated to yield the signal as a function of position along the fiber:

$$I'_s(z) = I'_s(0)\exp(a_p z) \qquad \text{Eq. 5.27}$$

where we defined the gain coefficient a_p

$$a_p = \frac{I'_p - 1}{I'_p + 1}\sigma_s \mathrm{N} \qquad \text{Eq. 5.28}$$

The signal grows exponentially, with a co-efficient proportional to the signal emission cross section and the degree of population inversion. The latter is determined by the pump intensity relative to threshold. When the pump intensity is very strong and several times the threshold, such that the erbium ions are all inverted, the gain coefficient becomes approximately [71]

$$a_p = \sigma_s N \qquad \text{Eq. 5.29}$$

From eq. 5.29 it is obvious that the gain of the EDFA is wavelength depended.

5.1.2 Gain wavelength dependency

The wavelength dependency of the gain can be further described by the black box model of the EDFA [72] presented in [73], according to which, the gain characteristic $G^{dB}(\lambda)$ of the amplifier, expressed in dBs, can be described as:

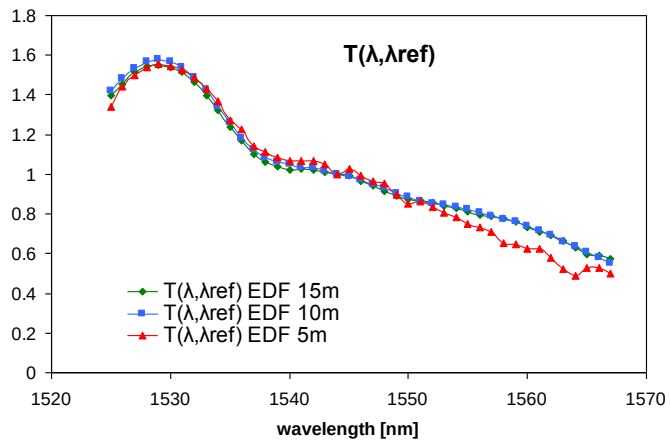

Fig. 5.3. Values of the tilt curve T(λ, λ_{ref}) for different lengths of the EDF HE980 for a pumping wavelength of 1480nm. The reference wavelength is λ_{ref} =1543.73nm, Pp=12 dBm and Pin=0 and -10 dBm for each EDF length

$$G^{dB}(\lambda) = T(\lambda, \lambda_{ref}) \cdot \left[G^{dB}(\lambda_{ref}) - G_{ref}{}^{dB}(\lambda_{ref}) \right] + G_{ref}{}^{dB}(\lambda) \qquad \text{Eq. 5.30}$$

With λ_{ref} is a reference wavelength and $G_{ref}{}^{dB}(\lambda_{ref})$ and $G_{ref}{}^{dB}(\lambda)$ are, respectively, a reference signal gain at λ_{ref} and a signal gain spectrum, at reference signal and pump input powers.

Finally, $T(\lambda, \lambda_{ref})$ is the named tilt function that can be experimentally measured from two gain spectrums measured at different saturation conditions, $G_1{}^{dB}(\lambda)$ and $G_2{}^{dB}(\lambda)$ without any knowledge about internal detail of the amplifier

$$T(\lambda, \lambda_{ref}) = \frac{G_1{}^{dB}(\lambda) - G_2{}^{dB}(\lambda)}{G_1{}^{dB}(\lambda_{ref}) - G_2{}^{dB}(\lambda_{ref})} = \frac{\alpha(\lambda) + \gamma(\lambda)}{\alpha(\lambda_{ref}) + \gamma(\lambda_{ref})} \qquad \text{Eq. 5.31}$$

where $\alpha(\lambda)$ and $\gamma(\lambda)$ are, correspondingly, the absorption and emission coefficients. They are related to the corresponding cross sections $\sigma_a(\lambda)$ and $\sigma_e(\lambda)$, by the expression: $\alpha(\lambda)=\sigma_a(\lambda)N_{Er}$ and $\gamma(\lambda)=\sigma_e(\lambda)N_{Er}$ [74], where $N_{Er}=\int dr_t n_{Er}(r_t)\left|\Psi(r_t)\right|^2$ represents the effective erbium concentration over the cross section of the fiber (r_t) overlapping with the signal propagation mode $\Psi(r_t)$. The Eq. 5.31 can be demonstrated knowing that the optical gain along the erbium doped fibers can be described by [73]:

$$G^{dB}(\lambda,L)=\left[\alpha(\lambda)+\gamma(\lambda)\right]\frac{N_2}{N_{Er}}\cdot L-\alpha(\lambda)\cdot L \qquad \text{Eq. 5.31}$$

where N_2/N_{Er} is the mean inversion and L is the EDF length. On one hand, the tilt function $T(\lambda,\lambda_{ref})$, as shown in eq. 5.31, should be independent of the length of the EDF. This is experimentally verified and shown in Fig. 5.3. It can be seen that the differences between the two tilt functions corresponding to 10m and 15m EDF are less than 0.05dB. Nevertheless, the 5m EDF shows higher deviations (max 0.15dB) at long wavelengths - due to the experimental error in $T(\lambda,\lambda_{ref})$ calculation- since the gain under two different saturation levels varies less at longer wavelengths.
Alternatively to Eq. 5.31, it can be shown, using Eq. 5.32 that

$$T(\lambda,\lambda_{ref})=\frac{G_1^{dB}(\lambda,L_1)\cdot L_2-G_2^{dB}(\lambda,L_2)\cdot L_1}{G_1^{dB}(\lambda_{ref},L_1)\cdot L_2-G_2^{dB}(\lambda_{ref},L_2)\cdot L_1} \qquad \text{Eq. 5.33}$$

by considering two gain spectrums $G^{dB}{}_1(\lambda, L_1)$ and $G^{dB}{}_2(\lambda, L_2)$ measured at different saturation conditions ($P_{in,1}$, $P_{p,1}$), ($P_{in,2}$, $P_{p,2}$) and different EDF lengths L_1 and L_2.
The black box model (Eq. 5.30) can be extended to predict the signal gain, $G^{dB}(\lambda, P_{in}, P_p, L)$, at any wavelength ($\lambda$), input signal power ($P_{in}$), input pump power ($P_p$), and EDF length (L), by using Eq. 5.33. Identifying: $G^{dB}{}_1(\lambda, L_1)$ as the signal gain spectrum at the target parameters (P_{in}, P_p, L), $G^{dB}{}_2(\lambda, L_2)$ as the gain spectrum at a reference configuration ($P_{in,ref}$, $P_{p,ref}$, L_{ref}), $G^{dB}{}_1(\lambda_{ref}, L_1)$ and $G^{dB}{}_2(\lambda_{ref}, L_2)$ as signal gain values at λ_{ref}, at the target and reference configurations respectively, in that case, the signal gain $G^{dB}(\lambda, P_{in}, P_p, L)$ can be obtained from Eq. 5.33 as:

$$\begin{aligned} G^{dB}(\lambda,P_{in},P_p,L)&=T(\lambda,\lambda_{ref})\cdot\\ &\left[G^{dB}(\lambda_{ref},P_{in},P_p,L)-\frac{L}{L_{ref}}G^{dB}(\lambda_{ref},P_{in,\,ref},P_{p,\,ref},L_{ref})\right]\\ &+\frac{L}{L_{ref}}G^{dB}(\lambda,P_{in,\,ref},P_{p,\,ref},L_{ref}) \end{aligned} \qquad \text{Eq. 5.34}$$

In comparison with previous black box model, an extra term, proportional to the difference between reference and target EDF lengths it is normally added to earlier expression Eq. 5.30

$$G^{dB}(\lambda, P_{in}, P_p, L) = T(\lambda, \lambda_{ref}) \cdot \left[G^{dB}(\lambda_{ref}, P_{in}, P_p, L) - G^{dB}(\lambda_{ref}, P_{in,\,ref}, P_{p,\,ref}, L_{ref}) \right] + \frac{L_{ref} - L) \cdot T(\lambda, \lambda_{ref})}{L_{ref}} \cdot \left[G^{dB}(\lambda_{ref}, P_{in,\,ref}, P_{p,\,ref}, L_{ref}) - G^{dB}(\lambda, P_{in,\,ref}, P_{p,\,ref}, L_{ref}) \right] \quad \text{Eq. 5.35}$$

where Eq. 5.35 is an expression equivalent to Eq. 5.34.

The characterisation of the gain G^{dB} (λ_{ref}, P_{in}, P_p, L) at the reference wavelength (λ_{ref}) can be done using the well known empirical expression [75, 76]

$$G(P_{in}, P_p, L) = \frac{G_0(P_p, L)}{1 + \left(\frac{P_{in}}{P_{sat}(P_p, L)} \right)^{a(P_p, L)}} \quad \text{Eq. 5.36}$$

where G_0 (small signal gain), P_{sat} (saturation power) and α are usually treated as fitting parameters. The values of G_0, P_{sat} and α depend on the input pump power and EDF fiber length (P_p, L). Once a set of representative experimental values are obtained, the value of $G_{dB}(\lambda_{ref}, Pin, P_p, L)$ at any arbitrary conditions can be obtained by interpolating $G_0(P_p, L)$, $P_{sat}(P_p, L)$ and $\alpha(P_p, L)$ and using Eq. 5.36. This is a similar procedure as the one proposed in [77] to include pump power dependency. While 1D interpolation is applied in [77], 2D interpolation is used to include EDF lengths dependencies.

Another mathematic expression of the total gain of the EDF is the following [78]

$$G = \Gamma_s \exp\left[\int_0^L \left(\sigma_s^e N_2 - \sigma_s^a N_1 \right) dz \right] \quad \text{Eq. 5.37}$$

where L is the length of the fiber, N_1 and N_2 are the population density in the level 1 and 2 as indicated already Γ_s is the confinement factor σ^e_s and σ^a_s are the signal emission and absorption cross-sections respectively.

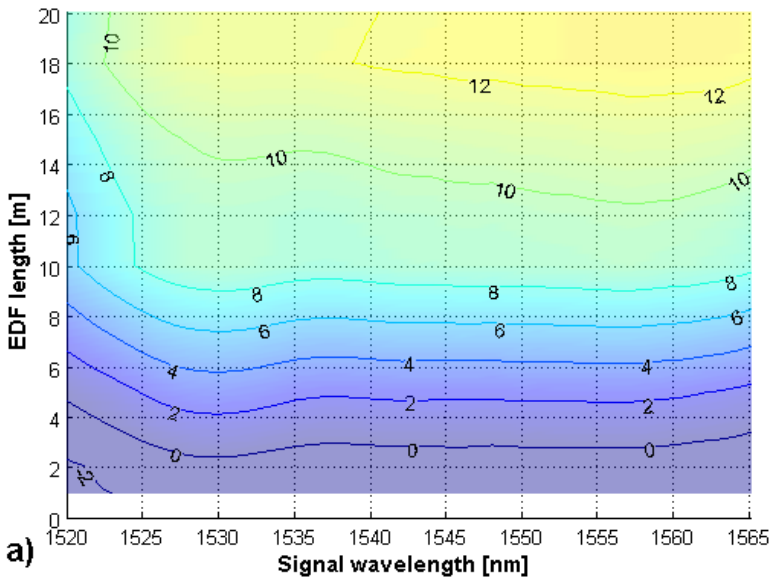

Fig.5.5. Signal gain variation for HE980, P_p -7dBm, as a function of EDF length and wavelength

The Fig.5.5 represents the signal gain variation, for a pump power of -7dBm and an EDF HE980. One can see the gain of the EDF as a function of the length and the signal wavelength.

The Fig. 5.6 demonstrates the saturation effect of the amplifier. For these cases, the efficiency of the amplification decreases for high input signal power, due to the saturation of the amplifier. In general, until the EDF reaches the saturation point, the lower the input signal power provided to the EDF is, the higher the signal gain. An exponential increase in the noise figure is achieved, when the amplification goes further into saturation. For an efficient amplification, one should not get further into the saturation mode as this causes lowering of the gain, higher pump consumption and higher degradation of the signal [79]

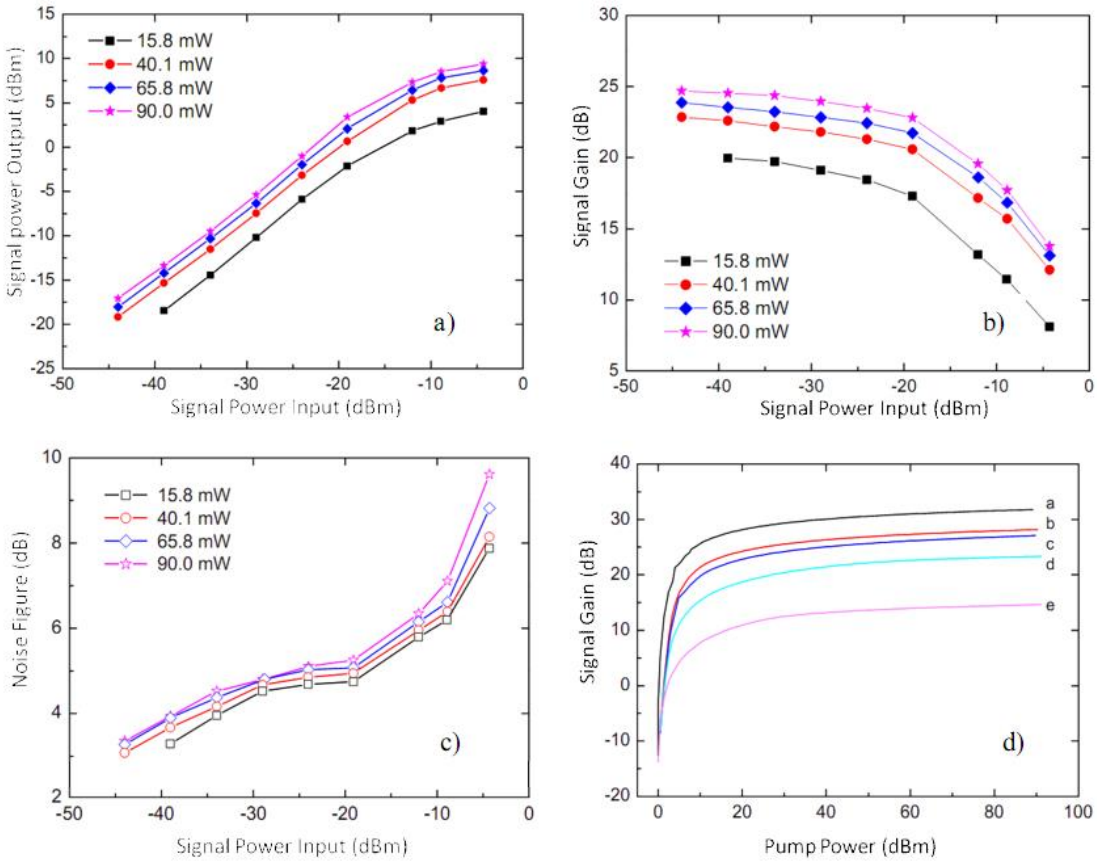

Fig. 5.6. a) Output signal power in function of the input signal power to various supplied pump power; b) Gain in function of the input signal power for different supplied pump power; c) Noise figure in function of the input signal power to various supplied pump power; d) Gain in function of the pump power to different values of signal input power [79]

As we will explain later on, the wavelength dependency of the EDFA gain can have a serious impact on the function of WDM/TDM PON using cascaded in-line EDFAs. As an effect by itself is neutral, can be used though to the benefit of the network, when the proper wavelength allocation is foreseen.

5.2 Theoretical approach of in-line amplification

5.2.1 General considerations

In-line EDF amplification refers to an alternative scenario of the original WDM/TDM PON (SARDANA), suggested in chapter 4, where the EDF is placed in the ring fibre rather than at the beginning of the distribution tree. Similar to the drop amplification case, in-line amplification can be constructed as part of the remote node by attaching the appropriate length of EDF before or after the add/drop filters. The pump distribution, carried over the upstream fibre is split accordingly, in order to provide the appropriate pump power level that in combination with the EDF length, offers the required gain.

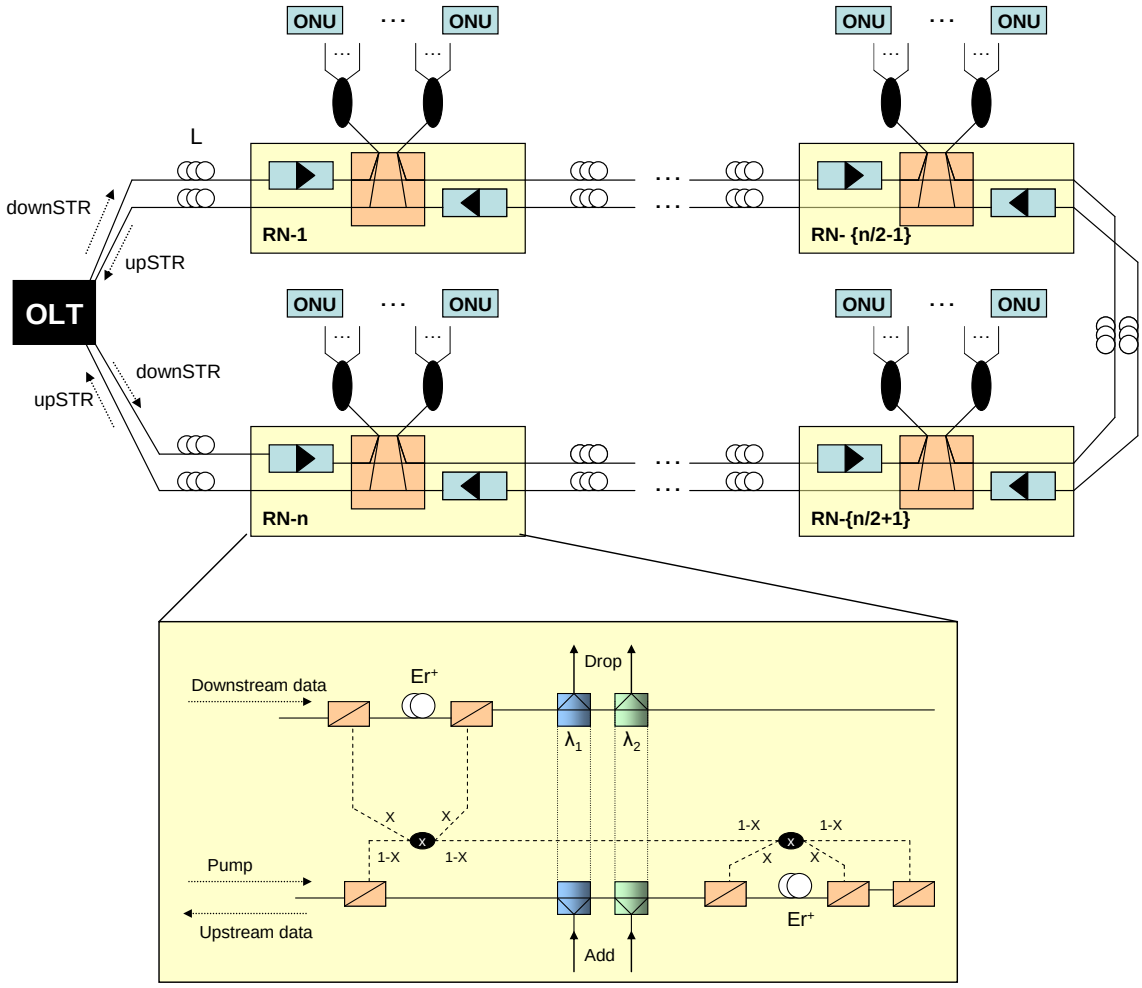

Fig. 5.7. Network architecture and Remote Node comprising in line remote amplification

The network set-up as well as the appropriate RN design are shown in the figure below.

The advantage of in-line amplification is that a small gain is only required in order to compensate the transmission and passive element losses of the intermediate distance between amplification stages. Therefore, in theory, all the signals can be kept on the appropriate level of signal power per channel with minimum requirements in terms of EDF length and portion of required pump power.

However, in practice, the fact that a group of wavelength channels require amplification, in combination with the wavelength dependent gain characteristics of EDF amplification in WDM channels, sets significant constrains in the design of the system. More specifically, the following limitations are observed:

- All the studied effects (gain, noise figure and OSNR) apply on WDM channels being amplified simultaneously. The wavelength dependent nature of EDF causes power variations due to unequal gain per wavelength.
- Any effects present in a system with in-line amplifiers must be studied for a cascade of amplification stages rather than single amplification per channel in the case of drop amplification. This reflects also in the design of such a system.
- The number of accumulated channels is not constant as channels are dropped or added in the system. This affects also the amount of gain received per channel.

These constraints complicate significantly both the design and the study of the network with in-line amplification. In general for the design of the downstream propagated signals, in-line amplification must provide a relative small gain in order only to compensate for the transmission losses and the losses of the passive elements. As the number of channels is reduced through a cascade of RNs, an even smaller total gain is required. Additionally, since the input power in the in-line amplifiers is strong and also the transmission losses are small, the added and accumulated noise level for the case of down stream propagation is expected to be limited, allowing good OSNR values at the ONU receivers. On the other hand, the high power levels per channels denote that the amplification operation will be performed in the saturation region of the EDF, where the obtained gain with respect to EDF length and pump is small.

The design of the upstream signals is totally different than that of downstream propagation. The main difference here is that the power level of the added channels is very small due to the losses in the distribution tree. This is expected to give a significant initial OSNR degradation. Moreover, the power level of the accumulated signals must be kept at relatively low levels so that we don’t have huge variation between the already added and amplified signals and those newly added at each RN. In this case, the pump and EDF length requirements are relaxed, since a good gain value can be achieved for low power signals that are away from the saturation region of the EDFA.

For the analysis of in-line amplification, the wavelength dependent nature of EDF is important to be considered. This depends on:

- the type of the EDF used
- the pump power
- the EDF length and
- the input wavelength channels and their power

In the following sub-sections first the simulation tool is described, providing its calculation capabilities as well as the common setting and parameters used. Based on this tool, an analysis on the wavelength and power dependent issues of amplification is given, with emphasis on the unequal gain per channel and the OSNR degradation effects.

The VPI simulation tool was used in order to estimate the effects of in-line amplification in a WDM signal. The analysis was based on the use of the test-amplifier module that among others it calculates the optical frequency/wavelength dependent gain, noise figure and OSNR per WDM channel. The analysis is performed by examining the input and output signals of each amplification stage.

5.2.2 Definitions and parameters used for the analysis

5.2.2.1 Input test signal

Since the main purpose of this study is to examine the gain and OSNR degradation of the signal and not other impairments, a simple WDM source was considered based on the generation of a comp of wavelength with certain wavelength position according to the ITU grid and power. In this case, each wavelength channel is considered to have all the power concentrated in a single frequency. The WDM comp source has been combined with a noise generation source that results in an initial OSNR of 40dB which is fixed for all cases.

5.2.2.2 Signal gain

The gain of the amplifier is calculated by the difference of the output signal power and the input signal power at each amplification stage.

$$G_i(dB) = P_{out,i}(dBm) - P_{in,i}(dBm) \qquad \forall i = amplification\ stage \qquad \text{Eq. 5.38}$$

Note: Each amplification stage includes the WDM coupler and splitter before and after the EDF fibre.

5.2.2.3 Giles parameters

A derivation of the Extended Black Box Model can be used, not only for providing an accurate description of the performance of EDFA, but as will be shown, for determining the cross sections in the form of Giles parameters of the studied EDFs. For the described Black Box Model, the Giles parameters depending on the emission and absorption cross sections, are given -as mentioned already- by the expressions found in [74]:

- $\alpha(\lambda)=\sigma_a(\lambda)N_{Er}$
- $\gamma(\lambda)=\sigma_e(\lambda)N_{Er}$

where $N_{Er}=\int dr_t n_{Er}(r_t) \left| \Psi(r_t) \right|^2$ represents the effective erbium concentration over the cross section of the fiber (r_t) overlapping with the signal propagation mode $\Psi(r_t)$

It can be demonstrated (publication pending) that the absorption Giles parameters, $\alpha(\lambda)$, can be determined by using the expression:

$$\alpha(\lambda) = \frac{1}{L_{ref}} \cdot \left[T(\lambda, \lambda_{ref}) \left[\ln\left(G\left(\lambda_{ref}, P_{in,ref}, P_{p,ref}, L_{ref} \right) \right) + \alpha_{ref} \cdot L_{ref} \right] - \ln\left(G\left(\lambda, P_{in,ref}, P_{p,ref}, L_{ref} \right) \right) \right] \quad \text{Eq. 5.39}$$

Once the absorption Giles parameters of the EDF are obtained, the emission Giles parameters can be determined as well, by using:

$$\gamma(\lambda) = T(\lambda, \lambda_{ref}) \cdot \left[\alpha_{ref} + \gamma_{ref} \right] - \alpha(\lambda) \quad \text{Eq. 5.40}$$

5.2.2.4 Excess noise power

The amplifier noise is the ultimate limiting factor for system applications [Agrawal, 2002]. The ASE noise, can be expressed by the following equation:

$$P_{ASE} = \mu \cdot [G_0 - 1] \cdot h \cdot \upsilon \cdot d\upsilon = \rho_{ASE} \cdot d\upsilon \quad \text{Eq. 5.41}$$

where ρ_{ASE} represents the ASE spectral density, that propagates in the same direction of the signal. The impact of ASE is quantified through the noise figure F_n given by $F_n = 2n_{sp.}$ The added noise power at the amplification stage is given by:

$$P_{ASE} = 2n_{sp} h\nu \cdot G \cdot \Delta\nu \quad \text{Eq. 5.42}$$

where n_{sp} is the spontaneous emission factor that depends on the relative populations N_1 and N_2 of the ground and excited states, hν the photon energy, G the amplifier gain and Δν the bandwidth over which the noise is calculated.

5.2.2.5 Optical signal to Noise ratio

OSNR is calculated at the output of the amplification stage by separately estimating the amplified channel power and the noise power. This is done by splitting the output signal in two components, i) the pure (parameterized) wavelength channel and ii) the remaining noise level within 100GHz around the signal integrated at 12.5GHz bandwidth. The ratio of these two values defines the OSNR parameter.

It is mentioned again that an initial OSNR value of 40dB is considered in all the examined cases.

5.2.2.6 Noise figure

The noise figure (NF) can be defined as the relation between the input SNR and the output SNR of the EDF [80]. Considering as the main limitation of the signal detection, the signal spontaneous noise power ($N_{S\text{-}SP}$), the noise figure can be calculated by the forward equation:

$$NF = \frac{P_{ASE}}{h\nu \Delta\nu G} \qquad \text{Eq. 5.43}$$

where P_{ASE} is the ASE power, hv is the energy of photon, Δv is the resolution bandwidth of the Optical Spectrum Analyzer (OSA) (0.1nm in the referenced case) and G is the gain of the EDF. Considering also the shot noise (N_{shot}) and the spontaneous-spontaneous noise ($N_{SP\text{-}SP}$) powers, the NF is calculated respectively with the equations:

$$NF = \frac{P_{ASE}}{h\nu \Delta\nu G} + \frac{1}{G} \qquad \text{Eq. 5.44}$$

$$NF = \frac{P_{ASE}}{h\nu \Delta\nu G} + \frac{1}{G} + \frac{P_{ASE}^2 (2B_0 - B_e) h\nu}{4(h\nu\Delta\nu)^2 G^2 P_{in}} \qquad \text{Eq. 5.45}$$

where B_0 is the optical bandwidth of the filter after the EDF, B_e the bandwidth of the electrical filter in the receiving circuit and P_{in} is the optical power at the input of the amplifier.

The analysis of noise figure is based on the electronic definition according to which the NF is related with the ratio of the input SNR_{in} over the output SNR_{out}. For this calculation with respect to optical noise and P_{ASE} the receiver characteristics must be considered and how this electronic circuit is affected by the noise factor. Assuming that the dominant contribution to the receiver noise comes from the beating of spontaneous emission with the signal and neglecting the contribution shot noise then the noise figure term can be simplified to the equation

$$NF = 2n_{sp} \frac{G-1}{G} \approx 2n_{sp} \qquad \text{Eq. 5.46}$$

Hence from the previous equation the following expression is derived:

$$NF = 10\log\left(\frac{1}{G}\left(\frac{P_{ASE}}{h\nu \Delta\nu}\right)\right) \qquad \text{Eq. 5.47}$$

This expression is according to the IEC 61280 definition on obtaining measurements for WDM systems spaced within the ITU grid and particularly applicable

in cases of cascaded EDFAs. The measurement bandwidth is defined again at 0.1nm (or 12.5GHz). The frequency ν refers to the operating wavelength or the central frequency of WDM channels.

5.2.2.7 Type of EDF

In all measurements the EDF type of fibre used was the HE980® fibre by Lucent-OFS. In Fig. 5.8 the gain spectrum and absorption is given. It is the most important feature of an EDFA as it determines the amplification of individual channels when a WDM signal

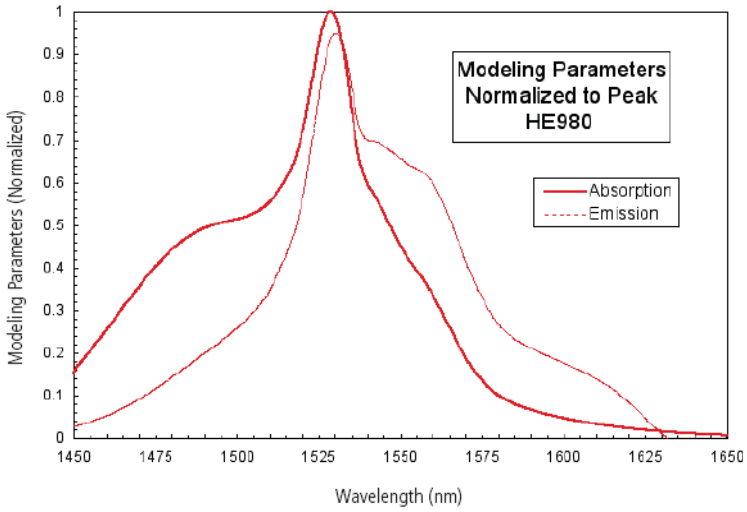

Fig.5.8. The parameters of the EDF type (Lucent Ofs HE980 ®) that was used in the simulation tool

is amplified.

The extracted Giles parameters (appearing in Table 5.1) were inserted in the EDF model of the VPI capable to emulate bidirectional signal propagation and amplification in doped fibers. The analytical model used, considers both the geometry of the fibre waveguide and the physical properties of the dopant ions determined by the Giles parameters. Since the gain and absorption properties in the model used for the studies presented here, is described using Giles parameters, very few additional parameters are required. This is because the measured gain and absorption per unit length in an actual fiber already include the effect of parameters such as the excited state lifetimes, and the details of how the optical field overlaps and interacts with the dopant ions. Both Giles parameters and additional fibre geometry related parameters have been provided by the manufacturer.

TABLE 5.1
Giles parameters for (Gain/Attenuation) for the EDF HE980 [OFS]

Wavelength (nm)	Gain (dB/m)	Attenuation (dB/m)
1400	0,00	0,00
1455	0,09	0,69
1480	0,61	1,88
1484	0,69	2,08
1510	1,56	2,43
1519	2,43	3,30
1528	4,00	4,34
1530	4,08	4,08
1534	3,26	3,21
1544	3,08	2,56
1559	2,78	1,48
1585	1,17	0,35
1614	0,52	0,13
1629	0,00	0,00
1656	0,00	0,00

5.2.3 Analysis of the expected OSNR degradation

5.2.3.1 Initial OSNR degradation after the 1st amplification stage

The first amplification stage in a cascade of amplifiers in a system is the one that determines the OSNR of the transmitted signal. According to the system design presented in the next chapter there two main cases that can be distinguished:

- In downstream signal propagation the initial WDM channels have sufficient power levels (0dBm per channel) at the output of the OLT. In this case, the signal attenuation between OLT and the first amplification stage as well as between the next amplification stages is relatively small. Additionally, the gain provided is also small since we are mainly interested in compensating for the losses in between amplification stages.

Therefore, the P_{ASE} contribution in the non-degraded (in terms of signal and noise power) input signal to the in-line amplifier is expected to be very small. Moreover since P_{ASE} depends on the achieved gain, its value will be also small.

- In upstream signal propagation the tributary wavelength channels initiated from ONUs are facing a strong attenuation within the distribution trees before being amplified by the in-line amplification stages in the ring.

Therefore, In this case the P_{ASE} contribution on the weak signal will be evident, causing an initial strong degradation through the first amplification stage.

Next an example is provided for both cases that proves this issue theoretically. The example is based on the actual values used in performance evaluation of the system and the target gain values required. In all cases an initial signal OSNR of 40dB is considered. Therefore, any comparison in terms of OSNR degradation must be made according to this initial value.

Assuming an initial $OSNR_{in} = S_{in}/N$ being amplified by the first in-line amplification stage with gain G, the output OSNR will be:

$$OSNR_{out} = \frac{S_{out}}{N_{out}} = \frac{GS_{in}}{GN + P_{ASE}} \Rightarrow OSNR_{out} = \frac{GS_{in}}{GN + 2n_{sp}h\nu \cdot G \cdot \Delta\nu} \qquad \text{Eq. 5.48}$$

5.2.3.1.1 Downstream OSNR degradation after 1st amplification stage

The power per channel of the signals being transmitted from the OLT is 0dB (1mW). With an initial OSNR of 40dB defined at 12.5GHz bandwidth, the noise power within the same bandwidth is N=1e-7 W.

According to the results that are presented in the next chapter, the first in-line amplification stage provides a gain of 7dB with a noise figure of 6dB. Assuming that the term $2n_{sp}$ is defined by the NF, and calculating the output OSNR from the last equation (for a channel frequency of 193.1THz, h=6.6261e-34 the Planck's constant, and BW=12.5GHz) we obtain: $OSNR_{out}$=39.7dB.

Therefore it is evident that in the case of downstream propagated signals, the OSNR degradation with respect to the initial transmitted signal OSNR (40dB) is only 0.3dB. If a pure initial signal is assumed with infinite OSNR (i.e. N=0) then the output OSNR of the first in-line amplification stage is $OSNR_{out}$ = 51.9dB. This value defines the absolute OSNR degradation due to the ASE noise in the amplifier. As the initial OSNR value of the transmitted channels is closer to this value then P_{ASE} becomes a more dominant factor and the OSNR degradation will increase.

5.2.3.1.2 Upstream OSNR degradation after 1st amplification stage

The power per channel of the signals being transmitted from the ONUs is 0dB (1mW) but due to the tree losses these signals are entering the in-line amplification stage with -20dBm (10uW). With an initial OSNR of 40dB defined at 12.5GHz bandwidth, the noise power within the same bandwidth is N=1e-9 W.

According to the design parameters for upstream signal a small gain is only provided at each RN in order to compensate for losses. An average value of 3dB gain

can be considered in this case. The noise figure increases compared to the downstream case and can be up to 7dB. Again the term $2n_{sp}$ is assumed to be defined by the NF; actually for low gain values a more accurate formula to use is $NF=2n_{sp}(G-1)/G$ from which $2n_{sp}$ is calculated. Finally, the output OSNR from the last equation (for a channel frequency of 193.1THz, h=6.6261e-34 the Planck's constant, and Δv=12.5GHz) is: $OSNR_{out}$=27.7dB.

Therefore, in the case of downstream propagated signals, the OSNR degradation with respect to the initial transmitted signal OSNR (40dB) increases significantly by 12.3dB. If a pure initial signal is assumed with infinite OSNR (i.e. N=0) then the output OSNR of the first in-line amplification stage is $OSNR_{out}$ = 27.8dB. This shows that the generated ASE noise is a dominant factor and affects significantly the output OSNR almost independently of the quality of the initial signal

5.2.3.2 OSNR degradation in a cascade of in-line amplifiers

For this case we assume that any additional in-line amplification systems do not provide extra gain in the signal but simply compensate for the losses between the amplification stages. On contrary ASE noise is accumulated. Therefore the signal power S and P_{ASE} after the i^{th} amplifier and compared to the $(i-1)^{th}$ amplifier can be expressed as:

$$\begin{aligned} P_{S,i} &= P_{S,i-1} = P_S \\ P_{ASE,i} &= P_{ASE,i-1} + 2n_{sp}h\nu G_i\,\Delta\nu \end{aligned} \qquad \text{Eq. 5.49}$$

Therefore the OSNR at the end of the i^{th} section is:

$$\frac{1}{OSNR_i} = \frac{1}{OSNR_{i-1}} + \frac{2n_{sp}h\nu G_i\,\Delta\nu}{P_S} \qquad \text{Eq. 5.50}$$

And after a cascade through N amplification stages this becomes:

$$\frac{1}{OSNR_N} = \frac{1}{OSNR_0} + \frac{\sum_{i=1}^{N} 2n_{sp}h\nu G_i\,\Delta\nu}{P_S} \qquad \text{Eq. 5.51}$$

where $OSNR_0$ is the initial OSNR of the transmitted signal.
Extending the example presented above for the case of a cascade of in-line amplifiers we can distinguish again the two cases of down- and up-stream propagation.

5.2.3.2.1 Downstream OSNR degradation through a cascade of in-line amplifiers

In this case the degradation term of $(P_s/2n_{sp}\cdot h\nu\cdot G\cdot\Delta\nu)$, has a very small contribution as it was calculated for the initial OSNR degradation. Additionally, P_s is assumed constant

and the gain G is relevant small (and even smaller than before) since it has to compensate for the limited losses in the system.

5.2.3.2.2 Upstream OSNR degradation through a cascade of in-line amplifiers

For upstream signals the term ($P_s/2n_{sp}\cdot hv\cdot G\cdot \Delta v$) is the dominant factor of degradation and affects significantly the output OSNR particularly in the first in-line amplification stages. As the OSNR value degrades after a cascade of amplifiers, the effect of ASE is also reduced since it is much larger than the degraded OSNR of the signal

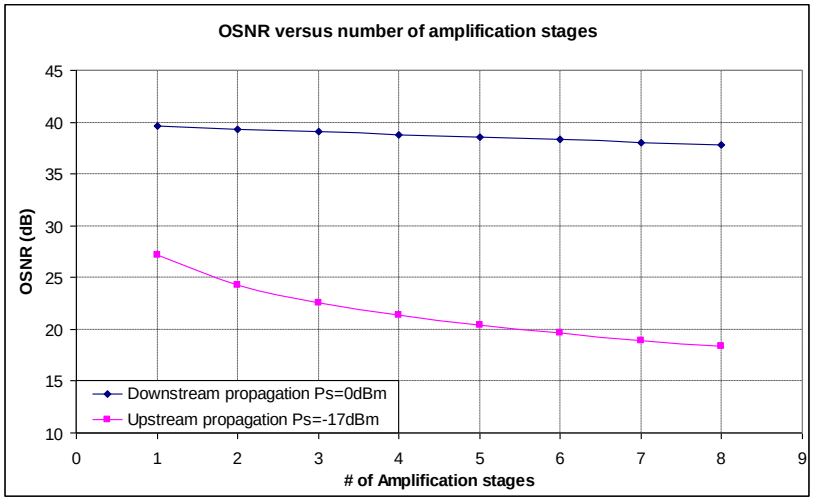

Fig. 5.9. OSNR degradation through a cascade of in-line amplification stages for the case of down- and upstream transmission with different characteristics

Table 5.2 Characteristics of up- and downstream transmission

Downstream Propagation
Ps = 7dBm (0.005mw)
G = 7dB
NF = 6dB
Upstream Propagation
Ps = -17dBm (20uW)
G = 3dB
NF = 7dB

The value of the accumulated OSNR for the two cases of downstream and upstream transmission is shown in Fig.5.9 and calculated based on the last equation for up to 8 accumulated in-line amplification stages. For both cases constant values of output power, gain and noise figure were considered in the calculations. These values are shown in the Table II, separately for each case.

From this figure it observed that for the downstream transmission where the signal power is preserved at high levels, the OSNR degradation is particularly small. A maximum OSNR penalty of 2.15dB (with respect to the initial OSNR value of 40dB) is achieved after 8 cascades. On the other hand the OSNR degradation is much more pronounced for the case of upstream propagation where the amplified signal levels are small. In this later case OSNR degrades rapidly within the first amplification stages and

tends to be stabilized for a larger number of stages. The maximum OSNR degradation is 21.62dB.

It should be noted that what is depicted in the figure above is theoretical approach that shows the trend on OSNR degradation for different parameters. However, in the system design that will be presented next the parameters of P_s, G and Noise figure are not constant for all RNs. This is because the pump is distributed from the OLT and therefore the amplification characteristics are changing through consecutive amplification stages. The values of gain and noise figure in remotely located nodes from the OLT are smaller as less pump power is available. As these values drop the OSNR degradation ratio is also improved. Comparing the theoretical results presented here with those in section 3 for the emulated in-line amplification system one may observe a perfect matching with respect to the initial OSNR degradation through the 1st amplification stage. However for the cascaded effect there is a small deviation from the theoretical values due to the reasons explained above.

5.3 Remote amplification approaches and design characteristics

5.3.1 Network design approach

As already mentioned, remote amplification is used in order to increase the power budget of the network, thus the volume of end users. The earlier proposed solution [3] has considered the use of remotely pumped EDFs in the drop part of the RN, after the wavelength channels distributed to the trees, are selected by the RNs. In this solution, the appropriate portion of the remotely distributed pump was extracted, in order to offer the required amplification in each RN. The main problem of this approach is that the RNs located further away from the OLT, require higher portions of the pump compared to the closely located ones, since the signal experiences larger attenuation due to propagation losses and passive losses in RNs. However, the pump power also attenuates significantly and therefore it is difficult to achieve the appropriate pump power levels for the distant RNs, unless high pump power lasers (offering several Watts) are used in the OLT.

In the study presented here an alternative design approach is considered, able to offer remote amplification by the use of in line amplification implemented in the interior of the RN and affecting directly the WDM signals rather than the individually selected signals after the RN. The target in this case is to offer the minimum possible amplification required to maintain the power of the signals as they propagate in the rings towards the more remotely located RNs.

In order to examine the amplification requirements of the network, the first critical issue is to evaluate the losses in the optical path between OLT and ONU. There are three main parts of the network that introduce losses, namely the transmission part (fibre), the add/drop module with the RN, and the distribution tree. This deployment, considers a total number of 16RNs each one of which drops 2wavelengths (32

wavelengths in total). The dropped wavelengths are split to 32 users (ONUs) resulting in a total of 32x32=1024 end users. The area is considered a densely populated one, therefore the distance between the RNs is considered small and it is set to 1km. The distribution tree at each RN spans to a maximum distance of 3km. Considering the total passive losses of the network, it is evident that these depend mainly on the high splitting ratio at the distribution trees and less on the fibre losses. According to the system design though, there are additional passive losses from the elements used in the network (WDM couplers, add/drop filters) as well as the splicing losses. According to the identified network parameters, the following design issues have been taken into consideration, for the practical implementation of in-line amplification.

First, in-line amplification stages have been placed in the network according to the normal (non-resilient) operation. This means that all even channels are handled by RN_1 to RN_8 and all odd channels are handled by RN_9 to RN_{16}. Therefore $RN_{1\text{-}8}$ show absolute symmetry with nodes $RN_{16\text{-}9}$ it terms of amplification stages, position, Erbium length and pump splitting factors. In the case of resiliency (and considering the worst case scenario), the signals will have to propagate through a maximum number of 16 RNs.

Second, optimization of the design parameters (wavelength allocation per RN, EDF length, and pump splitting ratio) have been performed for the worst case scenario of resiliency considering that the link between the last node and the OLT is down and that the signals have to propagate all the way to the OLT in the opposite direction. Since operation for the resiliency case can be guaranteed, then under normal operation, this is also guaranteed. However, with this approach the design requirements are stricter especially in terms of required resources (e.g. maximum pump power).

Third, other effects like non-linearities and dispersion limitations are not considered, although in practice are very important in order to identify not only the receiver's optimum input power level but also the required OSNR. In our studies, we tried not only to provide the appropriate gain that compensates for losses, but also to not exceed certain power limits that may trigger strong non-linear effects.

In all cases, the initial signals (either down- or up stream) are considered to have an initial OSNR value of 40dB. This is because noise sources exist in both ends of the system for the generated signals, i.e. a booster amplifier at the OLT and an RSOA at the ONU.

Another design issue relates with the allocation of the wavelength channels per RN. Considering the case of 32 wavelength channels and 100GHz spacing, the wavelength channels are split into two groups of odd and even channels with 200GHz spacing and these are distributed to the first 8 and last 8 RN respectively. Therefore for example, for a set of 32 wavelengths ranging between 192.0THz and 195.1THz the subset of the 16 wavelengths [192.0, 192.2, 192.4, …, 195.0](THz) is allocated to $RN_{1\text{-}8}$ and the subset of the other 16 wavelengths [192.1, 192.3, 192.5, …, 195.1](THz) is allocated to $RN_{16\text{-}9}$.

If it is assumed that all wavelengths receive the same gain through the amplification stages, then these can be freely allocated in any groups of two to any RN. However, in order to achieve this in practice, an optimum design is required with controllable pumps per in-line amplification stage. Now that the pump signal is centrally distributed, an optimum design per in-line amplifier is hard to be achieved. In our case, the system must be optimized as a whole so that we can have the total optimum operation for all amplifiers. Additionally, we must show a conservative approach on the use of pump so that the pump power to be adequately distributed to all amplification stages.

Non-optimum design per in-line amplifier -in terms of pump and EDF length- will result in unequal gain per wavelength. More specifically, longer EDF lengths for given pump powers, may provide more gain at lower frequencies rather than higher ones. If we reduce the EDF length then the gain is almost equalized for the different channels but it is small in order to compensate for losses. If we increase the pump (by increasing the splitting ratio) then we will be able to have more gain for all the channels but not enough pump power for the distant nodes to compensate losses, particularly in the case of resiliency where 16 RNs must be supported. Therefore, in practice, in order to compromise between gain per channel and available pump power, a more advanced approach must be considered, with optimum allocation of the channels per RN. In the non-optimum design a strong gain tilt will be observed after a cascade through a number of amplifiers.

The main purpose in an optimum design is to consider the worst case of resiliency and reserve those wavelengths that can have more gain, for the distant nodes. As the pump power fades out over longer distances, these wavelength channels that have received more gain in the previous stages, will be able to reach longer distances. Since this effect is evident for low frequencies, these must be allocated to the more distant RNs in the resiliency case which are RN_1 and RN_{16}, if we consider that the RN_1

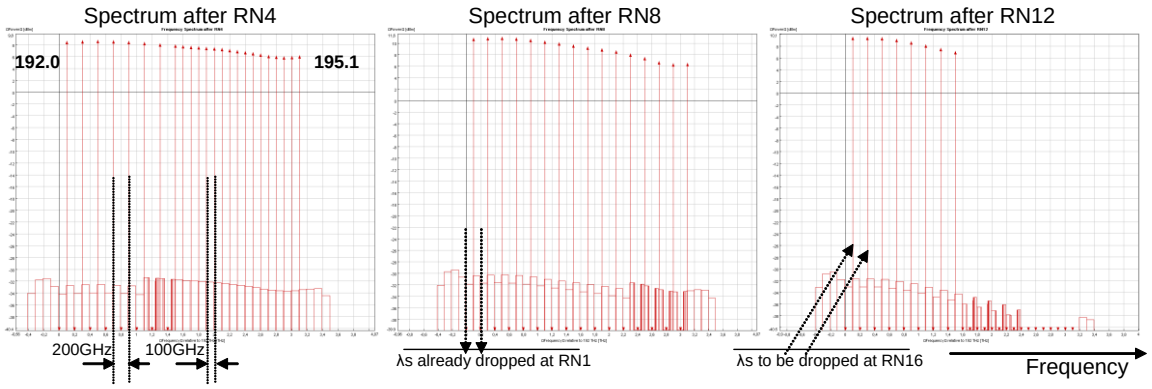

Fig.5.10 The RN design with in-line amplification at the down- and up-stream fibres indicating the main loss elements

to OLT or RN_{16}, to OLT connections respectively, are down. The effect of unequal gain per wavelength and according to optimum wavelength allocation scheme that is considered, is depicted in the example shown in Fig.5.10, for the case of downstream

propagation under resilient operation. The set-up details appear in a subsequent subsection.

5.3.2 RN design approach

As far as the RN is concerned, its design in this approach is implemented with two fixed filters that are used to drop the signals. The EDF is placed between the two drop filters and before the 50/50 splitter as shown in Fig. 5.11. The 50/50 splitters are used for resiliency in case of a fiber cut. The two predetermined wavelengths are dropped in each RN. Each wavelength is then driven to a tree. This of course creates the need to transmit in the downstream direction a signal with adequate power to reach the first tree (served by RN_1 in normal operation or RN_N when operating in resiliency mode in the case of a fiber cut between the OLT and RN_1) as the drop signal of the first tree in this design will not be amplified.

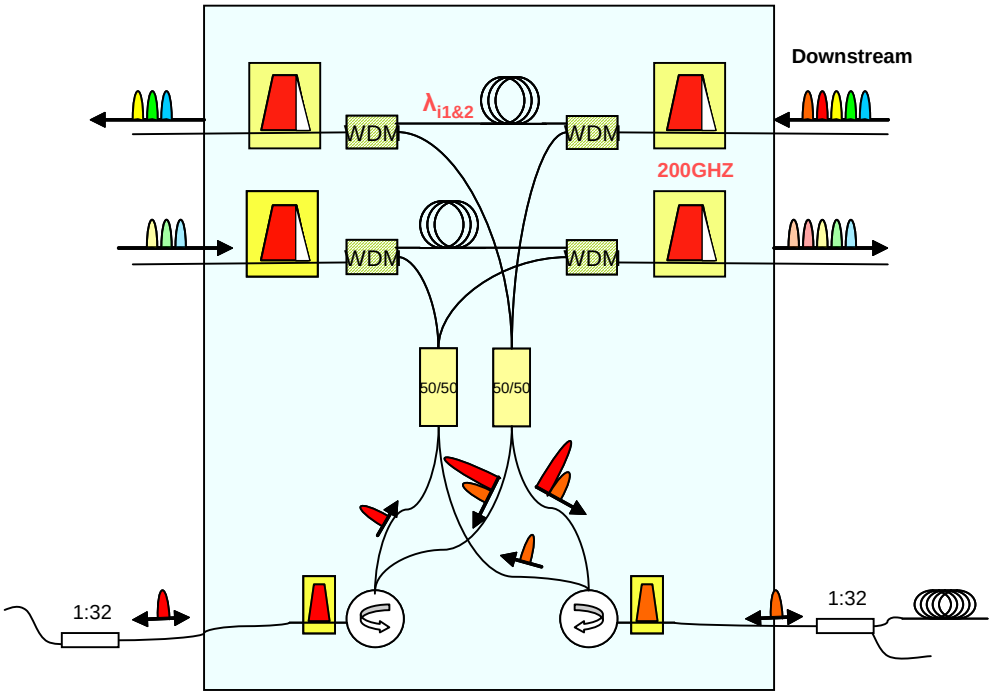

Fig. 5.11 RN design used for in-line amplification

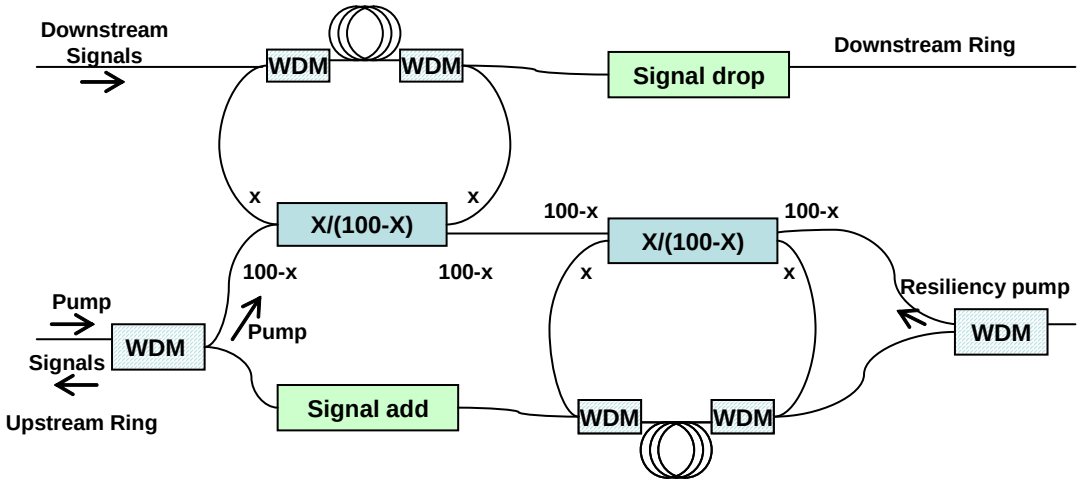

Fig. 5.12. Pump distribution scheme

The pump laser's emission power is predetermined in order to comply with safety regulations. The upstream signals' power is predetermined by the ONU's specifications and so is the receiver's sensitivity in both the ONU and the OLT.

Pump power, which counter propagates with the upstream signal, is distributed in each RN to be used in amplification of the downstream as well as the upstream propagating signals. The distribution is implemented by tap couplers with different percentages in each RN which select a portion of the pump for the EDF amplifying the downstream signals, and a portion for the EDF amplifying the upstream signals. The portion of the pump power used for the upstream is fixed. As far as the downstream propagation is concerned, the power required was determined by the need of each RN for amplification. The gain required, along with the dispensable pump power are the determining factors for the length of the EDF. Nevertheless, the gain provided to the signals by some RNs, makes it possible to surpass a number of them (RNs), while propagating towards the tree they are designed to be dropped, without the need of amplification. Therefore, some RNs don't contain an EDF in the downstream ring. On the contrary, in the upstream fibre ring, the in-line EDFs have the same length and are required in every RN.

In case of resiliency, there is another WDM coupler that operates similarly but from the opposite direction of the RN. This implementation of the pump distribution is depicted schematically in Fig. 3. When designing the network a conservative approach was considered on the use of the pump so as to be adequately distributed to all amplification stages.

5.3.3 Design emulation set up and parameters

In order to investigate the described design, we have considered a number of parameters, which are presented below.

The network consists of 16 RNs with 1km distance among them. The tree fiber length is equal to 3km. Therefore the ring size is 17 km and the maximum distance

between the OLT and an end user is 19km. The OLT transmits 32 wavelengths in the C band.

As far as the downstream transmission in concerned the OLT output is considered equal to 10dBm per channel. This power level could cause non linear effects during propagation, but the fact that the distances between the RNs as well as the tree fiber length are relatively small prevents the appearance of non-linearities. In the case of upstream transmission the ONU output is equal to 0dBm while the OLT input level is considered -28dBm. In RSOA based ONUs the input power required to achieve adequate performance and output power at 0dBm is considered -20dBm. The pump power is set to 31dBm.

The 32 aforementioned wavelength channels have 100GHz spacing and range within the C-band from 192THz-195.1THz. In order to achieve the same gain through the amplification stages for all wavelengths, an optimum design per RN and per in-line amplifier is required. The main purpose in an optimum design is to consider the worst case of resiliency and reserve those wavelengths that can have more gain for the distant nodes. The gain of the EDF is not flat for all frequencies. On the contrary it exhibits a gain tilt which favors some wavelengths in terms of gain received as can be seen in Fig. 5.8. As the pump power fades out over longer distances, these wavelength channels that have received more gain in the previous stages, as stated in the network design section, will be able to reach longer distances. Since this effect is evident in low frequencies, these are allocated to the more distant RNs in the resiliency case, which are RN_1 and RN_{16}, if it is considered that the RN_1 to OLT or RN_{16} to OLT connections respectively are down. The wavelength allocation used in the simulation set up, is the one appearing in Table 5.3.

Table 5.3 Frequency allocation

RN	1	2	3	4	5	6	7	8	9	10	11	12	13	14	15	16
f_1	192	192.4	192.8	193.2	193.6	194	194.4	194.8	195	194.6	194.2	193.8	193.4	193	192.6	192.2
f_2	192.1	192.5	192.9	193.3	193.7	194.1	194.5	194.9	195.1	194.7	194.3	193.9	193.5	193.1	192.7	192.3

In-line amplification stages were placed in the network according to the normal operation, meaning that the channels with the lower frequencies were handled by RN_1 & RN_{16}, RN_2 &RN_{15} handle the sequential, RN_3 & RN_{14} the next ones and so on. Therefore RN_1-RN_8 present a symmetry with nodes RN_{16}-RN_9 when referring to the downstream fibre ring in terms of amplification stages, EDF length, dedicated percentage of pump power and gain tilt.

The upstream fibre ring as already mentioned is equipped with the same length of EDF in every RN which depends on its OSNR performance and is in this case 2.2m.
As aforementioned the tree fiber has a 3km length. Considering the total passive losses of the network it is evident that these depend mainly on the splitting ratio at the distribution trees and less on the fibre losses. Therefore, in order to comply with the given values for transmitter-receiver power levels, the splitting ratio was set in 1:32 for each tree, which results in 1024 customers served.

The total losses considered at the RN are the losses of the filter, the WDM coupler, the 50/50 coupler, and the circulator. Their sum is 4.6dB.

5.3.3.1 Downstream scenario and set up

Each of the shaded areas represents a different RN starting from the first one on the upper left corner and ending on RN_{16} on the lower right corner. The schematic shown here actually represents the worst case scenario of full resiliency, in which all the 32 wavelengths with 100GHz channel spacing are propagating towards the same direction and the last pair drops at RN_{16}. In normal operation the same exactly set-up was used, up to RN_8 though and using the 16 of the 32 wavelengths with channel spacing of 200GHz.

The dashed circles in the schematic represent the positions of the in-line amplification stages. As it is observed, in-line amplification is not performed at every stage (Only RN1,4,7,10,13,16 have amplification). This is done because when optimizing the system for the worst case scenario it was shown that the signal level can be increased significantly allowing its transmission over a cascade of additional two nodes before amplification is again required; more details are given in the next subsection.

It is important to mention that the elimination of in-line amplification stages is allowed because the transmission losses are low between RNs (i.e. 1km of fibre + passive component losses). Alternatively, we have tried to have in-line amplification at every node using a very small percentage of the distributed pump and/or short EDF

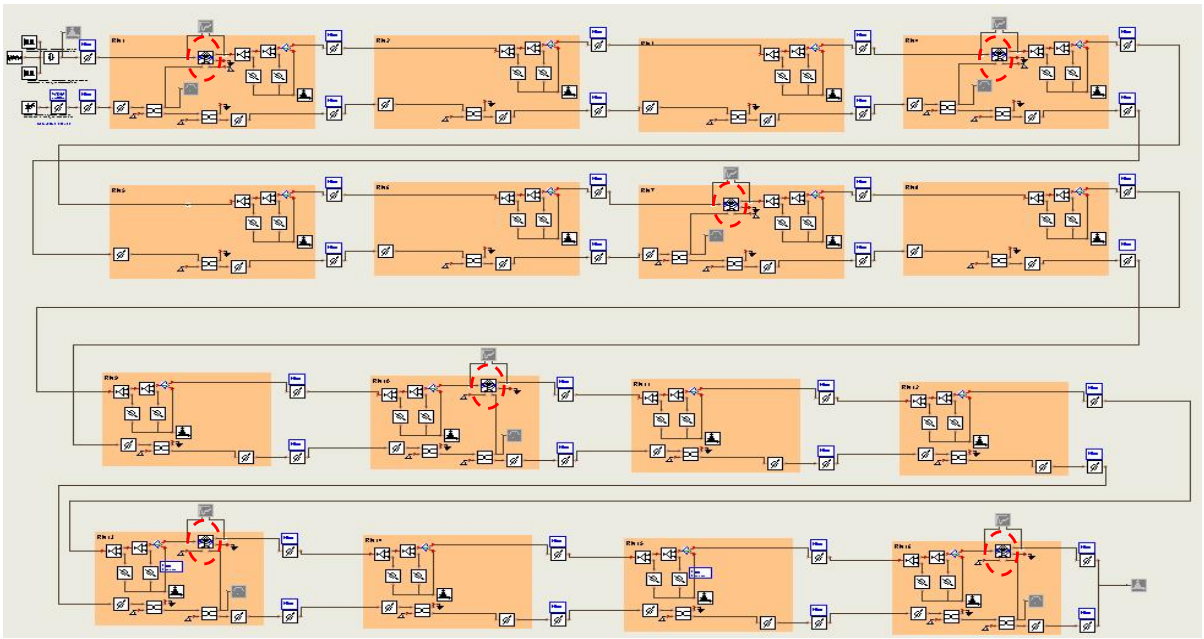

Fig. 5.13 Schematic of the network design for the case of downstream propagation under resilient mode. For normal operation the first 8 RNs are only used.

length. However, in this case, it was observed that due to the slightly unequal gain per channel obtained at each amplification stage, the cascade of in-line amplifiers was

resulting in a strong gain spectrum tilt in the more distant nodes. More specifically, this gives rise in the power of low frequency channels which prevents the large frequency channels to be amplified and reach the appropriate power level for correct reception at the ONU.

At each RN shown in the figure above, the upper link has an in-line amplifier (if this is required) followed by two drop filters centred at the wavelength of the drop channels. The lower link represents the pump distribution and contains the WDM splitters/couplers for the pump and the tap couplers that distribute the pump to both the down-stream and upstream directions.

The design was built following the rule about network symmetry. Therefore, for example the pairs of [RN_1, RN_{16}], [RN_2, RN_{15}], [RN_3, RN_{14}], … have exactly the same characteristics (splitting ratios and EDF length). In this case and under normal operation, the results obtained for the propagation through RN_1 to RN_8 will be the same as that from RN_{16} to RN_9; actually the only difference is that the wavelength channels in the last 8 RNs are shifted by 100GHz with respect to the first 8 RNs. Additionally, the internal design of the last 8 RNs, is symmetrical with respect to the first 8 RNs and therefore, the in-line amplification stage appears after the drop filters. This is true for the resiliency case, as after RN_8 the signals are propagating in the opposite logical direction compared to the propagation in the first 8 RNs.

Table 5.4. contains the optimum values of coupling factor and EDF length used in this set-up. The third column shows also the corresponding value of the pump power that is injected in the in-line amplification stages.

Table 5.4. Design parameters for the case of downstream scenario

#RN	Coupling factor	Optimal EDF Length [m]	Pump Power[dBm]
1	0.9	6	28.05
2	0	0	0
3	0	0	0
4	0.9	5	23.37
5	0	0	0
6	0	0	0
7	0.5	6	25.679
8	0	0	0
9	0	0	0
10	0.5	6	17.989
11	0	0	0
12	0	0	0
13	0.9	5	3.766
14	0	0	0
15	0	0	0
16	0.9	6	-3.925

5.3.3.2 Upstream scenario and set up

In the upstream propagation through the SARDANA ring, the added wavelength channels from each RN are propagating towards the OLT in the same fibre as the pump signal, but in a counter propagation mode. The critical difference between upstream and downstream propagation in terms of the amplification stage design, is that the added upstream channels are facing large losses through the distribution tree and when they are added in the ring fibre, their power level is less that -20dBm. Since this power level is away from the saturation region of the in-line amplifier, adequate gain can be provided in the expense of OSNR degradation. Therefore, the choice on the EDF length and the portion of the injected pump is critical in order to keep noise at moderate levels. The following figure provides the schematic used to emulate the performance of the upstream signal propagation. The schematic refers to the worst case of operation, under resilient mode, when all added channels propagate through the same direction upwards to the OLT. The position of the RNs are in reverse order with respect to the downstream scenario and therefore RN_1 is the one on the lower right corner of Fig.5.14 (followed by the OLT receiver) and RN_{16} is the one on the upper left corner.

The general design rule about symmetry is also implemented in this set-up and is observed between the first 8 and the last 8 RNs. At each RN, the upper link represents the signal propagation and the lower links the pump distribution system. Although pump and signal are propagated over the same fibre, within each RN these two are split and handled differently. Therefore, in terms of total passive losses, the upstream signals -when compared to the passive losses of downstream signals- are facing the additional loss from two WDM couplers, used to separate and recombine the counter propagated pump at each RN. Above each RN, is a system that distributes the appropriate wavelength channels pairs in the RNs.

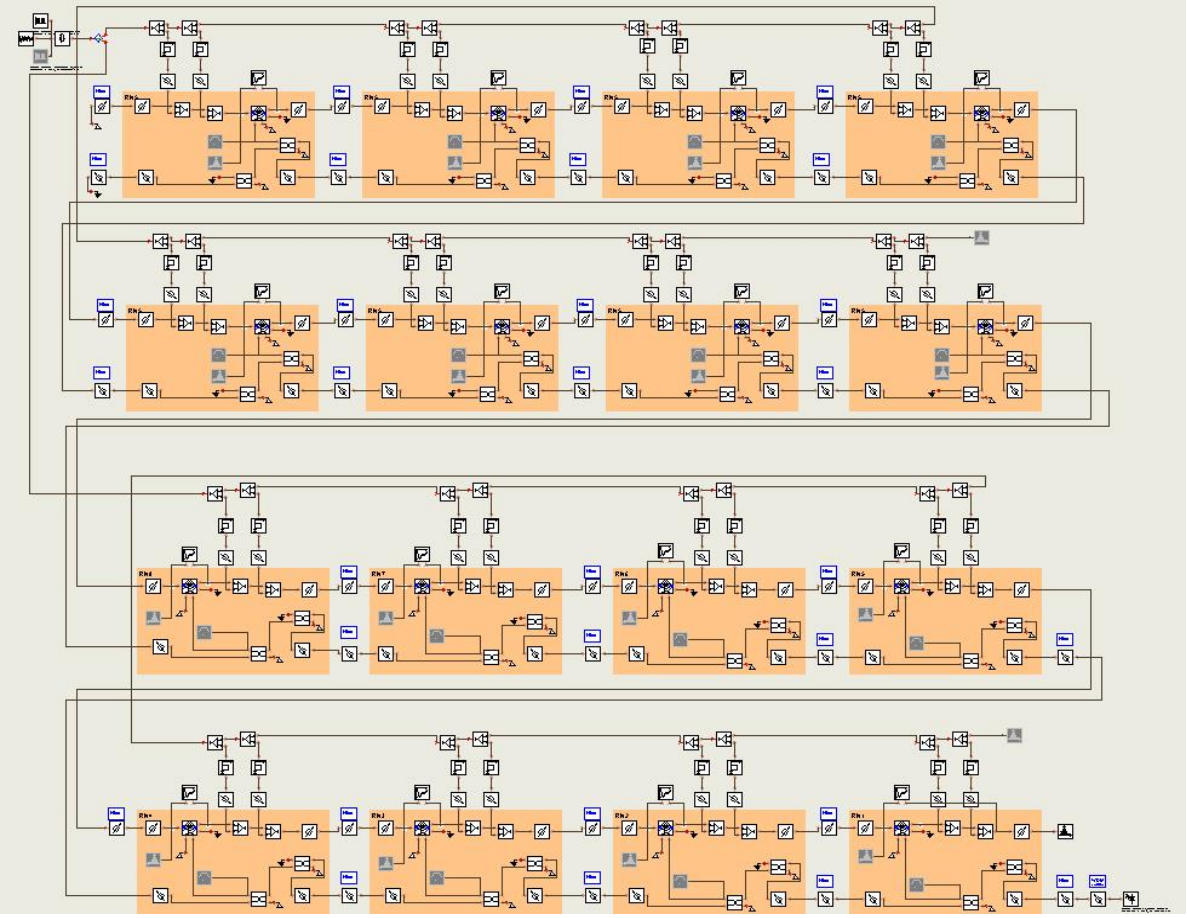

Fig. 5.14 Schematic of the network design for the case of upstream propagation under resilient mode. For normal operation the last 8 RNs are only used.

In this figure, it is observed that in-line amplification stages have been added at each RN. From the system performance point of view, this approach is mandatory, since we should not allow the already weak added channels to loose extra power. This would affect their OSNR performance. On the other hand, the provided gain must be kept low, by using small coupling ratios for the pump and small EDF lengths, so that all channels have almost the same power level after there are added and cascaded in the ring. If this is not guarantied, then any added signal with low power will be buried inside the noise level of the already added and cascaded channels with large powers. In the case of upstream propagation under normal (non-resilient) mode, the last 8 RNs (i.e. RN_8 to RN_1) in the schematic are only used.

Table 5.5 contains the optimum values of coupling factor and EDF length used in this set-up. It is observed, that coupling factors and EDF length parameters are much lower that what was used in the downstream signals.

#RN	**Table 5.5.** Design parameters for the case of upstream scenario		
	Coupling factor	**Optimal EDF Length [m]**	**Pump Power[dBm]**
1	0.95	1.2	24.582
2	0.95	1.2	23.405
3	0.95	1.2	22.228
4	0.95	1.2	20.598
5	0.95	1.2	19.42
6	0.9	1.2	21.254
7	0.95	1.2	13.825
8	0.95	1.2	12.648
9	0.95	1.2	11.726
10	0.95	1.2	10.548
11	0.9	1.2	9.376
12	0.95	1.2	4.954
13	0.95	1.2	3.776
14	0.95	1.2	2.146
15	0.95	1.2	0.969
16	0.95	1.2	-0.208

5.4 Evaluation of the design solution

The study performed, shows that the described architecture can serve 1024 end users with several hundreds of symmetric data rate in a maximum distance of 19km. More

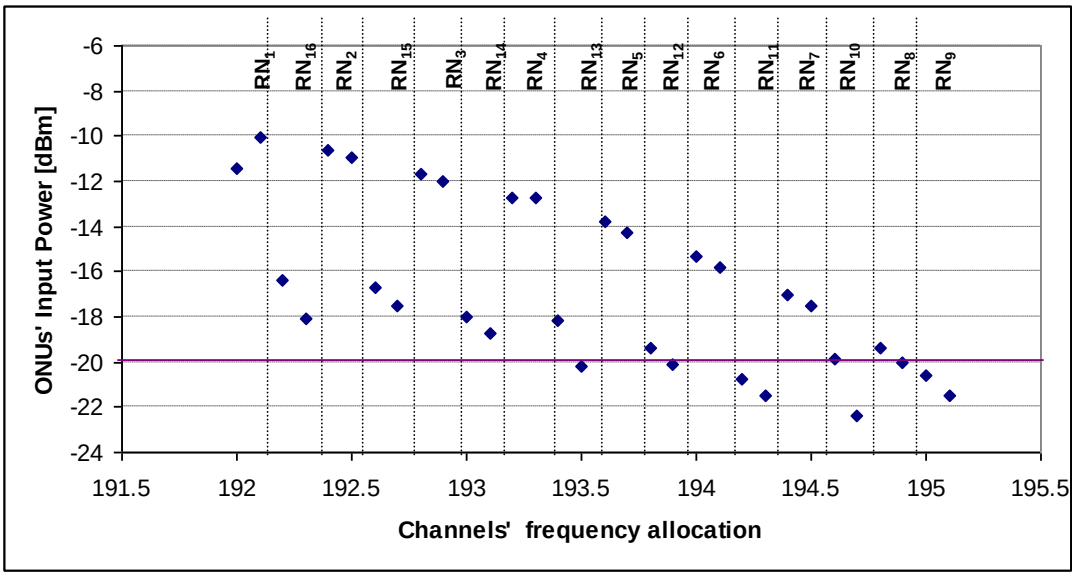

Fig. 5.15 Optical power of downstream signals when reaching the ONU

specifically, for downstream transmission, we observe that when operating in normal mode, all the ONUs are reached with a signal power higher than -20dBm. That means

that all ONUs used, could be based on RSOAs. The ONUs of the trees served by $RN_{1,}$ RN_2, RN_3, $RN_{4,}$ $RN_{5,}$ $RN_{6,}$ RN_7, RN_8, RN_{12}, RN_{13}, RN_{14}, RN_{15} , RN_{16} are reached with a signal higher than -20dBm, therefore RSOAs would be efficient in these cases in every operation mode (normal or resilient mode). In case of resiliency operation though, the signal can be received by standard GPON APD receivers in the ONUs served by $RN_{9,}$ RN_{11} and one of the trees of $RN_{10.}$

The upstream operation of the network is ensured in normal as well as in every case of resiliency operation. The reason is that the signal power level reaching the OLT (all frequencies considered) is above -28dBm which is the OLT receiver's sensitivity. The results for downstream and upstream signals are depicted in Fig. 5.15 and Fig. 5.16. respectively.

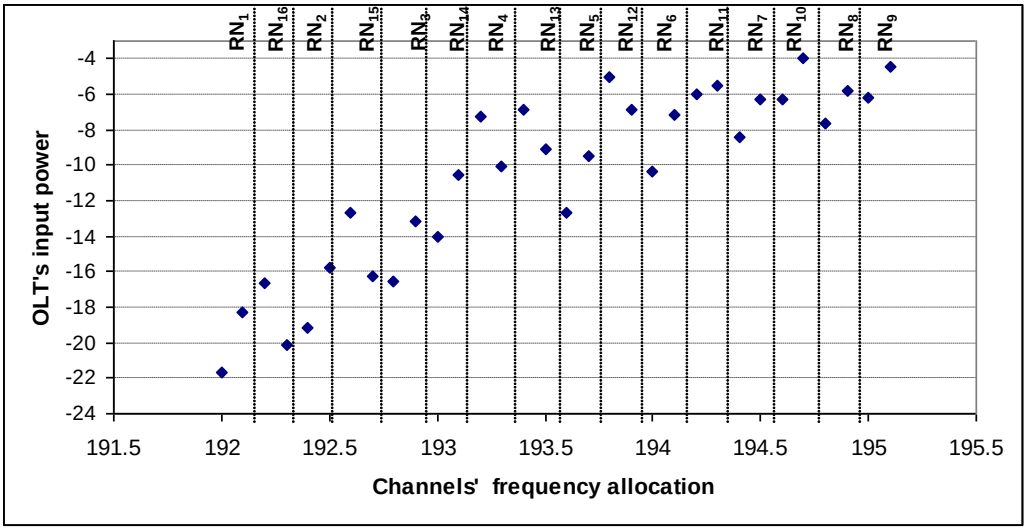

Fig. 5.16. Optical power of upstream signals when reaching the OLT receiver

As can be observed the trees connected to $RN_{9,}$ RN11 and one of the trees served by RN_{10} in the worst case of a fiber cut (thus a fiber cut between either the OLT and RN_1 or the OLT and RN_{16}) are reached by signals with power levels lower than the required for the operative use of an RSOA as a receiver/transmitter in the end part of the network.

The lower power level for the upstream signals that reaches the OLT's receiver is -21.64dBm that comes from the RN with the smaller distance from the OLT. The reason for that is that this signal doesn't acquire any gain as it doesn't pass through any amplification stage. A better performance of the network could be achieved with a smaller splitting ratio (e.g. 1:16 which corresponds to 512 users) or a larger value of pump power (e.g. 39dBm). In both the aforementioned cases the RSOA could be used in all ONU's and in any case of operation.

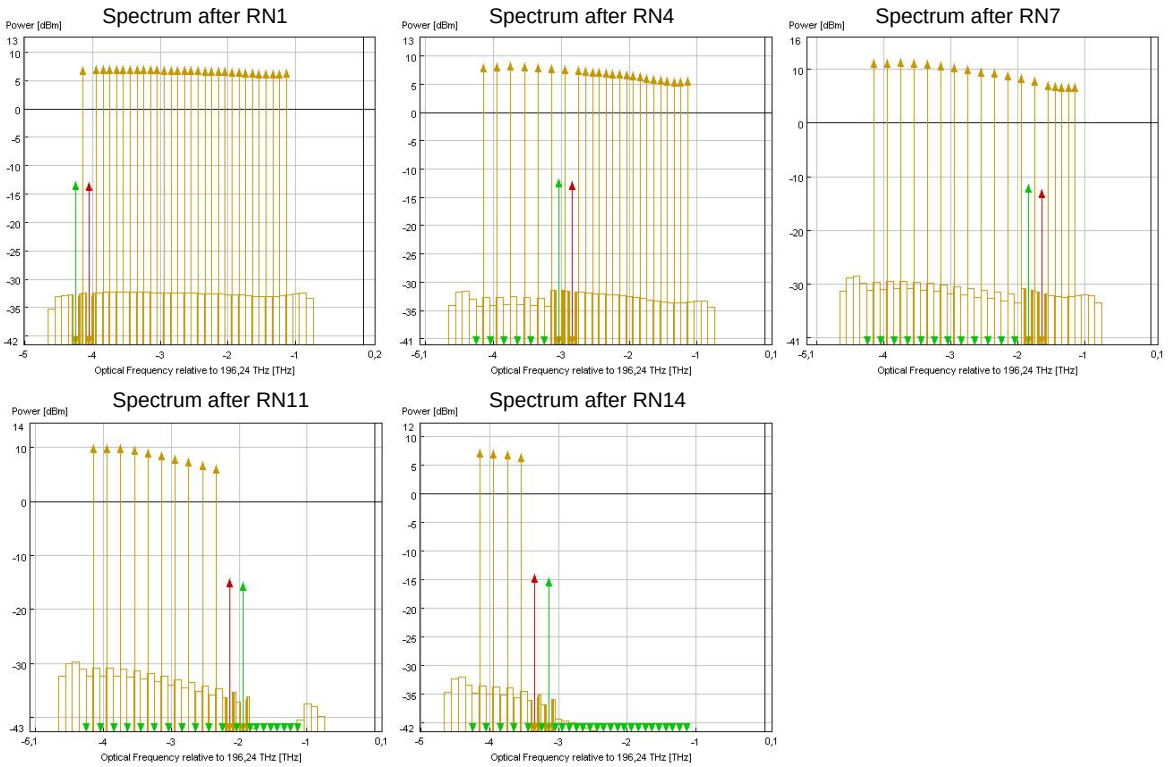

Fig. 5.17 Optical spectra with the through and dropped wavelength channels at RNs after each amplification stage for the case of downstream scenario in resiliency mode (Resolution Bandwidth = 0.1 nm)

The results for all the cases presented before are provided, in more detail in Fig.5.17-

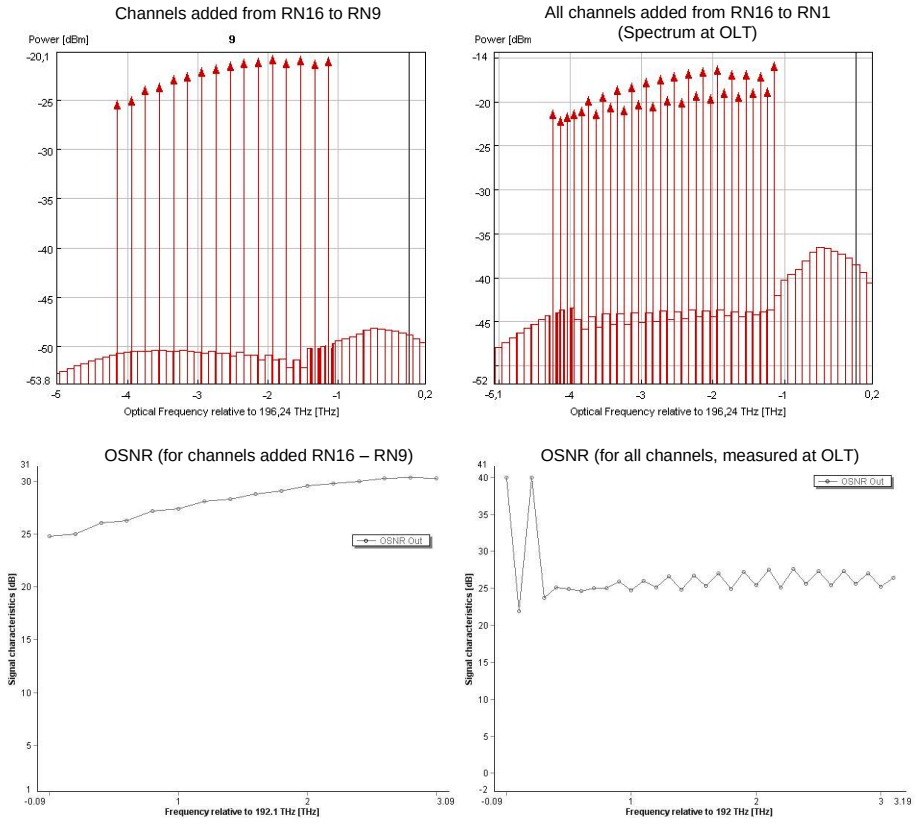

Fig. 5.18. Optical spectra with the through and dropped wavelength channels at RNs after each amplification stage for the case of downstream scenario in resiliency mode (Resolution Bandwidth = 0.1 nm)

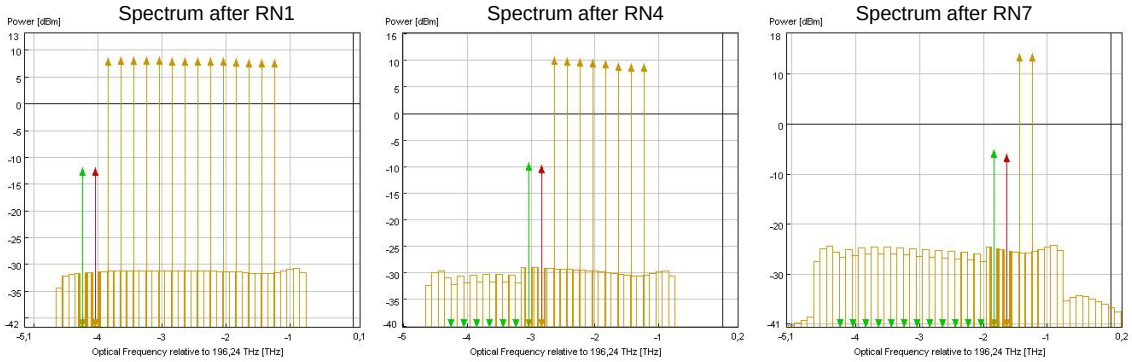

Fig. 5.19. Optical spectra with the through and dropped wavelength channels at RNs after each amplification stage for the case of downstream urban scenario in normal mode (Resolution Bandwidth = 0.1 nm)

5.20. More specifically the optical spectra after each amplification stage is shown. For the downstream signals the spectra show both the through channels and the dropped channels at the corresponding ONU. On the other hand, for the upstream signals the spectra show the newly added signals together with the already added signals from previous RNs for the middle and the last RN. Moreover in this case the OSNR per channel is provided.

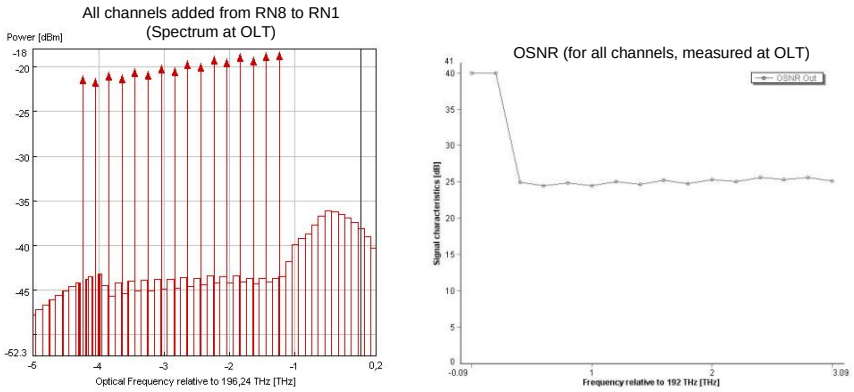

Fig. 5.20. Optical spectra with the added wavelength channels and OSNR per channel at OLT for the case of upstream urban scenario in normal mode (Resolution Bandwidth = 0.1 nm)

This investigation focused in an urban deployment. The same design can, with different parameters be optimized with response to the needs and the targets of the network. For example more users and stronger pump, longer distances and less users.

5.4.1 Conclusion

In this study we have shown that a network architecture based on SARDANA, using in-line amplification, can reach 19km while serving 1024 users with several hundreds of Mbps. Such a design can be applied in both, normal and resilient operation. If normal operation is considered, then all costumers can be serviced with the use of RSOA's

based ONUs. Nevertheless, in the worst case of a fiber cut, thus a fiber cut between the OLT and the first RN, the 160 users that are served by the RNs most affected can be served by standardized GPON APD receivers.

The proposed remote amplification solution consists of a fully passive architecture which can expand the limits of already deployed passive infrastructures, using remote amplification. The low pump power required, along with the extended use of RSOAs suggested, make this design very efficient in terms of OPEX. Furthermore, the overall cost of the RSOAs and the different components of the network, consist of a profitable solution in terms of CAPEX.

Chapter VI
Alternative band operation of a WDM/TDM PON

In order to increase the number of the end users, the solution of using an alternative frequency band has been considered. The limits of L-band for use on a WDM/TDM PON have not been investigated to the best of our knowledge and furthermore, this investigation can be expanded even more, so as to include operation in both C and L bands. In this framework, a special design of a WDM/TDM PON was implemented, based once more on the principle of cascaded in-line, remotely pumped EDFAs. In this chapter, we present the theoretical background of L-band EDFAs, several technologies for L-band amplification and some differences between C and L-band EDFAs. Furthermore, we expose some types of fibers for L-band EDFAs and the design of the aforementioned WDM/TDM PON, along with the special design considerations. Finally, the results of the study, in terms of the achieved maximum reach and number of end users on this alternative band PON are shown.

6.1 L-band EDFA

L-band EDFAs operate on the same principle as C-band EDFAs. However, there are significant differences in the design of L- and C- band EDFAs. The gain spectrum of erbium is much flatter intrinsically in the L-band than in the C-band.

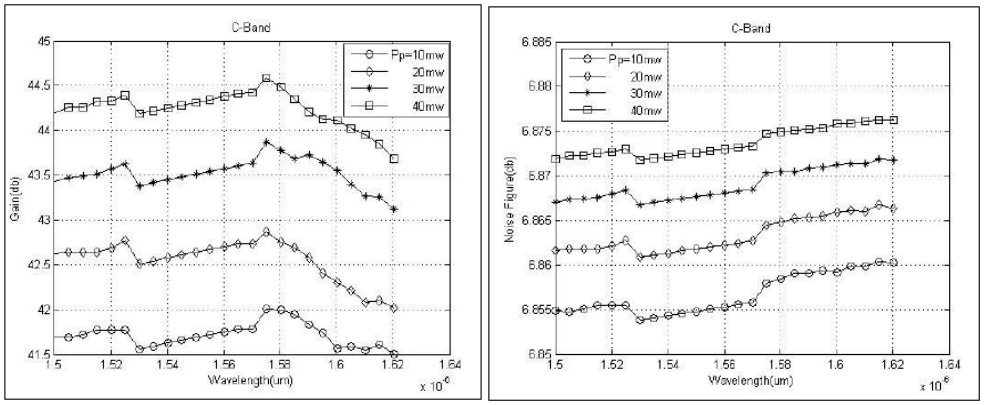

Fig. 6.1. C-band EDFA i) Gain vs. wavelength and ii) Noise figure vs. wavelength [82]

In typical EDFAs though, the erbium gain co-efficient in the L-band, is smaller than in the C-band. This necessitates the use of either much longer doped fiber lengths, or fiber with higher erbium doping concentrations. In either case, the pump powers required for L-band EDFAs, are much higher than their C-band counterparts. Due to the smaller absorption cross sections in the L-band, these amplifiers have also higher amplified spontaneous emission [81]. As one can see from Fig 6.1i) and 6.2i) that are based on a study appearing in [82], for a low initial pump power, the gain along the amplifier length will not be stable and there exists a saturation gain. For a larger pump power of 40mW, it is observed that the noise figure is below 6.875dB for C band while for L-band, for the same 40mW pump power, the noise figure is greater than 6.875dB (Fig

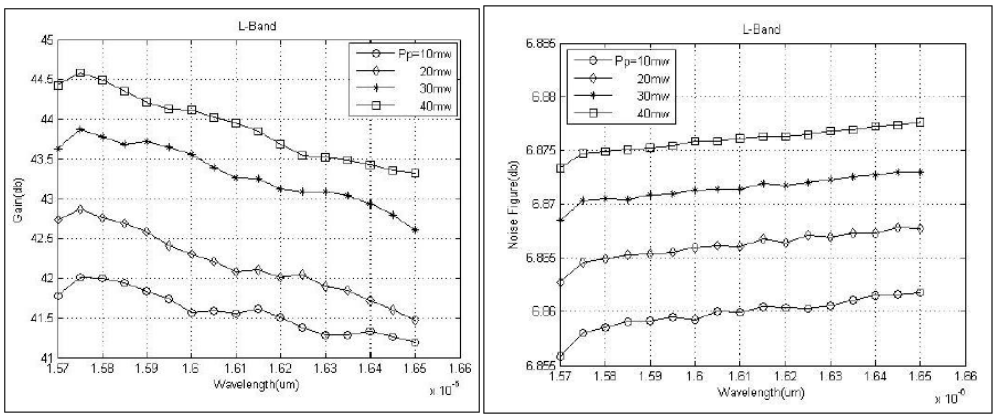

Fig. 6.2. L-band EDFA i) Gain vs. wavelength and ii) Noise figure vs. wavelength [82]

6.1ii), 6.2ii)).

In the WDM/TDM PON network study though, we have used a special doped fiber designed to operate in L-band, named iXF-FGL EDF.

6.2 L-band fibers

As already mentioned, in our study we have used a specially designed fiber that operates in L-band, named iXF-FGL EDF. The optical characteristics of the specially doped fiber can be found in Table 6.1.

TABLE 6.1. IXF-EDF-FGL CHARACTERISTICS

Fiber type	L band
Fiber name	IXF-EDF-FGL
Absorption @ 1530 nm (dB/m)	20-35
Absorption @ 1480 nm (dB/m)	9-16
Erbium consistency (%) 3km	+/−3.5
MFD @ 1550 nm (μm)	6.5
Background losses (dB/km)	<8
Cutoff wavelength (nm)	<1250
Splice loss (dB)	<0.15 (SMF28)
PMD factor (fs/dB)	<0.25

Below, the chart of the performance, as well as the characteristics of L-band erbium doped Nufern fibers (EDFL-980-HP, EDFL-980-HP-80 and EDFL-1480-HP) designed for use in L-band amplifiers. L-band erbium doped fibers, and these two ones in specific can be powered with 980nm or 1480nm pumps.

TABLE 6.2. EDFL-980-HP & EDFL-980-HP-89 CHARACTERISTICS

Fiber type	L band	L band	L band
Fiber name	EDFL-980-HP	EDFL-980-HP-80	EDFL-1480-HP
Absorption @ 1530 nm (dB/m)	25±2	25±2	30±3
Absorption @ 980 nm (dB/m)	≥7	≥7	≥12
MFD @ 1550 nm (μm)	5.5±0.5	5.5±0.5	5.3±0.5
Loss @ 1200 nm(dB/km)	≤15	≤15	≤15
Second mode Cutoff (nm)	920±50	920±50	1420±50
Numerical aperture(nominal)	0.25	0.25	0.25

In Fig. 6.3, one can see the gain and absorption curves of the EDFL-980-HP.

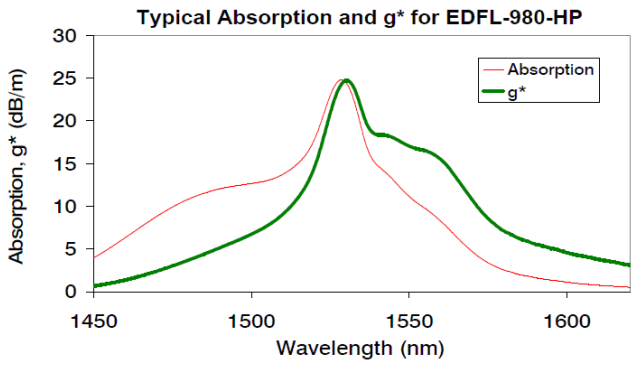

Fig. 6.3. Parameters of the EDF type: Nufern EDFL-980-HP

6.3 L-band amplification technologies

In WDM transmission systems and their related optical networks, one of the key technological issues is the achievement of broad and flat gain bandwidth for EDFAs. This trend of fast bandwidth consumption, as a natural extension, has resulted in the latest interest in optical amplifiers operating at longer wavelengths, which a conventional EDFA cannot handle. One solution to this demand includes either a new material composition for the fiber or higher concentration of Er3+.
Besides solutions involving new material composition or highly doped in Er3+ ones,

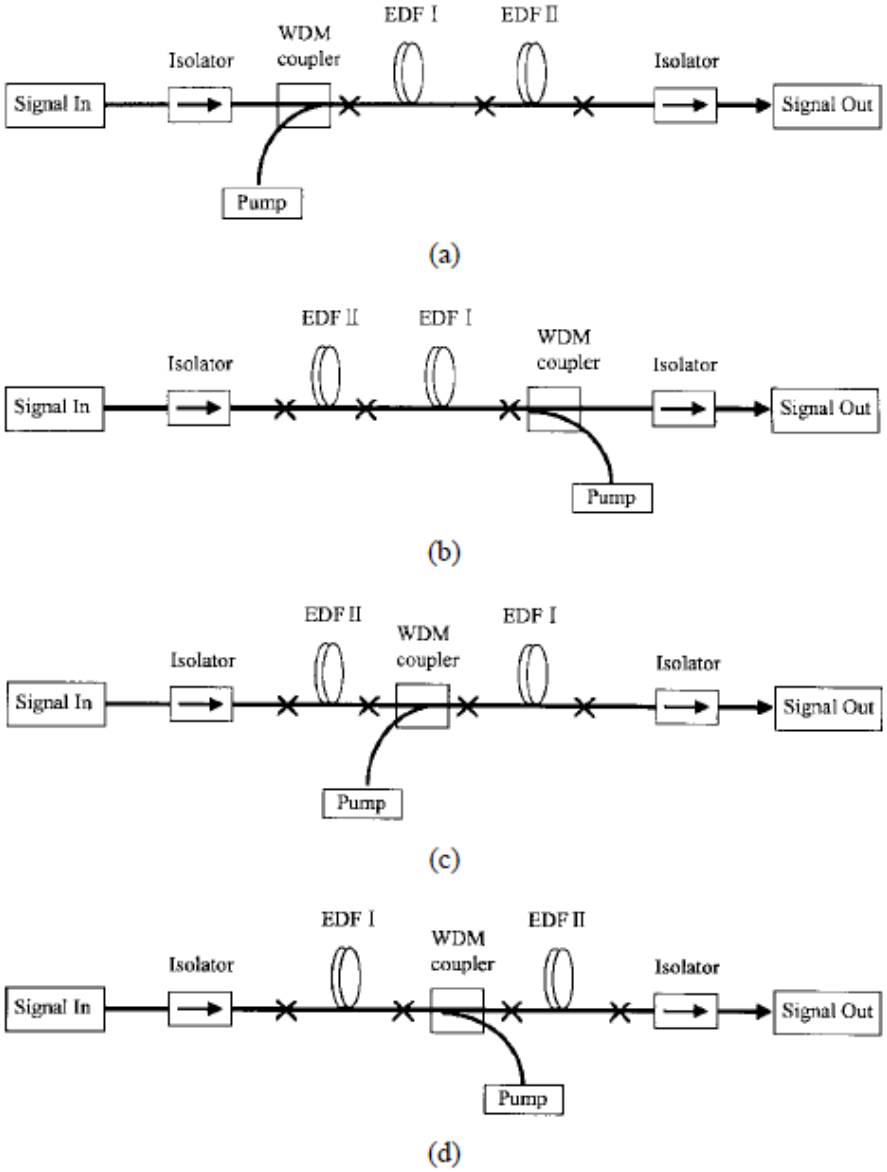

Fig. 6.4. Experimental examples of four types of L-band EDFAs a) Conventional forward pump, b) Conventional backward pump, c) Unpumped EDF section before forward pump, d) Unpumped EDF section after backward pump [86]

most efforts have been focused on silica-based erbium-doped amplifiers with various structures [83], [84]. For these approaches, relatively longer EDF's are commonly used with high pump power sources, to adjust the population inversion of the EDF at an

approximately 30%–40% level [83], and correspondingly to get the amplification in a long wavelength range (1570–1610 nm).

By using this L-band amplifier in parallel with the conventional (C-band, 1530–1560 nm) one the silica-based EDFA can now operate with a gain bandwidth of more than 80 nm, providing a wide open window for future high capacity WDM transmission systems [85]. It has been a common practice to use a cascade of EDFs and then use the backward ASE power of one of the EDFs as a pumping source for the unpumped EDF section. This principal has been used in the L-band EDFA presented in the Fig.6.4. c) and d) [86].

Another idea suggested, was the use of a 1540-1545nm pump, using the configuration appearing in Fig. 6.5 [87].

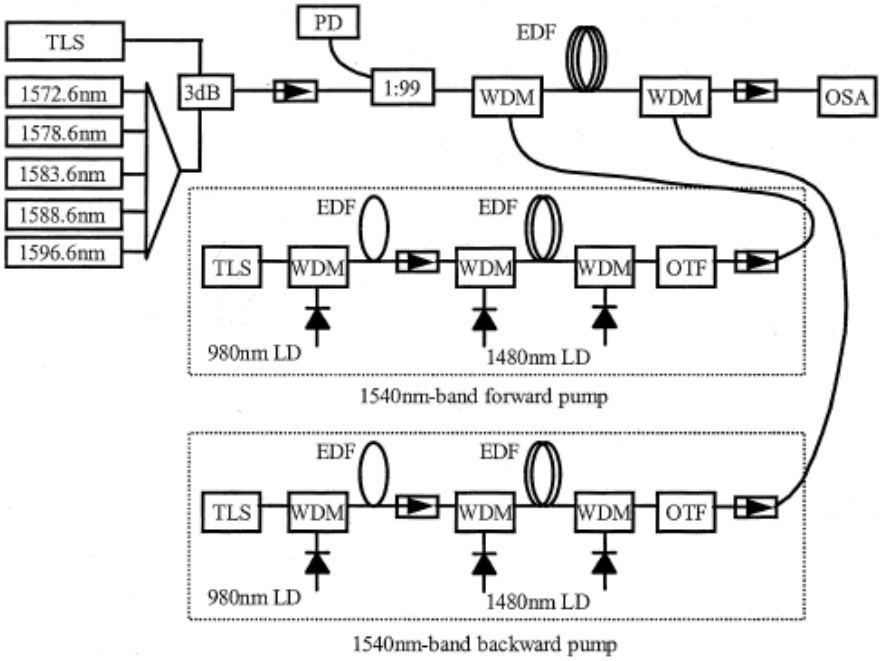

Fig. 6.5. Experimental configuration of 1540nm-band pumped L-band EDFA [87]

The results of 1540nm pumping, in terms of gain and noise figure vs. signal wavelength, can be found in Fig. 6.6.

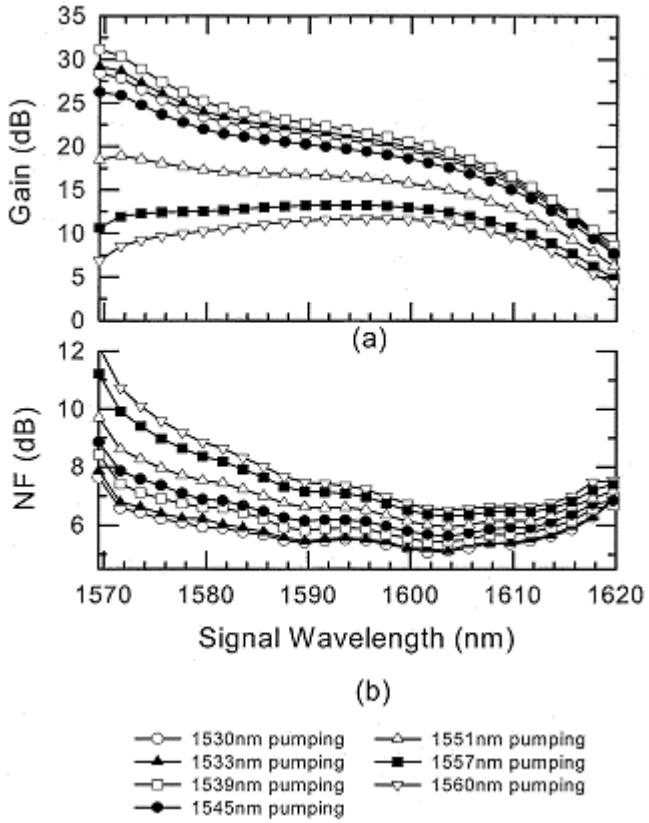

Fig. 6.6. (a) Gain spectra and (b) Noise figure spectra of 1540-nm-pumped L-band EDFA at 70mW pump power [87]

The pump source in this case is composed of a tunable light source and two C-band EDFAs in cascaded configuration. The gain co-efficient has proven to be 2.25 times larger than that of the conventional 1480nm pump. The reason for that is the backward ASE suppression.

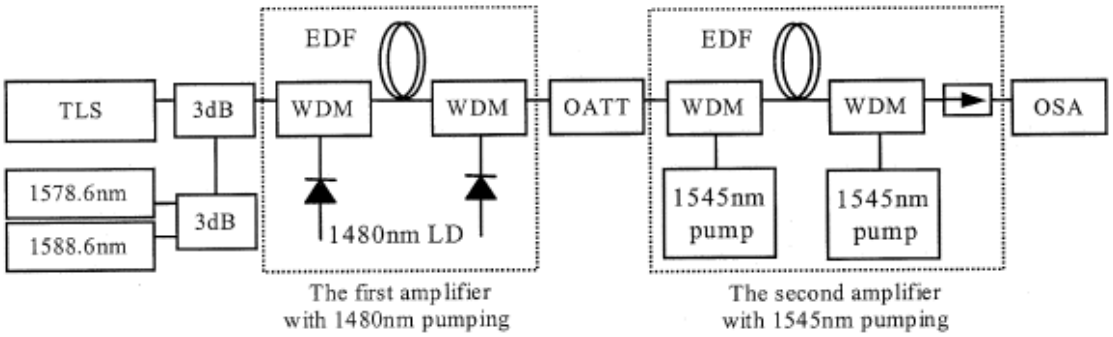

Fig. 6.7. Experimental setup of an in-line amplifier using 1545nm pumped L-band EDFA on cascaded amplification configuration[87]

This specially designed –band EDFA was applied in an in-line amplifier for an optical communication link as can be seen in Fig. 6.7. The in-line amplifier was composed of firstly a 1480nm pumped EDFA and secondly a 1545nm pumped EDFA in a two stage amplification configuration. This implementation has shown a very big power conversion efficiency improvement.

6.4 In-line and L-band operation of a WDM/TDM PON

Our approach, focusing on amplification and more specifically on in-line amplification using for transmission the L-band, is based and tested in a double ring fiber WDM/TDM PON that has been described in chapter 5, but with a few alterations [88]. The goal is to achieve, with given transmission and pump power, the longest reach possible from the OLT to the furthest user. At the same time, the aim is to serve more than 1000 users and retain the signal in a high level. In the scenario examined, the signal level as well as the OSNR obtained, allow the use at the customer's end of a RSOA.

The scalability of the network permits the implementation of several deployments, whose planning depends on the population density and the area considered. These characteristics determine the final number of the RNs as well as the distances among them. However, in every approach the need of remote amplification is necessary in order to have the appropriate input level in the ONU and to maximize the users while counterbalancing for the power losses throughout the network. On this study the use of in-line remote amplification has been considered. Moreover we have investigated the use of an alternative band of wavelengths, namely the L-band. 1024 users have been reached in a distance of 20km with a signal appropriate to be used with an RSOA.

6.4.1 Parameters of the network affecting its operation

The parameters taken under consideration are the number of RNs, the signal power, the pump power, the total length of the fiber between the OLT and the final user -which could be considered as the sum of the fiber distances from the OLT to the RN and the tree fiber length-, the losses induced by the RN, the splitting ratio of the tree, the length of the EDF, the percentage of the total pump power used in each RN to pump the corresponding EDF , the sensitivity of the receivers and the wavelength allocation in the sense of appointing which frequencies will be dropped in each RN regarding their distance from the OLT. Continuing, the parameters are analysed in more detail.

Number of RNs

The number of RNs depends on the number of end users we want to cover. In an urban area a number of 16RNs per fiber ring is considered. Increase of the number of nodes corresponds to increase of the users served and decrease of the power budget.

Signal power value

The downstream signal power's value has been set in 10dBm. The reason for that is that with the power link budget performed, the design of in line amplification requires 10dBm initial power in order to reach the users of the first tree, since no amplification is

performed for this frequency. Moreover the use of a stronger signal power was avoided, so as to prevent emergence of non linear effects at furthest propagation as well as for restraining OPEX. The upstream signals' value is set to 0dBm in order to comply with the capabilities of an RSOA.

Pump power value

The operation of in line amplification design was tested for two values of pump power, 31 and 39dBm respectively. Increase of the pump power makes the network more flexible in terms of users served. The reason is that it allows a more effective amplification in terms of greater gain, thus an increase in the power budget is achieved. Nevertheless, we examined the use of 31dBm, because a smaller pump power complies better with safety regulations as far as the CO is concerned. It should be marked however, in regard of safety regulations, that since the pump circulates only in the upstream fiber ring, there is no danger that it could come to the reach of the end user. The pump is counter propagating with the upstream signals as aforementioned, but in this investigation the loss due to pump depletion is considered negligible, because of the low signal power.

Losses induced at the RN

Each RN includes filters that perform Add & Drop operation. In the cases of RNs that include EDFs for in line amplification, the use of splitters and WDM couplers is additionally necessary. The filters used along with the splitters and the WDM couplers introduce losses at the RN. Losses are also induced by the WDM couplers and the attenuation of the fiber along the path to the end user. Their sum is 4.6dB. All these losses have to be counterbalanced by the gain of the EDF.

Splitting ratio

As aforementioned, the splitting ratio of the tree can vary from 1:32, 1:64 and 1:128 for an urban deployment. Since each node serves two trees each with a different λ, these splitting ratios are interpreted into 64, 128 and 256 users per RN respectively. It is obvious that increasing the splitting ratio the number of end users is increasing accordingly. One should take into account though, that this happens in expense of power losses induced to the network. In the scenario presented, a splitting ratio of 1:32 has been used.

EDF length

The length of the remotely pumped EDF affects the amount of gain achieved, the portion of the pump power consumed, as well as the OSNR. Therefore a careful choice has been made on the lengths of the EDFs used in each RN in respect of its position in the network (distance from the OLT) in order to counterbalance for all the

aforementioned variables. Different fiber lengths have been used in the downstream ring, symmetrically placed though, as described also in chapter 5 (i.e. same EDF lengths used in the first and last RN, so as to preserve a symmetrical design) in order to adapt in the case of resiliency operation (for example a fiber cut between the OLT and the first or the last RN). Furthermore, due to the elaborate design some RNs could be excluded (in this case as well as in the design of chapter 5) since the signal had the necessary power to serve the corresponding trees and no EDFs were placed in their interior. In the upstream propagation ring, all RNs were equipped with an EDF of the same length, but carefully optimized in terms of low pump power consumption and OSNR.

Distribution of pump power

Pump power is distributed in each RN to be used in amplification of both the downstream and the upstream propagating signals. The distribution is implemented by using different percentages in each RN for the amplification of the downstream signals, while the portion used for the amplification of the upstream signals is invariable. As far as the downstream propagation is concerned, the power required, was determined by the need of each RN for amplification. In some distances the signal had the power required to reach the customers' ONU without amplification, so, some RNs were excluded. A conservative approach was considered on the use of the pump so that it would be adequately distributed to all amplification stages.

Receiver's sensitivity

We consider the use of an RSOA. A power value of -20dBm is considered necessary in order to both obtain the downstream data and at the same time use the optical carrier for modulation with the upstream signal and achieve an output of 0dBm. Transmission with low input powers have been already demonstrated [84]. Finally, the receiver at the OLT is considered to have a sensitivity of -28dBm.

Frequency allocation

32 channels have been considered, with 100GHz spacing that range within the L-band from 187.4THz-190.5THz. In order to achieve the same gain through the amplification stages for all wavelengths, an optimum design per RN and per in-line amplifier is required. The main purpose in an optimum design is to consider the worst case of

Table 6.3 FREQUENCY ALLOCATION FOR L-BAND WDM/TDM PON WITH IN-LINE AMPLIFICATION

RN	1	2	3	4	5	6	7	8	9	10	11	12	13	14	15	16
f_1	187.6	188	188.4	188.8	189.2	189.6	190	190.5	190.3	189.9	189.5	189.1	188.7	188.3	187.9	187.5
f_2	187.7	188.1	188.5	188.9	189.3	189.7	190.1	190.4	190.2	189.8	189.4	189	188.6	188.2	187.8	187.4

resiliency and reserve the frequencies that can have more gain for the distant nodes. The gain of the EDF is not flat for all wavelengths, but exhibits a gain tilt which favors some of them in terms of gain received. As the pump power fades out over longer distances, the channels that have received more gain in the previous stages will be able to reach longer distances. This effect is evident in low frequencies therefore these were allocated to the more distant RNs in the resiliency case, which are RN_{16} and RN_1, if it is considered that the RN_{16} to OLT or RN_1 to OLT connections respectively are down. The wavelength allocation used is shown in Table 6.3.

6.4.2 Set up

The set up is considered to be applied in an urban area, therefore it consists of 16 RNs, with a distance of 1km among them, and an OLT connected with two fiber rings. One of them is used for downstream transmission, while in the other; the upstream signals are counter propagating with the pump signal. The tree fiber has a 3km length, therefore the maximum distance from the OLT to the end user is 19km. Considering the total passive losses of the network it is evident that these depend mainly on the splitting ratio at the distribution trees and less on the fibre losses. Therefore, in order to comply with the given values for transmitter-receiver power levels, the splitting ratio was set in 1:32 for each tree, which results in 1024 customers served.

The in line amplification is realized in the RN. With the use of fixed filters and splitters two wavelengths are dropped in each RN. The EDF is placed among the two drop filters and before a 50/50 splitter used for resiliency. Each wavelength is then driven to a tree. The placement of the EDF among the drop filters creates the need to transmit in the downstream direction a signal with adequate power to reach the first tree (served by RN_1 in normal operation or RN_{16} when operating in resiliency mode in the case of a fiber cut between the OLT and RN_1) as the drop signal of the first tree in this design will not be amplified. An overview of the network, as well as the RN design, is presented in Fig.6.7.

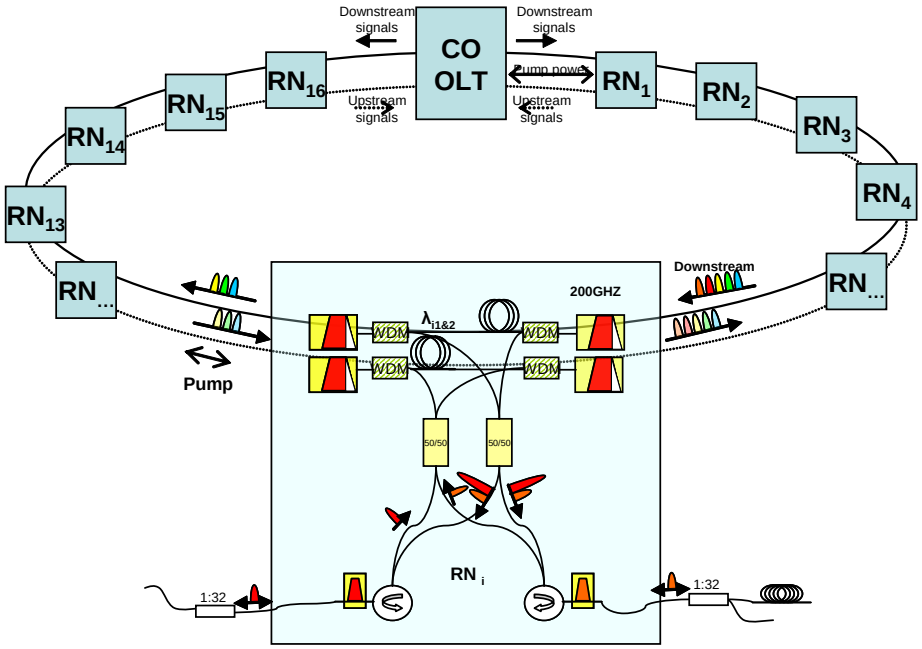

Fig. 6.7.Network architecture and Remote Node comprising in line remote amplification

6.4.3 Results

The study performed shows that the described architecture along with the use of L-band signals can serve 1024 end users with several hundreds of symmetric data rate in a maximum distance of 19km. More specifically for downstream as can be seen in Fig. 6.8, all the ONUs are reached with a signal power higher than -20dBm which means, they could be based on RSOAs .

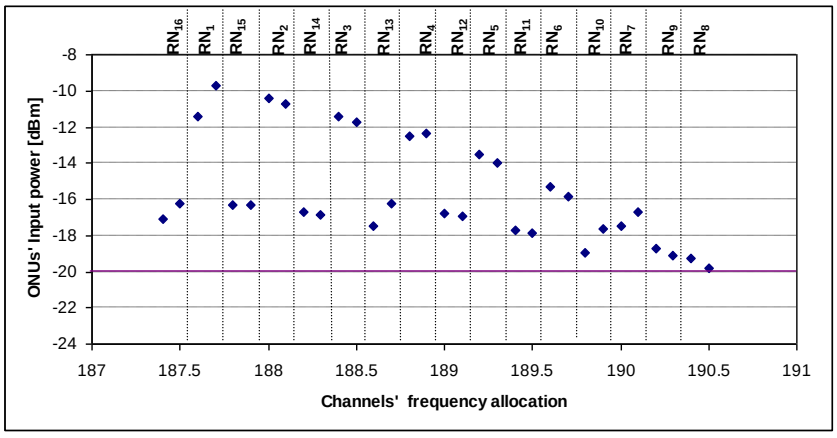

Fig. 6.8.Downstream signals

The upstream operation of the network is also ensured by the fact that the signal power level reaching the OLT is above -28dBm, as can be seen in Fig.6.9 which is the OLT receiver's sensitivity.

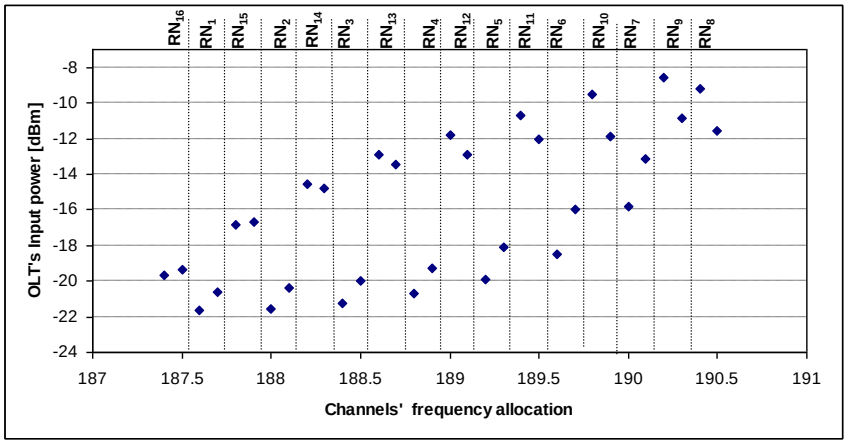

Fig. 6.9.Upstream signals

The gain of the special doped EDF has been experimentally investigated for different pumping power values and the results are depicted in Fig.6.10.

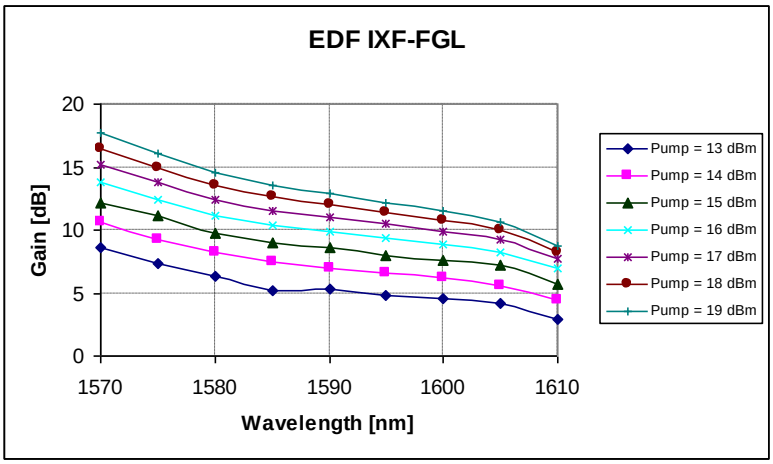

Fig.6.10.Characterization of the L-band amplifier in the RN

6.5 Conclusions

In this chapter we reviewed the idea of using an alternative band of frequencies for the implementation of a WDM/TDM PON. After exposing some technologies investigated in the past for L-band amplification and their performance we have reviewed some types of fiber for L-band amplification. Continuing we report the investigation we performed, on the L-band operation of a WDM/TDM passive optical network. More specifically, we have shown that a WDM/TDM passive optical network architecture using L-band in line amplification can reach 19km while serving 1024 users with several hundreds of Mbps while all costumers are serviced with RSOA's based ONUs. This solution consists of a fully passive architecture which can enlarge the limits of already deployed passive infrastructures, using remote amplification. The operational expenditures are expected to be decreased due to the low pump power required along with the extended use of RSOAs. In addition the overall capital expenditure can be reduced as the RSOAs consist of a profitable solution.

Chapter VII
Extended band operation of a WDM/TDM PON

In this chapter, we explore the possibilities of the expansion of a WDM/TDM PON with advancing and enhancing its band operation. Such a study can be considered very useful for infrastructure proprietors wishing to lease one fiber to more than one operator. The suggested designs can turn the network much more competitive, hence lowering the final services' prices and giving a financial boost to the whole technology.

A trial network design, due to operate in both C + L band, has been implemented. Further, the combination of Raman amplification with remotely pumped EDFs placed as in the previous chapters, in-line with the transmission path, thus distributed in the WDM ring is shown. Finally, we have investigated the limits and the performance of a WDM/TDM network operating in C + L band, which uses remotely pumped amplification in the drop part of the network, with the help of an especially designed RN.

Chapter 7 has been organised in three subsections. In the first we briefly explain the theoretical base of Raman amplification. On the second, the results of applying Raman amplification in a WDM/TDM PON are presented. Raman amplification mechanism is combined with in-line EDF amplification. On the third a RN design is presented, one that is predestined to operate in C+L band but using amplification on the drop part of the network. In other words, designed to enforce two wavelengths, the ones destined to the TDM trees connected to the specific RN.

7.1 Raman amplification

Stimulated Raman Scattering (SRS) is an interaction between light waves and the vibrational modes of silica molecules. If a photon with energy hv_1 is incident on a molecule having a vibrational frequency V_n, the molecule can absorb some energy from the photon. In this interaction, the photon is scattered, thereby attaining a lower frequency v_2 and corresponding lower energy hv_2. The modified photon is called a Stokes photon. Because the optical signal wave that is injected into a fiber is the source of the interacting photons, it is often called the pump wave, since it supplies power for the generated wave.

This process generates scattered light at a wavelength longer than that of the incident light. If another signal is present at the longer wavelength, the SRS light will amplify it and the pump-wavelength signal will decrease in power. Consequently, SRS can severely limit the performance of a multichannel optical communication system by transferring energy from short-wavelength channels to neighbouring higher wavelength channels. This is a broadband effect that can occur in both directions. Powers in WDM channels separated by up to 16 THz (125nm) can be coupled through the SRS effect, in terms of the Raman gain coefficient g_R as a function of the channel separation $\Delta\nu_s$ .This shows that owing to SRS, the power transferred from a lower wavelength channel to a higher-wavelength channel increases approximately linearly with channel spacing up to a maximum of about $\Delta\nu_c$ = 16THz (or = 125nm in the 1550-nm window), and then drops off sharply for larger spacing [89].

7.2 C + L band gain equalization – Hybrid Raman & in-line EDF amplification mechanism

The feasibility of gain enlargement and equalization on extended reach WDM-ring PON by means of hybrid Raman/EDFA amplification has been investigated with the use of simulation. This study has been performed in the framework of a collaborative effort with Berta Neto [90].

7.2.1 System description

The network examined, consists of a 80km WDM ring with 8 nodes in each one of which, 2 channels are added/dropped. It is therefore operated with 16 channels, 8 of which cover the C band while the other 8 cover the L one. In the CO, a bidirectional laser emitting at 1480nm is used to pump the spaced by 400 GHz 16 channels, that are distributed between 192.5 THz and 186.3 THz (see Table 7.1.). The channels leave the central office with 0dBm of optical power. The bypass losses are considered 0.53dB for channels and 1.01 dB for the pump, while the attenuation of channels and pump are set to 0.20dB/km and 0.25dB/km respectively. The channels drop losses are 3dB. In this framework two situations are analyzed, one with Raman amplification and the other with a hybrid amplification scheme composed by in line EDF with Raman. Therefore, an optimized span of EDF is inserted in the mid length of each link according to the dropping channels powers. This procedure was performed with total pump power of 1W (500mW in each direction). The results have demonstrated gain equalization with a ripple of 2.54dB over a bandwidth of 50nm by using spans of EDF with a total length of 22km.

7.2.2 Method used – Results

The 16 analyzed channels, with the exception of the last two, rely on the maximal bandwidth of Raman gain efficiency. In the following picture, the Raman gain efficiency is plotted for a standard single mode fiber, pumped at 1480nm, being the C and L bands represented by black and red arrows, respectively.

The optimization strategy followed is the following: (i) drop the channels with the higher gain first in order to settle a maximal gain level and decrease the effect of pump depletion, (ii) whenever the channel power reduction surpasses a predefined value, try several span of EDF fiber in the mid-link to minimize the gain ripple. The obtained optimized results were also compared with simple Raman amplification. The simulation is based on the implementation of Raman propagation equations [91] and Saleh [92] model for EDFA using the semi-analytical average power analysis method [93, 94]. This method leads to quick and accurate solutions.

The optimal dropping order is listed in Table 7.1. The idea is that the channels with the maximal Raman gain efficiency are dropped first and then move outwardly, as assigned in Fig. 7.1.

Table. 7.1 Channel dropping order along the ring (2 channels per node)

	RN #	f_1 (THz)	f_2 (THz)
C band	1	190.1	190.5
	2	190.9	191.3
	3	191.7	192.1
	4	192.5	192.9
L band	5	189.3	189.7
	6	188.5	188.9
	7	187.7	188.1
	8	186.9	187.3

The results for total pumping at 1W (500mW for each direction) are depicted in Fig. 7.2. The top graph displays the power after dropping spectra for optimized hybrid Raman/in line EDFA and simple Raman, while the middle one represents the optimized EDF span

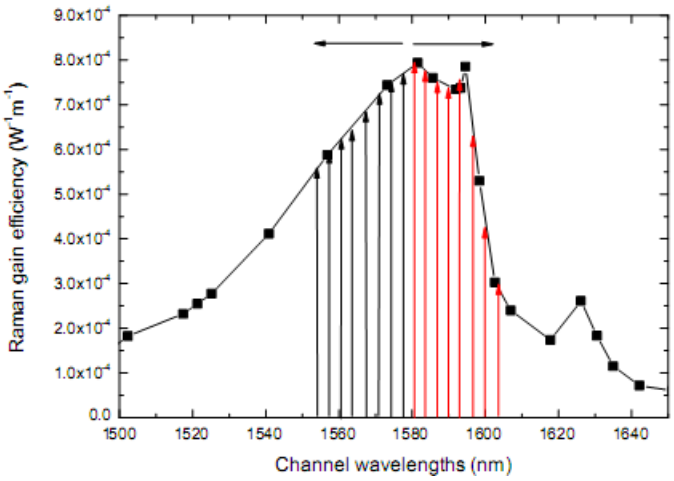

Fig. 7.1.Raman gain efficiency for pumping at 1480nm. The channels are represented by arrows (black –C band and red L-band). The curve was obtained by interpolation of experimental data. [95]

and their position in the ring (in terms of relative to the CO position). The bottom graph displays the available pump power for the EDF spans. On looking at the simple Raman results, we verify that just by choosing a dropping order compliant with the maximal Raman gain efficiency, the power is considerably flat in the 1567-1590nm range and then decreases as the channels' wavelengths move away from the maximal gain efficiency. On those links the insertion of an EDF span can increase the power above the 0dBm threshold. It should be noted that in order to provide gain in L band, longer spans of EDF are used. Looking at the pump power results, we notice that due to this methodology, the available pump power in distant links is still high enough to pump the EDF spans. Hence, in the hybrid approach a total span of EDF equal to 22m is used (2m for C band amplification and 20m for L band amplification) to attain a ripple of 2.54 dB over a bandwidth of 50nm.

7.3 Dual waveband remote node for extended reach full duplex 10Gb/s C + L band PON

The requirements of an extended WDM/TDM PON in terms of optical budget are increased when compared to simple PONs. Moreover, the requirements for extended reach and higher splitting ratios in their TDM segments increase the demands on the system, therefore additional amplification between the OLT and the ONU becomes mandatory. Although wideband C + L band Erbium Doped Fiber (EDF) already exist [96] the indispensable passiveness demands this kind of amplification to be performed remotely. This technique of remote pumping has been already demonstrated for long haul systems in both wavebands [97] and has been introduced also to PONs for the C-band, but with the use of EDFs in the drop part of the RN [98]. For this latter case, a pump is transmitted along its fiber plant towards the RNs. For the case of a hybrid PON from ring + tree architecture, these RNs, situated at the interconnection between the WDM ring and the TDM trees, also perform the task of signal drop and insertion between ring and tree segments.

In this experiment a remote node design for C+L band amplification is characterized and shown to cover the advanced optical power budget for a 55 km reach, 1:32 split hybrid passive optical network with symmetrical full-duplex 10 Gb/s transmission. Different types of Erbium-doped fibers, designed for the C- and L-band are evaluated in a bidirectional amplification stage at the remote nodes of a ring + tree network, providing 5-10 dB of power margin for the reception of down- and upstream despite degradation of the optical signal-to-noise ratio. The evolution of signal power and the noise accumulation along the light path is discussed for both wavebands. This work has been performed in a collaborative experimental study with Bernhard Schrenk.

7.3.1 Remote node design

The RN aims at serving the needs of combined C+L-band amplification in an extended reach PON (Fig.7.7) with a resilient dual fiber ring, where unidirectional rings for down- and upstream are connected via RNs to bidirectional trees that contains several ONUs. Since the used EDFs do not provide amplification in both wavebands, as can be seen in Fig. 7.8(a) that shows the spectra for the amplified spontaneous emission (ASE) of the HE980 and iXF-FGL EDF when being pumped at 1480 nm, a RN design with separate amplification stages for the wavebands was chosen. C/L waveband splitters (C_D, C_U and C_T) therefore divide the RN into sub-RNs, whereby each of them holds one of the two EDF types, which are designed for their dedicated waveband. While the ASE peak is located at 1530 nm for the HE980, it can be found at 1565 nm for the iXF-FGL EDF. According to the bidirectional nature of the tree, a sub-RN consists of two remotely pumped EDFs that are used for independent amplification of down- and upstream. This is necessary due to amplified reflection from the thin-film filters inside the pump/signal combiner which had a return loss of 54 dB and would lead after amplification to a power level for the reflected downstream signal that is then already comparable to the noise background of the ASE. For the case of a bidirectional amplifier, the reflection from the filter would be caused by a strong downstream signal and amplified back in upstream direction together with the upstream signal, which is in turn low due to the higher power splitting ratio in the tree. Therefore, not the background noise level of the upstream, but the reflection of the filter will degrade the upstream transmission in a bidirectional amplification scheme where down- and upstream have the same wavelength.

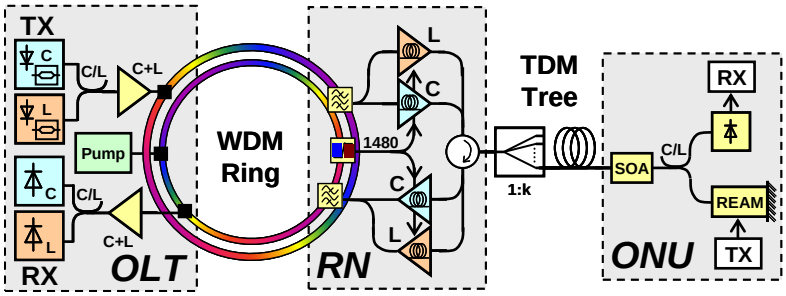

Fig. 7.7.Hybrid WDM/TDM-PON with remote C+L amplification between OLT and ONU, dedicating separated amplification stages for the two wavebands.

Besides that, the more critical degradation from bidirectional amplification is the effect of Rayleigh Backscattering (RB) in the EDF which is enhanced compared to a standard single-mode fiber (SMF), as can be seen in Fig. 7.8(b) for the EDFs used in the RN. While the RB coefficient, defined as the ratio between the Rayleigh backscattered light of a fiber and the launched light into the fiber, saturates at -33.6 dB for a standard SMF with a length of 18 km for both wavelengths of 1550 and 1585nm, the HE980 EDF saturates at -24.3 dB for a wavelength of 1550 nm and a length of 15 m, and the iXF-FGL EDF at -27.8 dB for a wavelength of 1585 nm and a length of 5m. Therefore, it is necessary to split the bidirectional amplification stage into two unidirectional stages to allow amplification inside the RN for counter-propagating data streams at the same

wavelength. However, bidirectional amplification itself is not prohibited since different wavelengths can be amplified in opposite directions, which is especially beneficial for the case of having two trees connected to the RN, where different wavelengths with different data streams can stabilize in the same amplification stage against gain transients in the presence of burst-like upstream traffic [99].

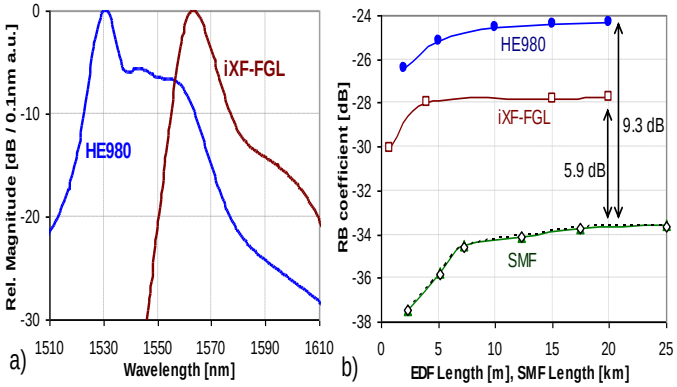

Fig. 7.8.(a) ASE spectra for the two EDFs used in the RN when being pumped at a wavelength of 1480 nm, and (b) amount of Rayleigh backscattered light relative to the light launched into the different EDFs of the RN and the SMF in the tree. The wavelength used is 1550 (filled) and 1585 nm (hollow markers).

A detailed scheme of the RN is shown in Fig. 7.9. Despite its complexity, it is kept fully passive and has no operating expenditures. The add/drop of the tree wavelengths from the ring into the sub-RNs was performed with four 200 GHz thin-film add/drop filters (A/D in Fig. 7.9), while resiliency is provided by a 50/50 coupler (C_R) that allows to receive and transmit the data stream to both directions of the down- and upstream ring for the case of a fiber cut. Another 100 GHz thin-film filters (R/M) are intended to allow for bidirectional amplification of the two tree wavelengths that have been dropped from the ring. After the EDFs, these two wavelengths are again multiplexed with 100 GHz filters (T/M), which also reject the ASE from the EDF or, in case of the upstream from the ONU, the noise of the reflective remodulator. Circulators are placed before the C/L splitters that feed the bidirectional tree. As there will be only one tree wavelength used in each waveband, the filters that are placed between the resiliency couplers and the EDFs are discarded, while the filters, originally situated between the EDFs and the tree interface are now placed at the bidirectional port of the circulator.

The insertion loss from the ring to the input of the EDF is then 4.5 and 6.9 dB for the C- and L-band, respectively. Another 1.5 and 3 dB of loss are located between the output of the EDF and the tree interface. The insertion loss values are higher for the L-band due to the higher pass insertion loss of the L-band filters. The pass-through loss between the two ring interfaces of down- and upstream was 1.2 dB. The remote EDFs were pumped at 1480 nm as this wavelength is suitable to be fed remotely from the OLT towards the RN. Two laser diodes (LD) of 19 dBm each for the downstream EDFs and two LDs with 16 dBm for the upstream EDFs were used locally, as strong pumps were missing for their transmission from the OLT. This shows a worse case where no extra Raman gain benefit was present.

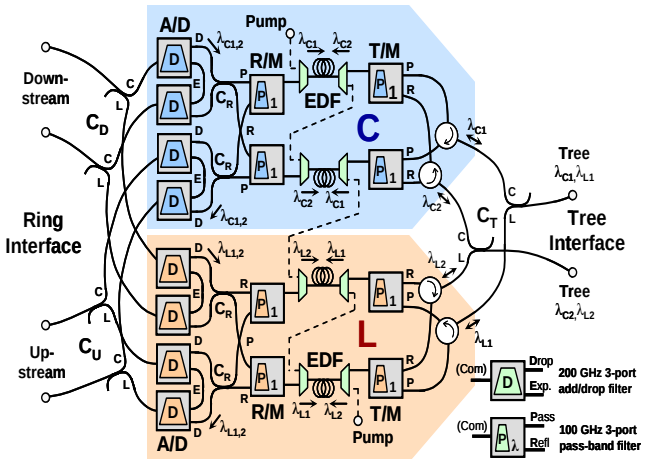

Fig. 7.9.Hybrid WDM/TDM-PON with remote C+L amplification between OLT and ONU, dedicating separated amplification stages for the two wavebands.

The weaker pump for the upstream reflects the better sensitivity in reception of the OLT compared to the receiver of the ONU, and also the constraints of the pump requirement in a PON.

For the C- and L-band, 15m of HE980 and iXF-FGL EDF was used for the downstream, while 15m and 10m were placed for the upstream light path. This choice is based on the investigation for both fiber types. Fig. 7.10(a) shows the gain for an input power of -10 dBm into the EDFs for C- and L-band wavelengths for different EDF lengths, and Fig. 7.10(b) and Fig. 7.10(c) the gain and the OSNR (measured for a resolution bandwidth of 0.1 nm) for a pump of 19 dBm for C- and L-band EDF, respectively. As can be seen, the gain profile of the HE980 EDF is quite flat over the whole C-band, and has a roll-off around 1560 nm. Although more gain can be provided in the region around 1530 nm, the Optical Signal-to-Noise Ratio (OSNR) is degraded by 1.4 dB over the centre wavelength of 1550 nm for a 15 m long EDF due to the presence of the ASE peak, as shown in Fig. 7.10(b). The gain profile of the iXF-FGL EDF has a slight roll-off over the whole L-band, giving a difference of 5.2 dB between the wavelengths of 1570 and 1600 nm for a 15 m long EDF, as can be seen in Fig. 7.10(c). However, for the same EDF length the OSNR degradation near the ASE peak is negligible when compared to a wavelength where the gain is still high and the ASE peak is sufficient far. For a possible application in a PON the gain for the longer wavelengths of the L-band may be too low to face the power budgets for data transmission. In that case, the spacing between the optical carriers in the L-band will have to be decreased to the next grid standard for the add/drop filters, for placing several wavelengths used for data transmission inside the range where sufficient high gain can be provided. Alternatively, the delivered pump power and the EDF length can be optimized so that a flat gain can be obtained for all L-band sub-RNs.

The optimum lengths of the EDFs were chosen according to the provided pumps and the achieved gain values. It has to be noted that for the C-band EDF, the gain is determined by length and pump power, as can be seen in Fig. 7.10(d) that shows the gain that is provided by the EDFs for C- and L-band for different lengths and different pump power values. For the C-band EDF, the gain curve is quite flat over the pump power, while for the L-band EDF the gain strongly depends on the provided pump. On the contrary to the C-band EDF, the difference in gain between different EDF lengths is much smaller for the same pump power. This behavior is pronounced due to the higher

pump consumption that longer EDF spans require, e.g. for the 20 m EDF, no additional gain is obtained compared to the 15 m EDF, as the provided pump of 19 dBm is already too low.

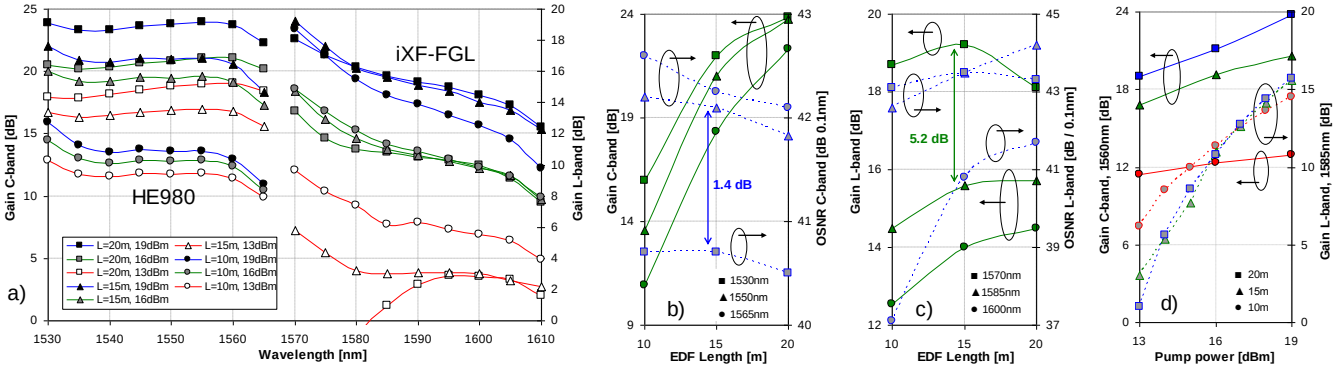

Fig. 7.10.(a) Characterization of the C- and L-band amplification stage in the RN, for an input power of -10 dBm and various pump power values, and achieved OSNR and gain for the (b) C-band and (c) L-band for a pump of 19 dBm, and (d) dependence of the gain for both EDFs on the pump power for different EDF lengths

For the downstream C-band EDF and an operating wavelength of 1560 nm, the latter chosen despite the falling gain spectrum of the HE980 EDF because of the preference of longer wavelengths in the available optical remodulator at the afterwards connected ONU, a length of 15m was used. Although some more gain could be provided with an EDF of 20m, this length was not chosen as the OSNR already starts to decrease. This criteria of selection is also pronounced due to the fact that the L-band EDF does not provide the same high gain as the C-band EDF. Therefore, the OSNR is an important parameter for the latter one as the power budget can be also reached with less gain. Considering operation at a wavelength of 1585 nm for the L-band, it can be seen that for the downstream with the stronger pump an EDF of 15m shows good performance as a longer one does not benefit. Although the gain is less than for the C-band EDF, a similar OSNR can be achieved.

For the C-band upstream, the same EDF length of 15m was chosen as this length provides sufficient gain for the power budget of the upstream which is more relaxed compared to the one of the downstream due to the better receiver at the OLT. The best choice for the EDF length in the L-band upstream amplifier is a short fiber of 10m as longer EDFs already miss gain due to insufficient pump. Although only one RN was placed inside the ring, the pass-through loss of 1.7 dB for the bypassed express wavelengths, considering also pump/signal splitters for the delivery of the pump for the RNs along the ring, could be partially compensated in the C-band by the extra Raman gain that is benefit from in a realistic scenario.

7.3.2 Remote Amplification in an Extended Reach PON

The experimental setup for the integration of the RN into a PON is shown in Fig. 7.11. This PON achieves full-duplex operation by dedicating different wavebands (C and L or vice versa) for down- and upstream. The optical carriers in the C- and L-band were located at 1560.61 and 1586.2 nm and modulated with Mach-Zehnder modulators (MZM in Fig. 7.11). The data rate was 10 Gb/s and a Pseudo-Random Bit Sequence (PRBS) of 2^7-1, equivalent to the block coding of Ethernet PON systems, was used. The extinction ratio (ER) of the modulator was better than 13 dB. The bias of the MZM was readjusted to pass the unmodulated carrier not to worsen the OSNR. Due to the long reach, DCF with a dispersion of -1365 ps/nm were placed. A first EDF amplifier (OA_{LC}, OA_{LL}) with 5m of HE980 (or iXF-FGL for the L-band wavelength) and a low noise figure is used before the booster amplifier (OA_{BC}, OA_{BL}). A C/L splitter then combines both wavelengths. A ring with 50 km of standard single mode fiber (SMF) connects RN and OLT. For simplicity, a single fiber ring is implemented. The 6 km SMF drop fiber was put after the 1:32 splitter to keep the RB low as no means of mitigation were utilized, and the high launched power from the RN to overcome the high splitter loss would lead to a low Optical Signal-to-RB Ratio (OSRR) considering also the limited gain of the ONU and the resulting low upstream power level.

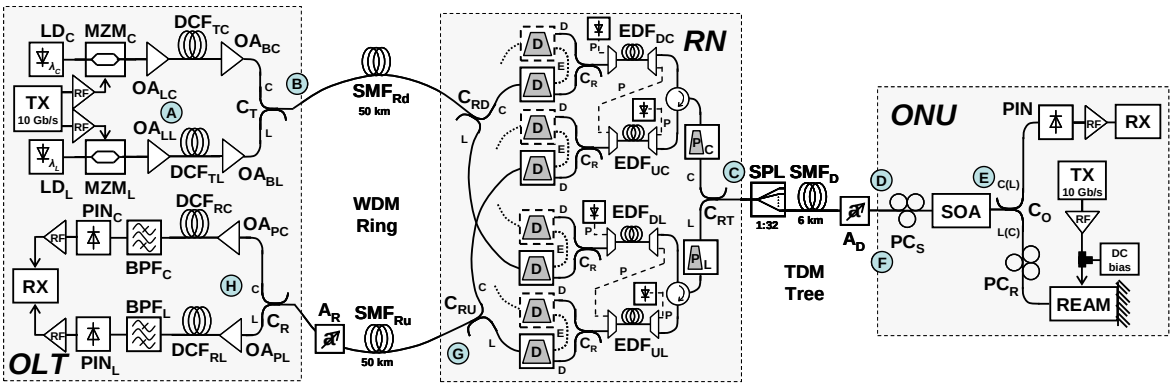

Fig. 7.11.Experimental PON setup. The RN provides remote amplification in the C+L band to provide two wavelengths at the ONU for downstream reception and upstream modulation.

At the ONU, a SOA with a small signal gain of 21 dB, centred in the C-band serves as preamplifier and booster, providing still 16.4 dB of gain in the L-band. The ONU has further a detection path, where a photo detector receives the downstream signal, and a remodulation path where a reflective modulator imprints the upstream on the incoming optical carrier. Both paths in the ONU are separated by a C/L waveband splitter and were further swapped by changing the output ports of the C/L splitter to show that they have in principle no preferred waveband. Although the L-band wavelength will miss gain in the SOA, the REAM that was used for remodulation was designed for the L-band where it has a slightly better performance in terms of ER and intrinsic loss. It was biased at -1.4V and -1.9V for the C- and L-band to achieve its optimum point of operation, and modulated with 3.5 V_{pp} at a data rate of 10 Gb/s with a

PRBS of 2^7-1, leading to an ER of 14 and 18 dB. With the intrinsic REAM losses of 15 and 11 dB, no cross gain modulation between down- and upstream was observed in the SOA, even with a bias of 200 mA. A PIN diode with a sensitivity of -18.5 dBm was used as detector in the ONU. For the Bit Error Ratio (BER) measurements, attenuators (A_D, A_R) were placed to vary the input power into the ONU and the OLT receiver.

The high splitting ratio in the tree makes the signal power level and the OSNR subject to strong dynamics along the transmission system, as can be seen in Fig. 7.12. The power levels and/or OSNR for the C-(L-)band were 47.5 (46.6) dB after the first amplifier (point A in Fig. 7.11), 6 (6) dBm and 44.5 (44.7) dB after the booster (B), 4.9 (2.6) dBm and 39.5 (41.1) dB at the tree interface of the RN (C), -13.3 (-15.4) dBm at the ONU input (D), 35.4 (35.8) dB after preamplification (E), 2.5 dBm (-1.8) dBm and 34.1 (33.4) dB after being remodulated and boosted (F), resulting in a net gain of the ONU of 15.8 (17.2) dB, and -3.7 (-9) dBm and 32.2 (32.6) dB when injected into the upstream ring fiber (G). The OLT preamplifier (OA_{PC}, OA_{PL}) with a noise figure of 4 (4.1) dB (H) was followed by a 60 GHz bandpass filter and a PIN diode with a sensitivity of -18.5 dBm. The OSRR at the tree was determined by the high splitting ratio and the high net gain of the ONU. The downstream signal arrives with quite low power at the drop fiber, and together with the relative high launched power from the ONU the OSRR for the upstream is higher than 40 dB for the C- and also for the L-band wavelength. However, the downstream transmission is more critical as the upstream that is boosted by the ONU will cause a significant distortion for the downstream due to RB in the drop fiber. The downstream OSRR for the C- and L-band wavelength was ~21 dB, but will not cause BER floors above 10-10 as will be proven later in this section.

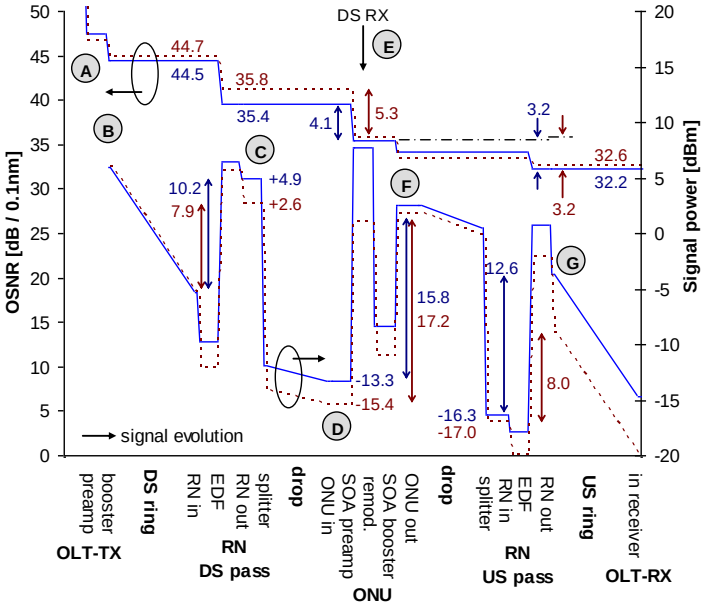

Fig. 7.12.Evolution of OSNR and signal power for C- (solid) and L-band (dashed line) along the PON for downstream and upstream.

The net gain of the RN, defined between the ring and the tree interface for the downstream or vice versa for the upstream, is 10.2 (7.9) dB for the downstream and 12.6 (8.0) dB for the upstream. Looking at the drop amplification of the downstream, the EDF of the C-band wavelength already becomes saturated for the downstream

amplification while the EDF for the L-band wavelength does not due to the higher drop losses from the ring. The upstream gain in the RN benefits from the limited net gain in the ONU, which causes low input powers for the EDFs. Slightly higher gain values can be therefore obtained even for a lower pump. However, this unsaturated gain conditions are gathered at the cost of another 3.2 dB of OSNR degradation, which could be avoided with increased ONU net gain.

Consequently, most problematic in the PON is the high loss in the splitter, as there is a high OSNR degradation in the consecutive amplifying stage due to its low input power. Especially for the downstream this is critical as the SOA has a high noise figure of 6.4 (6.6) dB in addition. Keeping several input power levels moderate at the input of the amplification stages along the way from the modulator at the OLT transmitter towards the ONU, the ONSR stays at a high level but is also vulnerable to noise that is accumulated at the following amplification stages. The preamplification in the SOA of the ONU degrades the input OSNR therefore by 4.1 (5.3) dB. However, the OSNR for the downstream detection is high enough to have acceptable sensitivities for the downstream detection, as can be seen in the BER measurements shown in Fig. 7.13.

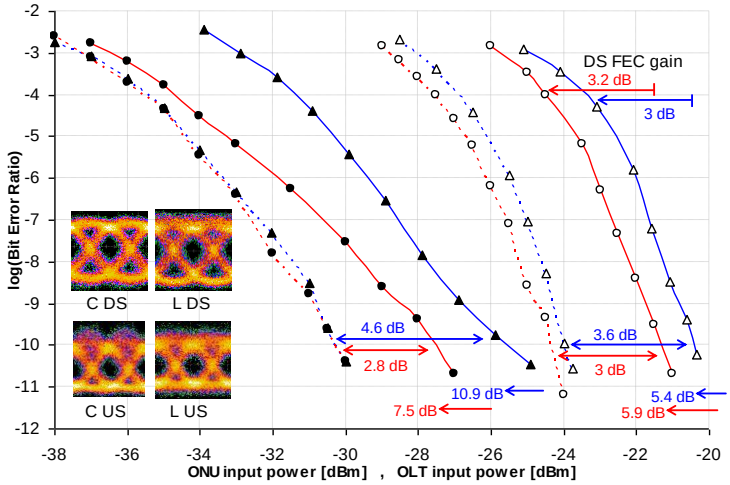

Fig. 7.13.BER curves for full-duplex 10 Gb/s downstream (DS, hollow markers) and 10 Gb/s upstream (US, filled markers) transmission. Single ended arrows indicate the reception margins for a reach of 56 km and a split of 1:32 in the tree. Dashed lines correspond to the back-to-back case, while solid lines indicate the presence of ring+tree fiber. ▲,● markers show measurements in the C- and L-band, respectively.

The sensitivity for a BER of 10^{-10} in the back-to-back case, where the ring+tree fibers were replaced by their equivalent attenuation, is -24 and -24.3 dBm for the C- and L-band wavelength, respectively. When fibers and DCFs are added, an additional penalty of 3.6 and 3 dB is obtained. Therefore, a power margin of 5.4 and 5.9 dB is obtained for a BER of 10^{-10}, large enough to cope for additional splices and other unforeseen losses that may arise over time in a PON.

The upstream sensitivities for the C- and L-band are -30.2 and -30.3 dBm for the back-to-back case and a penalty of 4.6 and 2.8 dB is caused when fiber and DCFs are used. Nevertheless, for a BER of 10^{-10} power margins of 10.9 and 7.5 dB for the upstream are provided even without additional error correction techniques.

The obtained margins could be used to increase split or distance further. The sensitivity of the downstream which is limiting this extension in split or reach, would allow to increase the splitting ratio in the tree to 1:64 or an increase in reach of about 25 km. If Forward Error Correction (FEC) with an acceptable BER of 10^{-4} is taken into consideration for the ONU receiver, the margin would increase to 8.4 and 9.1 dB for the C- and the L-band wavelength (Fig. 7.13). This in turn would then allow increasing the splitting in the tree up to 1:128 or the distance by 40 km.

7.3.3 Conclusion

An RN design for dual waveband operation, which satisfies the requirements of an extended reach and high split WDM/TDM-PON, has been characterized. Depending on the waveband, a net gain of 8-12 dB was obtained next to incorporating dual wavelength drop functionality and resiliency for the ring-based PON. Despite the reduced OSNR of 32 dB at the OLT receiver, error-free operation can be obtained with a margin of 5-10 dB for C- and L-band, whereas the downstream transmission has been shown to be more critical

With the covered wavelength range from 1530-1563 nm in the C- and 1570-1600 nm in the L-band, in which sufficient gain can be provided for the given power margins, a PON with data transmission on 32 wavelengths in each waveband can be considered, serving with a splitting ratio of 1:32 in the tree altogether 1024 users with a full-duplex data transmission of up to 10 Gb/s. Together with the nominal reach of 56 km for the PON, a capacity-length product of 17.9 Tb/s km is provided.

When the margins are eroded for the benefit of increasing the splitting ratio or the reach, a split of 1:128 or additional 40 km of distance can be provided when error correcting codes are utilized at the downstream receiver.

Chapter VIII
Dispersion compensation in optical networks

In this chapter, we present the study of the dispersion imposed restrictions on a WDM/TDM PON. In the first part, we examine the operation of the transmitters and how the laws of physics applied both on the light sources and propagation mean explain the dispersion on the network. Next, we present two possible tools to help combating these limitations, namely, dispersion compensation fiber and electronic equalization. Then, an experimental study performed with the use of those two dispersion compensating mechanisms on a WDM/TDM PON is presented, along with the relevant results, some comments and conclusions on them.

8.1 Dispersion, source induced chirp and fundamentals of equalisation

An optical signal becomes increasingly distorted as it travels along a fiber. This distortion is a consequence of intramodal dispersion and intermodal delay effects. These distortion effects can be explained by examining the behavior of the group velocities of the guided modes, where the group velocity is the speed at which energy in a particular mode travels the fiber. Intermodal dispersion or chromatic dispersion is pulse spreading that occurs within a single mode. The spreading arises from the finite spectral emission width of an optical source. This spectral width is the band of wavelengths over which the source emits light. It is normally characterized by the root-mean-square spectral width α_λ. Laser diode optical sources have a spectral width of typical value of 10^{-4} [100].

In this study we have tested the behaviour of two different transmitters in a WDM/TDM PON. Namely, a distributed feedback (DFB) laser source, externally modulated by a Mach-Zehnder modulator and an integrated DFB - Electroabsorption Modulator (EAM), have been examined. One of the characteristics strongly affecting the performance of the transmitters is the laser frequency chirp. The fundamentals of the modulators operation are described below.

The MZM is configured as an interferometer, thus it is referred to as Mach-Zehnder Interferometer (MZI). It uses two separate beam splitters to split and

recombine the beams, and has two outputs. The optical path lengths in the two arms may be nearly identical or may be different, e.g. with an extra delay line. In one state, the signals in the two arms of the MZI are in phase and interfere constructively and appear at the output. In the other state, applying a voltage causes a π phase shift between the arms of the MZI, leading to destructive interference and no output signal. The chirp can be controlled very precisely in such devices.

The EAM can be fabricated with the same material and techniques used to fabricate semiconductor lasers. This allows the EAM to be integrated along with a DFB laser in the same package, which results in a compact and low cost solution. The EAM uses a material such that under normal conditions, its band gap is higher then the photon energy of the incident light signal. This allows the light signal to propagate through. Applying an electric field to the modulator, results in shrinking the band gap of the material, causing the incident photons to be absorbed by the material. This effect is called Franz-Keldysh effect or Stark effect [101].
The chirping parameter can be estimated by the following expression [102]:

$$\alpha_{chirp} = \frac{4\pi}{\lambda}\frac{\Delta n_R}{\Delta \alpha} \qquad \text{Eq. 8.1}$$

Where, Δn_R is the change of the real part of the refractive index, which happens with the change of absorption coefficient, when electric field is applied. $\Delta\alpha$ is this change of the absorption coefficient. Two effects cause the phase response or chirp of the device. The modulator section presents some transient chirp due to the fact that the refractive index of the medium where the light is propagating changes when it is modulated. If the modulator were isolated from the laser section, there will not be other chirp effects. But due to reflections in the laser modulator interface there is some optical feedback that affects the laser behavior although it is being operated in CW mode. In particular, optical feedback causes a change in the threshold carrier density of the laser that originates a modulation in the effective refractive index of the laser section and a change of the lasing wavelength. This leads to some extra transient chirp and adiabatic chirp. Transient chirp is the responsible of frequency variations when the output optical signal changes and adiabatic chirp represents a change in the optical emitted frequency for different power levels (marks and spaces in a digital signal).As mentioned already, this is the main cause of dispersion in an optical fiber network.

The dispersion management is a way to ameliorate the performance of an optical fiber network, thus expand its dimensions. This objective can be reached with several techniques. Two of the ways to reduce the impact of chromatic dispersion, are, using external modulation in conjunction with DFB lasers and chromatic dispersion compensation. In this experimental study and in this thesis we have tried to combine those two factors. We have combined an externally modulated source, as well as an integrated one, with dispersion compensating fiber and electronic equalization. The principles of electronic equalizers and more specifically of the model used are presented subsequently.

8.2 Dispersion compensating fiber

The dispersion of a transmission fiber can be compensated with sections of fibers with different designs or with other optical elements. Dispersion compensation modules (DCMs) can contain, e.g., long pieces of dispersion-shifted fibers.
Dispersion-shifted fibers have modified waveguide dispersion so as to shift the zero dispersion wavelength into the 1.5-μm region. This is achieved by modifying the refractive index profile of the core. Common index profiles of dispersion-shifted fibers have a triangular, trapezoidal or Gaussian shape. There are also dispersion-flattened fibers with relatively constant group delay dispersion over some wavelength range, i.e., low higher-order dispersion. They can, for example, exhibit near zero dispersion in the telecom C band. Such fibers are important for data transmission with wavelength division multiplexing and for adiabatic soliton compression. They often have a W-shaped profile of the refractive index, although profiles with a graded index and multiple steps have also been developed. In this study we have used, 2.39km of a DCF with a total dispersion compensation value of -680ps/nm, corresponding to around 40km of SSMF.

8.3 Electronic equalizer

Electronic dispersion compensation can be used to counterbalance the accumulated

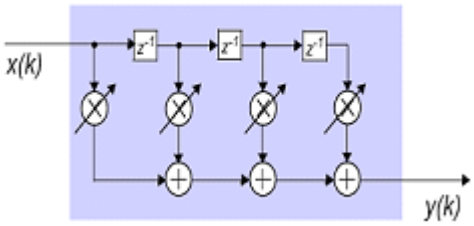

Fig. 8.1.The structure of an FFE

dispersion increasing the transmission length of the system. The scheme can be adaptive to the total dispersion depending on the transmission distance. As mentioned already in chapter four, there are three main architectures for ECE and the most basic scheme is the FFE (Fig. 8.1). In this structure, after the optical-to-electrical conversion a FIR filter is added to the transmission line. The filter has several stages. Every stage, consists of a delay element, a multiplier and an adder. After every delay element, an image of the non-delayed input is multiplied with a coefficient and added to the signal. The number of filter stages used and the coefficients chosen are essential for effective dispersion cancellation. Automatic control of the filter coefficients is crucial.

A second approach is the DFE appearing in Fig. 8.2. This structure is an FFE with a second FIR filter added to form a feedback loop. Again, the coefficients of both filters require active control. Today's integration levels, permit either FFE or DFE to be built into a clock-data recovery or demultiplexer chip, with an extra power requirement of about 500 mW.

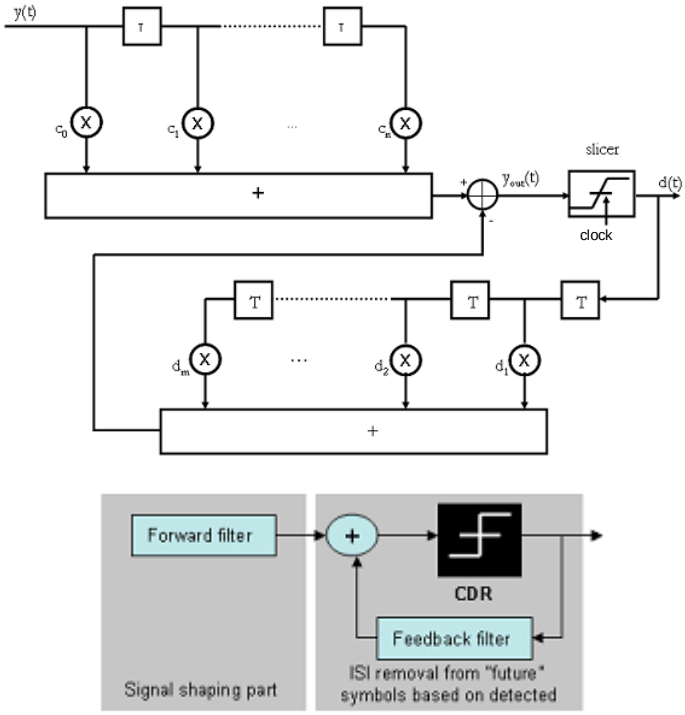

Fig. 8.2 The structure of DFE. {CDR: Clock and data recovery module, ISI: Intersymbol Interference}

The tap coefficients of the filter are calculated and adjusted in an adaptive operation according to an algorithm that runs in parallel. The purpose of this is the minimization of the error. The type of the algorithm and more significantly the way that this algorithm is optimized, are particularly important in order to minimize the error and enhance the transmission properties of the system. Training and decision mode are the operating modes of the adaptive equalizer. During the training mode the algorithm adjusts to the channel characteristics and calculates the filter taps to compensate for the introduced impairments. In the decision mode, small variations in the taps allow for the compensation of the time varying effects of the channel. The LMS algorithm is the most common algorithm used, in order to calculate the taps. The goal of that algorithm is to minimize the MSE between the desired equalizer output and the actual equalizer output. It is controlled by the error signal which is derived by the output of the equalizer with some other signal which is the replica of transmitted signal. The DFE version of the equalizer is a non- linear process that uses the same algorithm but subtracts the interference by the already detected data offering advanced performance characteristics. In this study, the examined EDC, is a FFE-DFE integrated circuit.

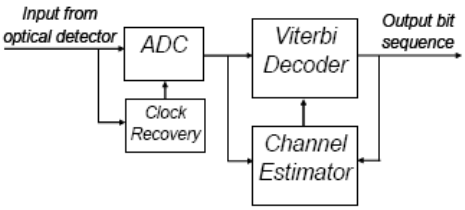

Fig. 8.3.Digital implementation of MLSE. (ADC: Analog – to digital converter)

8.4 Experimental study

Our suggested WDM/TDM PON architecture considers the use of reflective ONUs at the end users, in order to achieve colorless operation. This in general can be achieved either with the use of a dedicated CW signal fed by the optical line terminal (OLT) [103] – [105] or by re-modulating the down-stream propagated signal. In the former case the maximum achievable performance of the reflected ONUs is exploited but bandwidth utilization is reduced to half since each TDM PON tree requires two wavelengths. Furthermore the CAPEX of the network increases as the number of the required optical sources is higher. . In the latter case, the upstream signal is modulated on top of the downstream signal, which in turn must have an increased DC power level (i.e. low extinction ratio (ER)), in order to assure an adequate power level at the ONU for re-modulation [105] and to avoid residual crosstalk on the up-stream data. The increased DC bias corresponds to an increased optical power offset being applied to the downstream signals. Despite the optimized bandwidth utilization, due to the use of a single wavelength for upstream and downstream transmissions, the transmission performance of the downstream signal must be intentionally reduced, in order to allow the re-modulated upstream signal to be transmitted efficiently. Therefore, despite the optimized bandwidth utilization, due to the use of a single wavelength for upstream and downstream transmission, the transmission performance of the downstream signal is significantly reduced.

Evidently, and as it has been studied in [105], there is a compromise between the downstream ER and the overall transmission distance that can be achieved. When the ER of the downstream signal is reduced, the performance of the re-modulated upstream signal is increased. At the same time the performance of the downstream signal is reduced. By applying certain performance improvement schemes, either in the optical [106] or electronic domain [107], or both combined, the performance of the downstream signal with reduced ER can be significantly increased. In this case, an upstream signal with increased performance can be generated after re-modulation. It is noted that latest advances in coherent modulation systems are applied in PONs [108], however, due to the extensive use of electronics that is required, such schemes are still too expensive to be complemented at the ONU.

The general purpose of the work performed, is to study experimentally, different transmission performance improvement methods applicable in 10Gb/s optical signals,

with typical and reduced ER values, generated by two different types of transmitters, with different chirp characteristics. More specifically, a MZM and an EAM type of transmitter have been considered and operated at two different sets of driving voltages, resulting in ER values of 3dB and 9dB. The signal improvement methods considered were based on: a) the use of fixed dispersion compensation fiber able to compensate for half the maximum transmission distance, b) the use of electronic equalization and c) the combination of the aforementioned techniques. The performance was evaluated for typical, moderate and long reach PON applications up to 100km, for both types of transmitters and ER values and for all the signal improvement methods.

The two values of ER that have been considered in this study (3dB and 9dB), are proven to be appropriate for use in WDM/TDM PON in combination with colourless ONUs. First, a signal modulated with a high value of ER, namely 9dB, was tested in the testbed created. This signal could be used in combination with a CW dedicated to upstream remodulation. The value of ER =9dB has been shown to be appropriate for all optical cancellation in the case of colourless ONUs, as in [109]. Second, the case of low ER, namely 3dB, is shown to be ideal for efficient signal remodulation [106], but also for the more advanced feed forward cancellation method presented in [110].

In the case of the 3dB ER, the reduced receiver sensitivity, due to the poor downstream signal quality, becomes a major issue in long reach PONs, mainly because of the chromatic dispersion penalty. This penalty can be mitigated with the use of either DCF, or electronic dispersion compensators (EDCs). In long reach PONs, due to the specific network design considerations and in order not to increase the signal power losses, it is possible to use the DCF as pre-compensator at the OLT side of the PON, providing partial compensation around half of the maximum transmitted distance. The wide operating bandwidth of DCFs allows the sharing of the DCF module among all users in a WDM/TDM PON, reducing significantly the additional cost per user. On the other hand, EDC can be used only as post-compensator, at the receiver side; therefore it must be included at each ONU increasing its cost. However, EDC offers adaptive dispersion compensation with respect to the transmission distance and optimizes the transmission performance particularly for long distances. The extra cost of the EDC can thus be counterbalanced by the consequent reach extension of the PON. It should be noted that currently, WDM/TDM PONs (e.g. Next generation PONs-NGPON2) use tunable filters in ONUs as an alternative way to achieve colourless operation, we have taken under consideration though, that a possible increase in the number of wavelengths used, could render the use of RSOA, more cost effective.

In the case of the 9dB ER signal, the behaviour of the network is intensely affected by the existence of chirp. When no chirp is present, it is possible to reach the maximum distance using no means of signal improvement. Overall, it has been observed that with both transmitters – regardless of the chirp- the application of such methods evidently offers a much more uniform behaviour in terms of OSNR vs. BER for several lengths of the network. Therefore it is apparent that, from a practical point of view, the design of a long reach PON with improved performance can become

problematic when transmitters with different chirp characteristics are considered. In this work, the performance of 10Gb/s MZM- and EAM-based sources, operated at two different low-driving voltages (resulting in 3 and 9dB of ER correspondingly), considering additionally, both, the aforementioned dispersion penalty and the improvement methods of partial pre-compensation with DCF and adaptive post-compensation with EDC, is practically evaluated.

8.4.1 Experimental set-up

The complete experimental setup for all the examined cases is shown in Fig.8.4. The two types of low-driving voltage sources examined are:

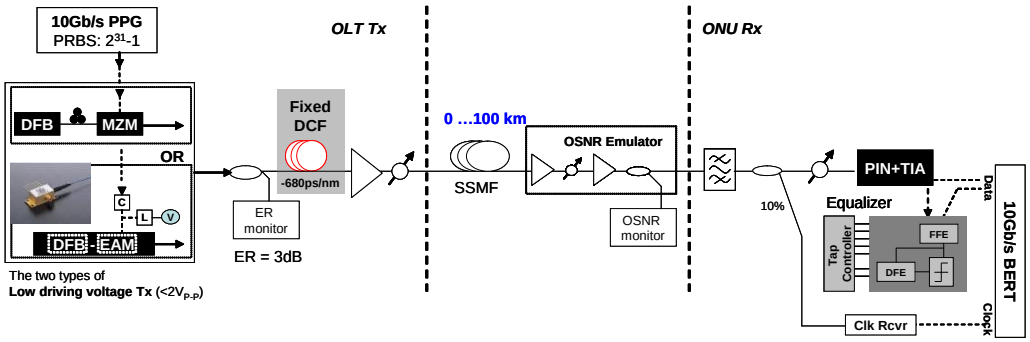

Fig. 8.4. Experimental set up for the performance evaluation of low-driving voltage DFB-MZM and DFB-EAM transmitters, over 0 to 100km links and for two dispersion compensating schemes DCF partial pre-compensation and FFE-DFE post compensation

a) An externally modulated DFB -by the use of a MZM- source, operating at 1541.35nm with peak-to-peak voltage (V_{P-P}) of 1.2V and amplifying bias voltage (V_{bias}) of 1.3V, being applied at the MZM for the 3dB ER and 2V of V_{P-P} with 1.3V of V_{bias}, to achieve 9dB ER.

b) An integrated DFB-EAM source, emitting at 1539.46nm and being driven at the EAM section via an external bias-T at 530mV_{P-P} and V_{bias} of - 2V for 3dB ER and at 2V_{P-P} with V_{bias} of -1.7V for 9dB ER. A 9.952Gb/s signal with 2^{31}-1 long PRBS pattern was used and was launched directly by the pattern generator to the modulators, without the use of electrical amplifiers. The V_{P-P} and V_{bias} values in each case resulted in optical signals of 3 and 9dB ER. The signals are then launched on variable lengths of standard single mode fiber (SSMF), ranging from 0km (back-to-back (b2b)) to 100km. The launch power was fixed at 6dBm in all cases. Before the receiver, an OSNR emulator is used, consisting of a variable optical attenuator (VOA) and an EDFA, in order to alter the level of OSNR for the measurements and emulate the extender box or remote amplification process in long-reach PONs. At the receiver end, the signal was filtered with a 0.8nm Gaussian filter and received by a p-i-n photodiode (PIN) followed by a trans-impendence amplifier (TIA). The receiver input power at the PIN was always adjusted via an optical attenuator at -10dBm. The two compensating schemes considered are indicated with the grey shaded areas in Fig.1. For the case of partial

optical pre-compensation, a fixed length of DCF was used before the booster EDFA at the output of the OLT, with a total dispersion compensation value of -680ps/nm, corresponding to around 40km of SSMF. For the case of post-compensation with EDC, an integrated 5-tap FFE and a 2-tap decision-feedback equalization DFE circuit was used and controlled by properly adjusting the taps for optimum BER. A BER tester was connected, either directly on the PIN-TIA output, or the EDC output for the cases of DCF- and EDC-based compensation, respectively. The reference clock for the measurements is provided either via an external clock recovery circuit, or directly by the EDC circuit, depending on the compensation method.

Finally, it should be noted that in the results, presented next, the performance has been studied in terms of BER versus OSNR, since in long-reach access-metro networks, the use of amplification (either with remote amplification schemes [103], or with optical amplifiers [104]) is considered in the network. In these cases, the power budget issues are resolved, but the input signal level in the amplification sections, as well as the type of amplification, affect the signal's OSNR.

8.4.2 Results

For nearly zero-chirped, externally modulated sources (DFB-MZM), the increase of ER, highly decreases the required OSNR (ROSNR), for an error-free transmission without FEC (BER=10^{-9}) [111], as can be seen in Fig.8.5.

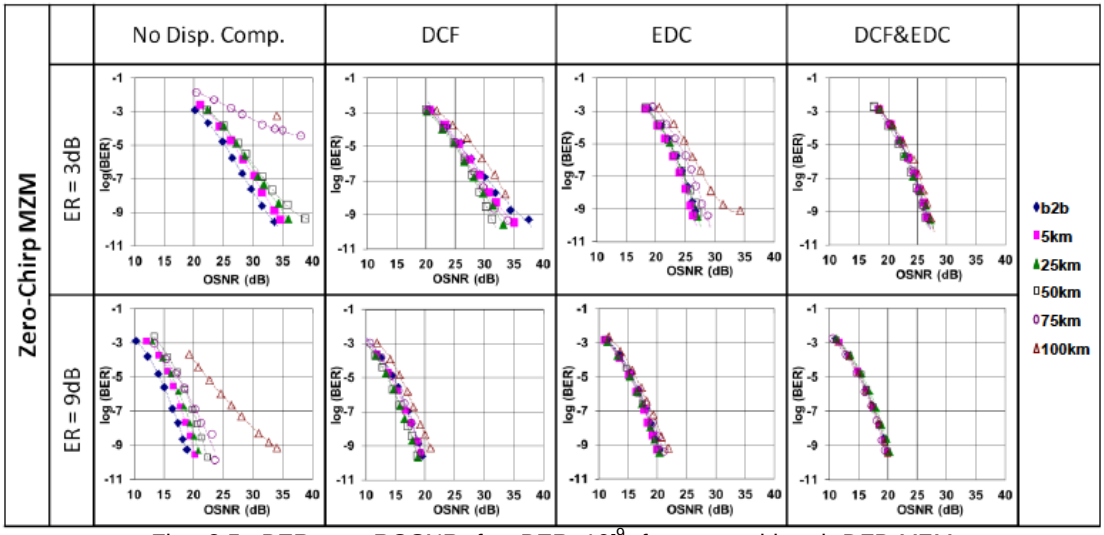

Fig. 8.5. BER vs. ROSNR for BER=10^{-9} for zero chirped DFB-MZM transmitter in the cases of: no dispersion compensation, DCF only, EDC only, DCF and EDC when signals of 3 and 9dB ER are transmitted

Even though in commercialized 10Gb/s PONs the use of FEC is nowadays mandatory, in our effort to give a complete study of the behaviour of the system, performance for both BER=10^{-9} and BER=10^{-3} has been investigated. Moreover, in Fig.8.5 we observe that when no compensation or equalization is applied, error-free performance is possible, with an ER of 9dB, for lengths that it was impossible with an ER of 3dB. With the use

of DCF, for ER=3dB, high ROSNR values such as 32dB were observed for very long distances such as further than 50km, while for ER=9dB any distance up to 100km is possible with a ROSNR value less than 21dB. For the 3dB ER signal, the DCF decreases the ROSNR in the case of 50km transmission length, which is expected, as the value of the DCF has been chosen to compensate for half the maximum SMF length, but in all other cases it does not offer a substantial improvement. In fact, the extra 40km of fiber that the signal has to propagate through, cause attenuation, this results in higher ROSNR. In the case of 9dB ER, partial pre-compensation by using DCF, improves system performance for all distances up to 100km. With electronic compensation (EDC) for ER=3dB and up to 75km, system performance improves significantly -more than 5dB- while for ER=9dB, no performance improvement is observed in comparison with the use of partial DCF compensation. With combined partial DCF and EDC, independently to the operating ER, the system becomes almost dispersion independent, manifesting just about the same performance for all distances between 0 and 100km both for 3 and 9dB of ER. The reduction in the ROSNR, when the ER increases from 3 to 9dB, in this last scenario, is about 6dB.

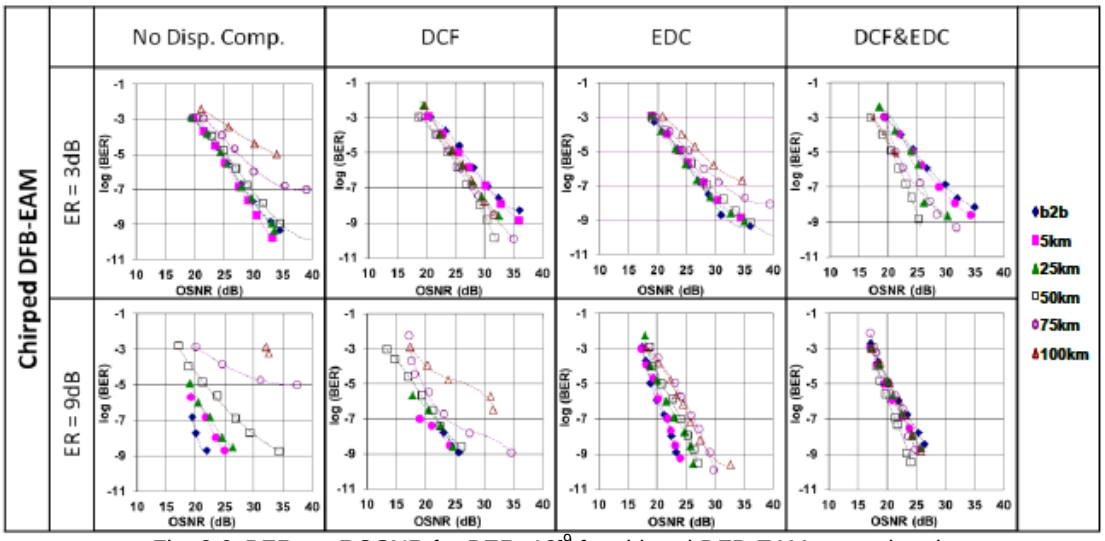

Fig. 8.6. BER vs. ROSNR for BER=10^{-9} for chirped DFB-EAM transmitter in the cases of: no dispersion compensation, DCF only, EDC only, DCF and EDC when signals of 3 and 9dB ER are transmitted

The results collected for the chirped DFB-EAM transmitter appear in Fig.8.6. It is noticed that i) when no means of signal improvement are used, the lower ER helps achieving a more constant operation compared to the high ER, whilst ii) when means of signal improvement are applied, the performance of a high ER is evidently better and clearly very efficient when the combination of EDC and DCF is applied on the transmission of the signal. As it has been remarked in [112] and as one can observe from the results, there is a trade-off between a high ER and dispersion control. This is most obvious in the case of no dispersion compensation or equalization. With the generated chirp and without any compensation, it is noticed that an error-free performance is possible only for link lengths up to 50km. The performance improves first with the distance and starts degrading after 25-30km indicating that the utilized

EAM has a negative chirp. In the case of high ER, the chirp dependent power variation caused by the reflections in the fiber, generates interference that gives a reduction in the eye-opening at the receiver [10], which proportionally, is larger then in the case of the low ER. Therefore, the dispersion penalty is larger on the high ER signal, than on the low ER one. When DCF is used, the performance improves for long distances in the range of 50km for both ER values, but performance for short distances is degraded. It is detected that no error-free transmission (BER=10^{-9}) can be achieved for very long distances such as 100km. The reason is, that the applied DCF compensates for half the maximum SMF length, therefore the cases of 0 and 100km namely, are the ones with the worst performance. When EDC is used and ER=3dB, there is no actual benefit in comparison to partial dispersion compensation, except some limited improvement for very long lengths. When the signal has an ER of 9dB, there is significant performance improvement, allowing error-free transmission over any distance up to 100km with a ROSNR lower than 30dB. Finally, when partial dispersion compensation and EDC is combined, there is a small performance improvement for the case of the 3dB ER and larger improvement for the case of the 9dB ER.

TABLE 8.1
Mean value of ROSNR decrease (dB) for the several transmission lengths to achieve a BER of 10^{-9}

Decrease of ROSNR when ER increases from 3 to 9dB		
	DFB-MZM	DFB-EAM
NoDCF	12dB	
DCF	14dB	7dB
EDC	7dB	4dB
EDC&DCF	6dB	2dB

A part of the significant findings are reported in Tables 8.1, 8.2 and 8.3. Table 8.1 represents both transmitters' decrease of the ROSNR for an error-free transmission, when the ER increases from 3 to 9dB. The values chosen are the mean ROSNR values in all transmission lengths and in each case. The DFB-EAM, due to the inability to reach a BER of 10^{-9} without the use of signal improvement means, has no value in the first row. Additionally, what has been detected regarding the shift of the ROSNR when the ER increases, is that it can reach even 12 dB in the case of no dispersion compensation or equalization and 14dB in the case of DCF use. The second value is larger in this case, as the use of DCF causes considerable attenuation on the 3dB ER signal which is not the case when the ER increases.

TABLE 8.2
Spread of the ROSNR (dB) for the several transmission lengths to achieve an error free signal without FEC (BER=10^{-9})

ROSNR spread				
ER	3dB	9dB	3dB	9dB
	DFB-MZM		DFB-EAM	
NoDCF	4 dB	15 dB	0.8 dB	- dB
DCF	4 dB	2 dB	2.5 dB	- dB
EDC	5 dB	1 dB	4 dB	- dB
EDC&DCF	1 dB	0.1 dB	6 dB	5 dB

It is observed, that the two values of ER have less difference in ROSNR for error free performance when EDC is used, either alone, or in combination with DCF. In the case of no dispersion compensation or equalization, as the spectrum is broadening due to dispersion, the receiver sensitivity worsens; therefore the increase of ER has a significant impact on the ROSNR for DFB-MZM. For chirped DFB-EAM, the spectral broadening, when no dispersion compensation is applied, is so intense, that an error-free signal was impossible to be achieved. The behaviour of the system, thus the considerable decrease of ROSNR in the case of dispersion compensation is due to the use of partial compensation scheme with affixed DCF that corresponds to the full compensation of 40km of SMF, for the case of DFB-MZM but not for the case of DFB-EAM, due to its negative chirping. Moreover, the combination of DCF and EDC proves to give a homogenous behaviour on the transmission system even in the case of varying the ER, as from the results one can see that the decrease of ROSNR is rather small when compared to all the other scenarios.

TABLE 8.3
Spread of the ROSNR (dB) for the several transmission lengths to achieve an error free signal with FEC (BER=10^{-3})

	ROSNR spread			
ER	3dB	9dB	3dB	9dB
	DFB-MZM		DFB-EAM	
NoDCF	2.5 dB	4 dB	4 dB	4.5 dB
DCF	2 dB	1 dB	1.5 dB	4 dB
EDC	2 dB	1 dB	1.5 dB	2.2 dB
EDC&DCF	1 dB	1 dB	3 dB	0.7 dB

Finally, DFB-MZM as well as DFB-EAMs have an optimum ER which is ideal for achieving the least dispersion in long distances transmission, therefore the lower dispersion power penalty for long distances. It is detected from the results presented, that the DFB-MZM has a larger optimum ER while the chirped DFB–EAM has a low one. So, as one can see on the left column, for the DFB-MZM there is a larger decrease of ROSNR than on the right column of the DFB-EAM. Table 8.2 depicts the spread of ROSNR, for error-free transmission without FEC (BER=10^{-9}), along the several transmission lengths, for 3 and 9dB of ER and for all scenarios for both transmitters. The values of DFB-MZM ROSNR for BER=10^{-9}, when no means of dispersion compensation or equalization are used, have a spread of 4dB for ER=3dB and 15dB for ER=9dB. These spread values strongly decrease when the dispersion is compensated and the signal equalized. As observed in Table 8.2, for both values of ER, the spread in the case of combined use of EDC and DCF takes a value of 1 and 0.1dB correspondingly, which means that the performance of the system can be easily predicted. In the case of DFB-EAM, due to the high chirp, an error-free performance could not be achieved for ER=9dB in any other case, then in the combined use of DCF and equalization.

On the other hand, as far as the evaluation of the system in the case of FEC use is concerned, in Table 8.3, where the ROSNR for BER=10^{-3} is presented, it is indicated, that the spread of ROSNR is smaller for the 9dB ER signal of the DFB-MZM in all

cases, but the one where no dispersion compensation or equalization are being used. Evidently, this combination of transmitter and ER offers a very good solution in terms of behaviour predictability. The DFB-EAM modulated with 9dB ER, has in most cases, a large spread of ROSNR, while it is depicted that, in the case of application of both dispersion compensation and equalization, it displays the most homogenous behaviour of all the combinations of transmitters, ERs and signal amelioration techniques.

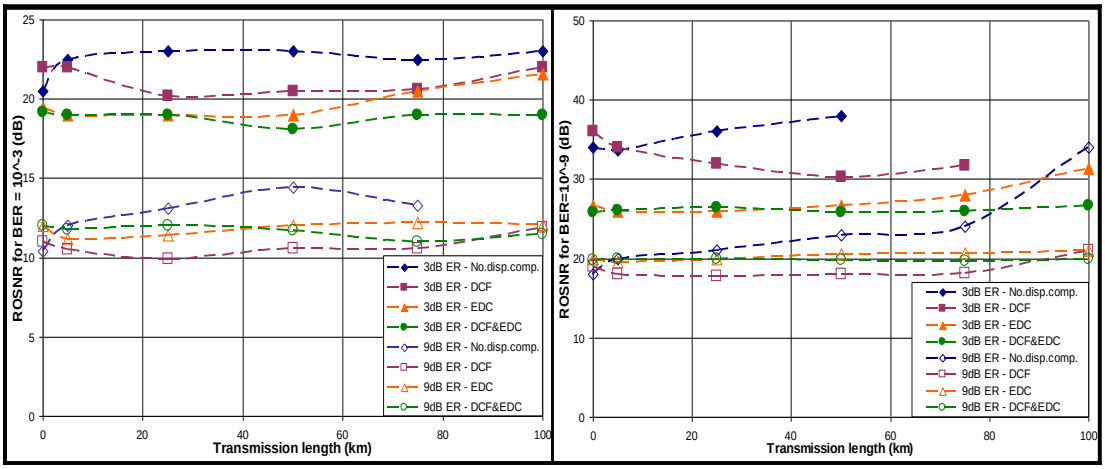

Fig. 8.7. ROSNR vs transmission length for DFB-MZM transmitter for the cases of: i) BER=10^{-3} and ii) BER=10^{-9}

From Fig.8.7., where the ROSNR for error-free transmission i) with and ii) without FEC correlates with the DFB-MZM signal transmission length, it is observed that the most homogenous behaviour is the one of the 3dB ER for a BER of 10^{-3} when no dispersion compensation is applied, while requiring the highest OSNR. In the case of FEC usage, the best performance is depicted for 3dB ER when the use of DCF is combined with EDC, while in the case of 9dB the combination of the two signal improvement techniques gives the more stable behaviour and overall provides one of the less requiring solutions in terms of OSNR. In the case of ROSNR for BER=10^{-9} the same observation can be made. Once more, the combination of DCF and EDC offer the best performance and the most stable ones, both in the case of 3 and 9dB. This time though, the numerical difference between the ROSNR is much less –in the order of 6dB- than in the case of 10^{-3}-BER.

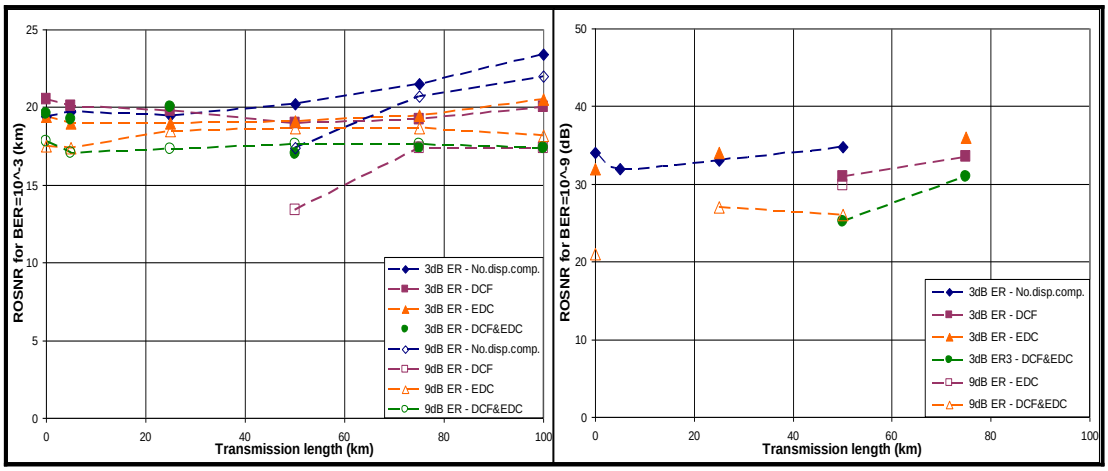

Fig. 8.8. ROSNR vs transmission length for DFB-EAM transmitter for the cases of: i) BER=10^{-3} and ii) BER=10^{-9}

In Fig.8.8., the corresponding results are depicted for the DFB-EAM transmitter. In 5i) the required OSNR for an error free transmission with the use of FEC (BER=10^{-3}), versus the transmission length is presented, for signals with ER of 3 and 9dB. The scenarios examined are the following: a) no dispersion compensation, b) only DCF fiber is applied right after the transmitter; c) only equalization takes place in the receiver's end d) DCF in the transmitter and EDC in the receivers end are combined. In 5ii) the results for the same signals and the same scenarios, but for achieving an error-free transmission of BER=10^{-9}, are presented. As one can see in 8.8i), the 10^{-3} BER can be achieved with both ER in some scenarios. Furthermore it is observed that the response of the system, despite the chirp of the transmitter can be easily predicted due to the homogenous behaviour presented, especially when equalization is applied. Once more the best performance is achieved with the combination of EDC and DCF for the 9dB ER. The required OSNR is quite low in this case, varying around17dB. In 8.8ii) one can observe that the induced chirp makes impossible for the EDC to lock in a frequency allowing the taking of the measurements. The dispersion caused due to the chirp is so strong, that it is not achievable to take measurements for any other case then the case of 3dB and no dispersion compensation or equalization.

8.4.3 Conclusions

The results have shown that the behaviour of the network depends on two very important parameters. The first is the chirp of the transmitter and the second one the value of the ER. The different signal improvement methods contribute differently in each case. The best combination, as it can be seen in Fig.8.4 and Fig.8.5, is the one of 9dB ER with DCF and EDC regarding signal improvement, which offers a dispersion independent uniform behaviour and an error-free performance at all lengths up to 100km with an OSNR value of up to 20dB. The 3dB ER with the same improvement method is a lower energy consumption solution that requires up to 26dB OSNR.

Moreover, it has been observed that the transit from ER=3dB to ER=9dB causes a significant decrease on the ROSNR, which especially when no means of signal improvement are used, or when low cost (due to its attribute of being shared among end users) DCF is used, can reach even the 14dB. In other words, even when the lowest CAPEX solution is chosen, with a very small change in the value of driving voltage, the quality of the transmission can significantly improve. On the other hand, the choice of combining DCF in the transmitter (OLT) and EDC in the receiver (ONU) gives a very constant behaviour for all different lengths, therefore it can be easily suggested when the standardization of a PON is the main target. Finally, the combined use of EDC and DCF can help improve the transmission by a range of 10dB of ROSNR which is translated into cost savings.

Chapter IX
Combination of in-line and extended band and equalization for WDM/TDM PON

The combination of all the techniques used throughout this thesis, for the optimization of a WDM/TDM PON, was realized in the framework of an experimental study. The scope of this experiment was to use all the designs and solutions studied up to now into one implementation, in order to achieve the maximum performance possible. In this sense, the in-line amplification by means of remotely pumped EDFAs was combined with C + L band operation of the WDM/TDM PON. For this reason a special C + L band remote node was designed and mounted. Raman amplification was used for the upstream signals and the use of equalization was studied in the downstream signals. The first paragraph of chapter 9 gives an outline of the WDM/TDM PON design examined. In the second paragraph a description of the experimental set up is given, while in the third part the results of the study are presented.

9.1 Technical description

A double-fiber ring WDM/TDM PON has been implemented. The design was based on an existing ring-tree based architecture [1]. A number of signals emitting on both C- and L-band were multiplexed with the use of an Arrayed Waveguide Grating (AWG) and then launched into the downstream fiber. For the amplification of the signals, in-line remotely pumped EDFAs were used. A pump laser emitting at 1480 nm was launched in the upstream ring, so as to offer Raman gain to the upstream propagating signals.

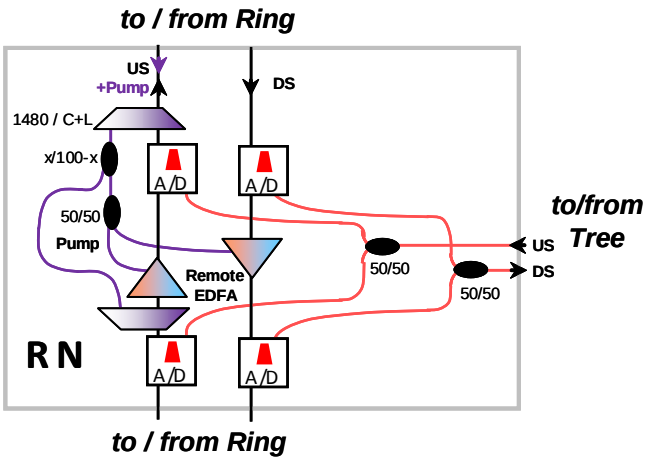

Fig. 9.1.Remote node design operating in C + L band with the use of remote amplification of EDFAs placed in-line with the propagating signals

The signals were dropped with the use of three-port thin-film filters before entering the corresponding in-line remotely pumped EDFA. When this RN design (Fig. 9.1) is used for the implementation of the WDM/TDM PON, the signal serving each tree needs to have the adequate power to reach the furthest ONU of the tree, without receiving extra amplification in the RN in which it is being dropped. In other words: if S_1 is the signal being dropped in the first TDM tree and RN_1 the RN serving this tree, then the signal S_1 will be dropped with the use of a filter, before entering the in-line EDFA situated in this RN. This becomes clearer in Fig. 9.1.

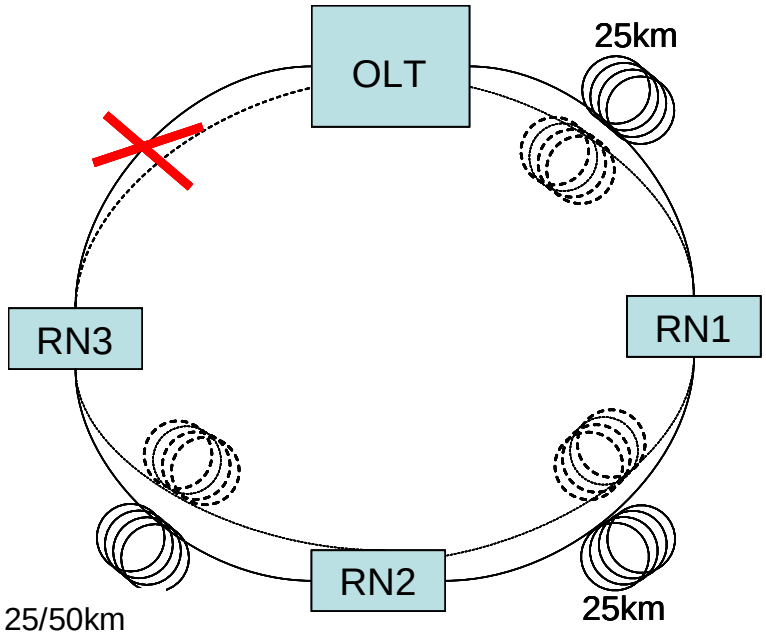

Fig. 9.2. WDM/TDM PON design operating in C + L band with the use of remote amplification of EDFAs placed in-line with the propagating signals

On the contrary, the rest of the signals, namely S_2, S_3, …S_N that are dedicated to the TDM trees T_2, T_3, … T_N correspondingly, will pass through the EDFA placed between the two thin-film filters in the RN_1, all of them being amplified simultaneously.

In this experiment we consider a double-fiber WDM ring with 3 RNs positioned in a distance of 25km from the CO, 50km and 75km correspondingly, as they appear in Fig. 9.2. This design is transformed, in the worst case of a fiber cut (e.g. between the OLT and RN_1 or RN_3), into a 75km double-fiber WDM trunk. Furthermore, in an attempt to extend the limits, a RN has been placed in a 100km distance from the CO for the last set of measurements. The TDM trees have 6km reach and several splitting ratios have been examined. The ONU receivers are implemented with the use of APDs and in some cases the use of an integrated 5-tap feed-forward equalization (FFE) and a 2-tap decision-feedback equalization (DFE) circuit is considered for the equalization of the signals. The ONU transmitter is implemented with a continuous wave (CW) transmitter, a REAM and an RSOA.

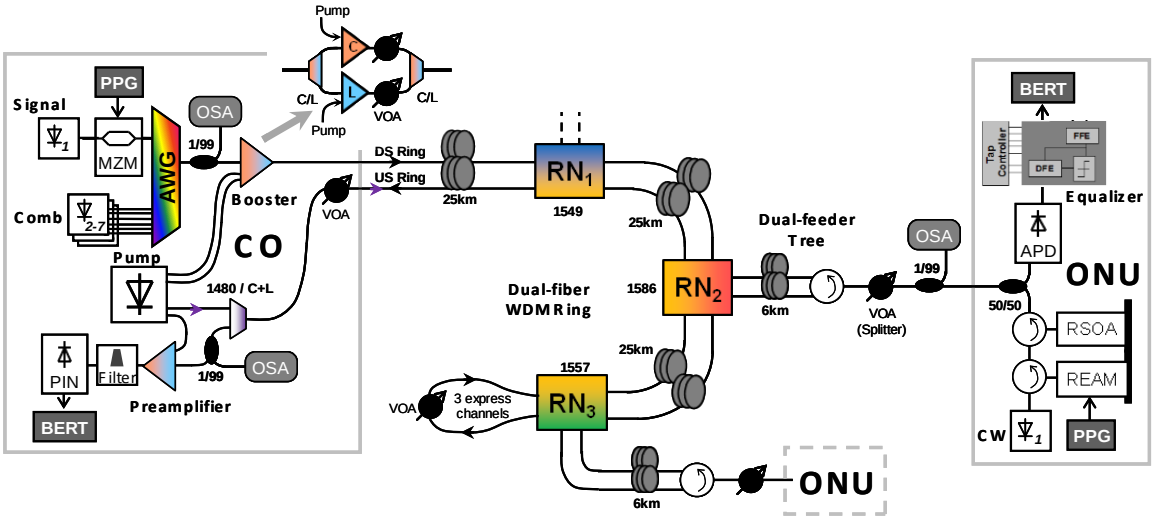

Fig. 9.3. Experimental set up used to test a WDM/TDM PON operating in C + L band with the use of remote amplification of EDFAs placed in-line with the propagating signals

9.2 Experimental set-up

The system investigated consists of seven laser sources emitting on the wavelengths: 1541.1, 1549, 1557, 1571, 1586.2, 1598 and 1600nm, correspondingly. Three RNs, especially designed for in-line amplification in both C+L band (Fig. 9.1.), where placed in distances of 25, 50 and 75km, respectively, as can be seen in Figures 9.2 and 9.3.

As a maximum reach evaluation, a 100km WDM ring was tested. That was implemented by increasing the distance between RN_2 and RN_3 by another 25km. The downstream signal is modulated at the CO on a CW signal with the use of a Mach-

Zehnder modulator (MZM) at 10Gb/s, using a PRBS 2^{31}-1. The downstream has been implemented as continuous data stream. The modulated channels under study were coupled together with the remaining wavelengths forming the dummy comb, using a 40-channel AWG with 100GHz grid. The modulated channels were namely: one emitting at 1549nm with 2.4dBm, one at 1557nm with 3.6dBm and one emitting at 1586.2nm with 3dBm. The dummy comb consists of wavelengths of both C and L band. More specifically, we have used the following wavelengths: 1541.1nm emitting with a power of -0.6dBm, 1571nm emitting with 2dBm, 1598nm emitting with 4dBm, 1600nm emitting with -4dBm. These signals have not been modulated, just multiplexed with the 3 modulated signals that were dropped in the 3RNs of the network. After the AWG a C/L combiner splits both bands for the booster stage, where a dedicated booster for each band is used. After the booster stage a C/L combiner is used to combine again both bands and launch the comb in the downstream ring. A variable optical amplifier (VOA) controls the total output power. The launch power was 4dBm per channel. No means of dispersion compensation were used at the OLT.

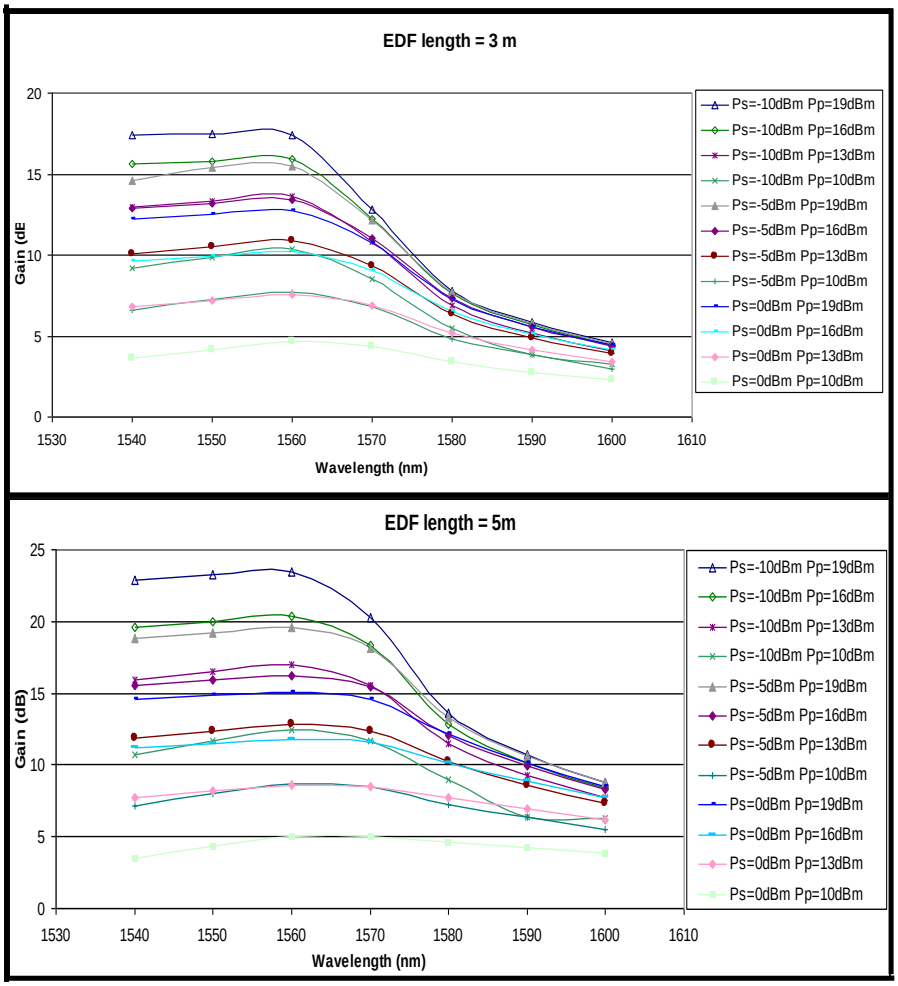

Fig. 9.4.) Characterization of the EDF used in the amplification stage of the RN, for a) 3m, b) 5m of length and 0dBm, 5dBm,10dBm of input power and various pump power values of 10dBm, 13dBm, 16dBm and 19dBm respectively

The dual fiber 75km WDM ring is made of 6 SMF spools of 25kms, 3 for downstream and 3 for upstream. This set-up corresponds to a 75km trunk with 3RNs in the worst-case resiliency scenario (i.e. fiber cut between OLT and RN_1 or RN_3). The RN drop channels are distributed as follows: 1549nm is dropped at 25km, 1586.2nm at 50km and 1557 at 75km. The TDM tree is composed by 6km of dual-fiber feeder to avoid strong Rayleigh backscattering at the bidirectional tree. A VOA is used to emulate the splitter stage between RN and ONUs.

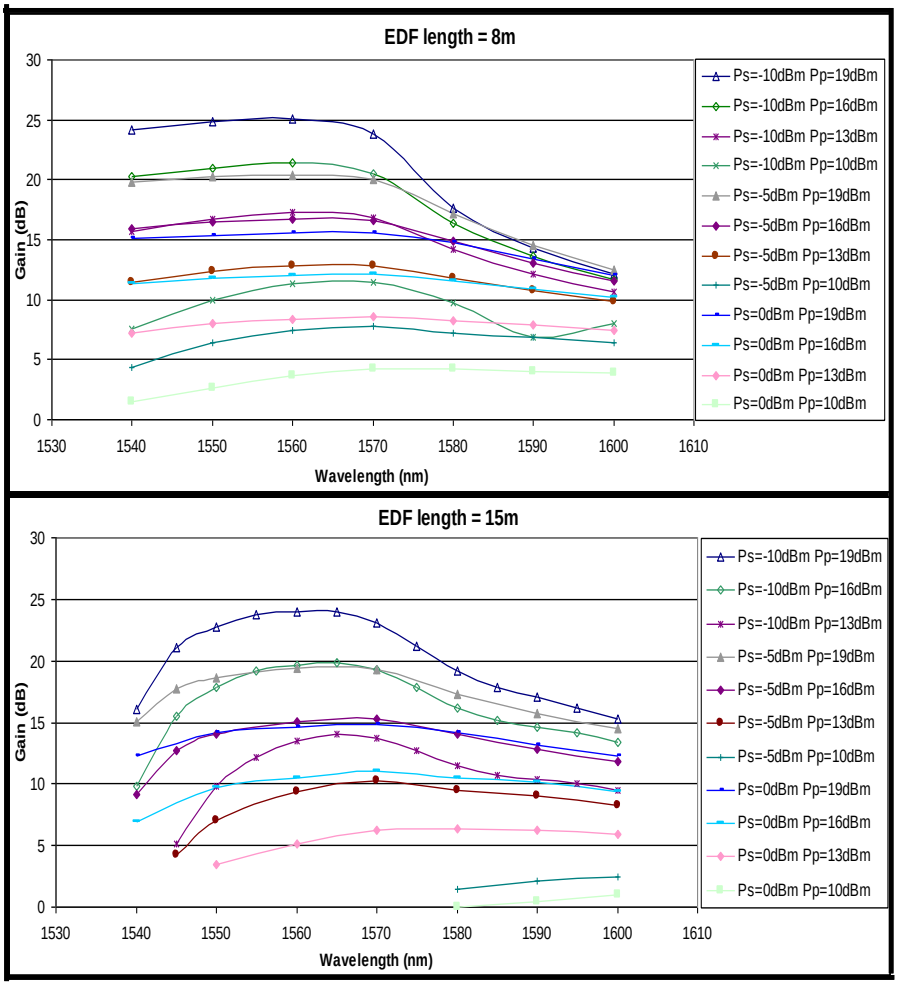

Fig. 9.5.) Characterization of the EDF used in the amplification stage of the RN, for a) 8m, b) 15m of length and 0dBm, 5dBm,10dBm of input power and various pump power values of 10dBm, 13dBm, 16dBm and 19dBm respectively

An avalanche photodiode (APD) is used as the ONU receiver. The signals are equalised with the use of an FFE-DFE equaliser in half of the measurements. As ONU transmitter, a CW seed light was used in combination with a REAM and a RSOA. The upstream was modulated at 10 Gb/s in order to demonstrate symmetric data transmission. The upstream path is symmetrical to the downstream one. At the OLT input, a WDM waveband combiner is used to inject the counter propagating remote pump at 1480nm. The signal is then split in the two bands, C and L, with a C+L splitter. A band-dedicated optical preamplifier is then used to enhance the reception sensitivity. Finally, the channel under study is selected with the help of a tuneable optical bandpass filter and detected by a PIN diode.

The RN is a key element in order to increase the reach of the proposed topology as well as a key element for enhancing the resilience performance. The suggested design is based on the SARDANA RN [1]. The add/drop functionality of the tree wavelengths from the ring into the sub-RNs was performed with 3-ports thin-film add/drop filters, while resiliency is provided by a 50/50 coupler (CR) that allows to receive and transmit the data stream to both directions of the down- and upstream ring for the case of a fiber

cut. Since a dual-feeder is used at the tree, no circulator is required at the RN to separate downstream and upstream. This circulator can be rather found at the VOA emulating the tree splitter. For the proposed RN design an in-line amplification approach has been used in order to amplify the upstream or downstream signals. The EDF is placed between the two thin-film filters, connecting both express ports, amplifying in this way all the channels, except the one that is being dropped in the RN (Fig. 9.2).

When working with C- and L-band at the same configuration, the usual approach is to split both bands using a C+L coupler and amplifying each band independently, with a specific EDF for each one, as in [113]. This design has some drawbacks, such as an increase in both the complexity and the cost of the designed RN by including C+L splitters, as well as doubling the number of amplifiers requiring extra pump power. In this experiment, this drawback has been overcome by the use of an EDF appropriate for the amplification of both C- and L-band signals and the appropriate wavelength allocation in the network. The wavelength allocation was performed by means of appointing the right wavelength drop, according to the gain each frequency band receives, while taking into account the distinctiveness of this RN design. This distinctiveness lays on the fact that the wavelength dropped has received amplification in the previous amplification stages, but needs to have adequate power to reach the ONU of the RN in which it is being dropped, without receiving any extra gain in this specific RN. In Figures 9.4 and 9.5 one can see the EDF characterization as a function of the signal wavelength and the pump power at 1480nm, for four different EDF lengths and four different signal power levels. As can be observed, even with low pump power values such as 10 or 13 dBm, the EDF can provide gain in the whole spectrum of C+L bands. From Figures 9.4 and 9.5 it is observed that the L-band signals receive less gain than the C band ones, therefore we have dropped the one belonging in L band (1586.2nm) in RN_2, placed in the middle of the network, as in this case, the signal is being amplified when going through RN_1 and on the same time does not need to travel the whole distance of the network but a moderate one. The two signals belonging to C-band are dropped as following: the one in RN_1 (1549nm) without going through any amplification stage and the second in RN_3 (1557nm) going through two amplification stages so as to ensure adequate power to reach the last ONU (at 100+6km). The required gain is around 14dB in both EDFs (upstream and downstream) in RN_1 and RN_2 while the launch pump power is 30dB and when reaching the two RNs it is 24dB and 17dB correspondingly. Therefore, from Fig. 9.4, we have chosen a 3m EDF for RN_1 and 5m EDF for RN_2. It is also observed, that with low pump power values the gain tilt is rather flat, in contradiction with the case of high pump power such as 16-19dBm. Since we are using a remote pump, this small tilt towards the C-band can be compensated by the extra Raman gain expected for the L-band, as the maximum Raman gain will be located at 1580nm when using a pump at 1480nm [114].

With the use of this elaborate network design, theoretically, the number of the users can be doubled, by the use of both C and L bands, allocating the signals belonging to the second one, to the RNs placed in the middle of the WDM ring. On the contrary, the

signals belonging to C-band, that apparently receive more gain when going through the several amplification stages, which is in fact accumulated, are allocated in the RNs placed near the CO, which transform into the more distant RNs in the worst case of a fiber-cut, as mentioned before.

9.3 Results

The MZM was operated at two different sets of driving voltages, resulting in ER values of 3 and 10dB respectively. A value of ER =9dB has been shown to be appropriate for all optical cancellation in the case of colourless ONUs in [109]. Second, the case of low ER, namely 3dB, is shown to be ideal for efficient signal remodulation [115], but also for the more advanced feed forward cancellation method presented in [116]. Therefore, and based on these previous results, we have used two similar values for the signal modulation.

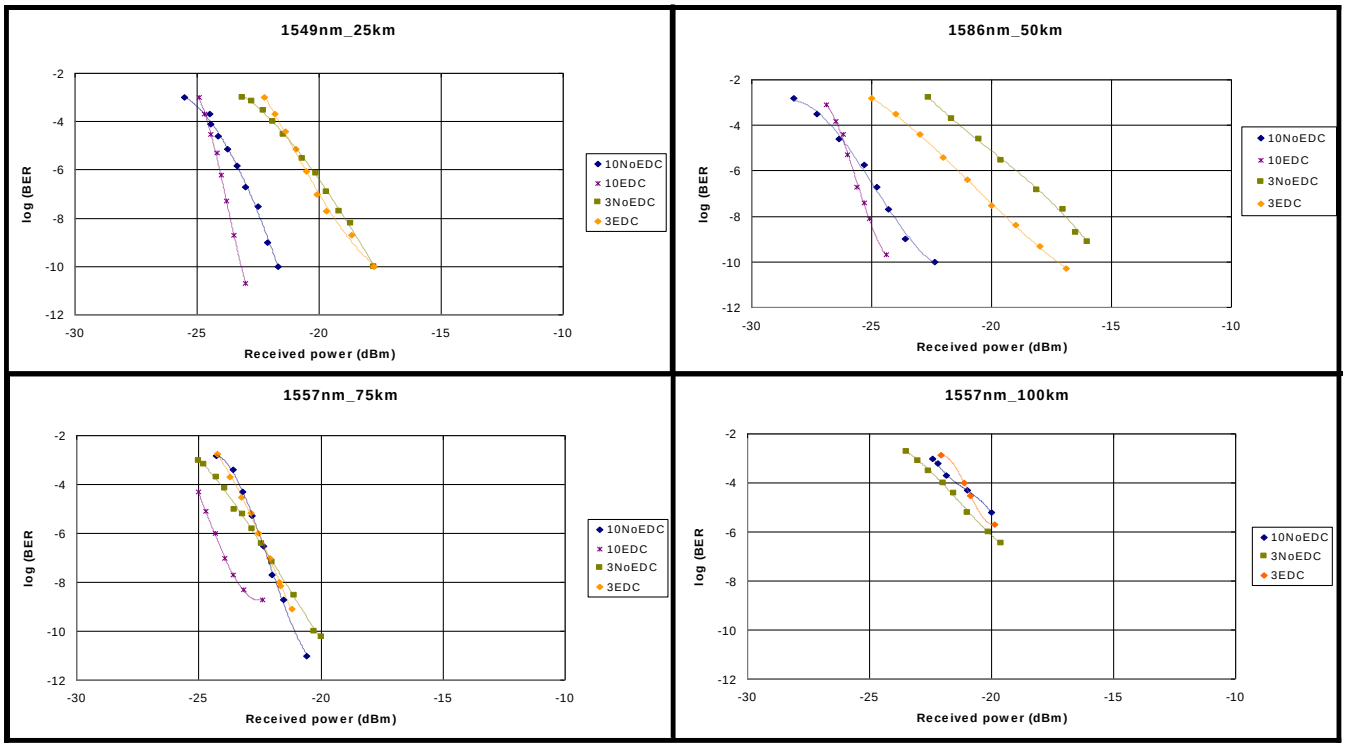

Fig. 9.6. BER vs. received power for a)RN_1 (λ=1548nm, 25km), b)RN_2 (λ=1586.2nm, 50km), c) RN_3 (λ=1557nm, 75km), d) RN_3 (λ=1557nm, 100km), in the cases of i)10dB ER and no EDC use, ii) 10dB ER and EDC use, iii) 3dB ER and no EDC use, iv) 3dB ER and no EDC use

In the results, presented in Fig. 9.6, the performance has been studied in terms of BER versus received power. Measurements were taken in the ONU part for the following cases. First we consider RN_1, which is situated 25km away from the OLT, where the wavelength of 1549nm is being dropped and the results shown in Fig.9.6 correspond to an ONU situated 6km away from the OLT, therefore in a total distance of 31km from the OLT. Next, an ONU of RN_2 at 50+6km with drop wavelength of 1586nm was examined and subsequently we have examined RN_3 (1557nm drop wavelength) and its

ONU for two different distances. In this framework, the RN_3 is situated 75km away from the OLT (therefore its ONU is situated at 75+6km) and then with the use of 25km of SMF, we place the RN_3 at a distance of 100km from the OLT (subsequently the ONU is placed in a distance of 100+6km from the OLT).

Observing the results for the downstream propagation, it is obvious that the MZM modulated signal has a better performance when modulated on a high ER [112], in this case 10dB, than in the case of a low 3dB ER. Furthermore, the EDC equalizer offers a decrease in the range of 3-5dB of required received power in order to have an error free ($BER=10^{-10}$) performance.

One can notice in the results the existence of chirp even if we have used a MZM modulator. As it has been remarked in [112] and as one can observe from the results, there is a trade-off between a high ER and dispersion control. This is evident in the case of 10dB ER and long distance (RN_3-100km) where the dispersion effect in combination with the small but existent chirp is so high that does not allow for acquiring measurements while using EDC. On the contrary the 3dB ER signal arrives at the 106km with less dispersion as the chirp counteracts with the dispersion caused by the propagation of the signal in the fiber. The behaviour of the 3dB ER signal, is again anticipated as in the case of 25km and C-band signal, the EDC offers a small improvement, but when moving in the 50km, without any dispersion compensation and with a larger chirp parameter since the signal belongs in the L-band [117] we observe that a) the results have a great difference from the 10dB ER ones, b) especially in the case of no EDC the performance of the network is much lower and the EDC offers good results in controlling the dispersion. Nevertheless, as can be observed from the results and shown in [116], the use of EDC is not compulsory in order to achieve results that can be used for proper remodulation while using RSOA in the ONU.

9.4 Conclusions

We have combined in an experimental set-up and an experimental study, the ideas that have been examined throughout this thesis achieving to reach by means of in-line amplification and C+L-band utilization, 106km in a WDM/TDM ring PON architecture, adding this way 6km to our previous studies, while at the same time increasing the number of users. The capacity of the network with the use of the C + L band and the proper design in the sense of wavelength allocation can theoretically be doubled. This is a subject for further investigation though. The special RN design has helped the realization of this goal. The use of equalization has been examined and it does increase the performance of the network especially in the case of a larger ER in a scale of 4-6dB. Nevertheless, even the 3dB ER without the use of equalizer can offer an acceptable performance, so the cost of an equalizer at least at the ONU part, can be avoided. Further studies should take place for the examination of the equalizer at the OLT part. The C+L band use can offer both an increase on the number of end customers as well as the possibility in infrastructure proprietors to lease one fiber to more than one operator.

The suggested design can render the network much more competitive, giving this way an impetus to the whole technology.

Chapter X
Conclusions

This chapter summarizes the knowledge acquired throughout this thesis project and presents suggestions for possible future work.

10.1 Conclusions

The aim of this study was to shed light on the economic and technical aspects of the emerging technology of WDM/TDM PON FTTH networks. To evaluate, in terms of cost, those networks position in the global telecom market; and to suggest as well as to investigate ways to improve their performance.

A study on the economic and technical aspects of the FTTH networks, has shown that the most cost effective solution is the one of WDM/TDM PON implemented in P2MP architecture. More specifically, a model has been created that compares -using OSP, active equipment and implementation cost- several architectures and technologies. The possible implementations were presented along with some technical details on the FTTx infrastructure and a description of the model. To give a more complete and thorough estimation, we have compared the costs of different FTTx infrastructures. When estimating the OSP cost of a FTTH metro network with EP2P on the access part with the metro-access FTTH solution of WDM/TDM PON we conclude that there is a 40% reduction when we choose the second option, while in the case of a FTTH metro network with GPON the decrease is one of 20%. When we compare the overall cost of the three FTTH implementations (OSP and active equipment cost) we end up in the result that the PON is 20% less costly than the active solution while the WDM/TDM PON has a maximum cost of approximately 2000€ in the most scarcely populated area, while the prices decrease for every other population density. In general, it is evident that the most cost saving technology in terms of OSP cost is the WDM/TDM PON. The explanation for that is the competent use of the fiber resources, as the feeder and the distribution part, is shared between a higher number of end-users than in any other technology.

In continuance, a presentation of the network design used as a reference for WDM/TDM PONs takes place, along with the challenges such a design presents. These are namely signal attenuation, chromatic dispersion and non linear effects. The suggested solutions for overcoming limitations in a fully passive optical network

infrastructure are the results of a combination of two requirements. The first is to fight the challenges presenting themselves in optical networks due to natural phenomena, with the effective use of other phenomena, without the use of electro-optical conversion; and the second to avoid the use of any active equipment whatsoever in the field. The solutions suggested are, amplification with the use of EDFs, use of dispersion compensating fibers and signal equalization. Furthermore, the use of reduced OLT power is recommended.

Following, we examine the idea of using remotely pumped EDF amplification, placing the EDF in-line with the signals propagation direction. A special RN design has been proposed for this reason, as well as a special wavelength allocation plan in order to exploit the gain tilt of the EDF. The design solution has been tested with the use of simulation tool and it has proven to be able to serve 1024 end users with several hundreds of symmetric data rate in a maximum distance of 19km.This design can be applied in both, normal and resilient operation. If normal operation is considered, then all costumers can be served with the use of RSOA's based ONUs. Nonetheless, in the worst case of a fiber cut, hence a fiber cut between the OLT and the first RN, the very few users served by the most affected RNs can alternatively be served by standardized GPON APD receivers. The proposed remote amplification solution consists of a fully passive architecture which can expand the limits of already deployed passive infrastructures, using remote amplification. The low pump power required, along with the extended use of RSOAs suggested, make this design very efficient in terms of OPEX. Furthermore, the overall cost of the RSOAs and the different components of the network, consist of a profitable solution in terms of CAPEX.

Subsequently, the solution of using an alternative frequency band has been considered. The reason for this was to enhance the number of the end users. Another reason was the idea that this investigation can be expanded even more, so as to include operation in both C and L bands. In this framework, another special design of a WDM/TDM PON was implemented, based once more on the principle of cascaded in-line, remotely pumped EDFAs. The design of the RN used is similar to the one used for the design of the aforementioned network operating in C band only. A number of parameters have been taken under consideration for the implementation of this network design and again a special wavelength allocation has been considered. We showed that a WDM/TDM passive optical network architecture using L-band in line amplification can again reach 19km, serving 1024 users with several hundreds of Mbps while all costumers are serviced with RSOA's based ONUs. This solution consists also of a fully passive architecture which can enlarge the limits of already deployed passive infrastructures, using remote amplification. The operational expenditures are expected to be decreased due to the low pump power required along with the extended use of RSOAs. In addition the overall capital expenditure can be reduced as once more RSOAs can be used for te implementation.

After that, a trial network design, due to operate in both C + L band, has been implemented. Further, the combination of Raman amplification with remotely pumped

EDFs placed as in the previous chapters, in-line with the transmission path, thus distributed in the WDM ring is shown. The feasibility of gain enlargement and equalization on extended reach WDM-ring PON by means of hybrid Raman/EDFA amplification has been investigated with the use of simulation. The network examined, consists of an 80km WDM ring with 8 nodes, operated with 16 channels, 8 of which cover the C band while the other 8 cover the L one. The results have demonstrated gain equalization with a ripple of 2.54dB over a bandwidth of 50nm by using spans of EDF with a total length of 22km.

Next, we have investigated the limits and the performance of a WDM/TDM network operating in C + L band, which uses remotely pumped amplification in the drop part of the network, with the help of an especially designed RN. With the covered wavelength range from 1530-1563 nm in the C- and 1570-1600 nm in the L-band, in which sufficient gain can be provided for the given power margins, a PON with data transmission on 32 wavelengths in each waveband can be considered, serving with a splitting ratio of 1:32 in the tree altogether 1024 users with a full-duplex data transmission of up to 10 Gb/s. Together with the nominal reach of 56 km for the PON, a capacity-length product of 17.9 Tb/s km is provided.

Following, an experimental study has been performed, in which we have tested the behaviour of two different transmitters in a WDM/TDM PON. Namely, a distributed feedback laser source (externally modulated by a Mach-Zehnder modulator) and an integrated DFB – Electroabsorption Modulator have been examined. Two possible tools to help combating the dispersion imposed restrictions on a WDM/TDM PON that is, dispersion compensation fiber and electronic equalization have been investigated. The results have shown that the behaviour of the network depends on the chirp of the transmitter and the and on the value of the ER. The different signal improvement methods contribute differently in each case. The best combination is the one of 9dB ER with DCF and EDC regarding signal improvement, which offers a dispersion independent uniform behaviour and an error-free performance at all lengths up to 100km with an OSNR value of up to 20dB. The 3dB ER with the same improvement method is a lower energy consumption solution that requires up to 26dB OSNR. Moreover, it has been observed that the transit from ER=3dB to ER=9dB causes a significant decrease on the ROSNR, which especially when no means of signal improvement are used, or when low cost DCF is used, can reach even the 14dB. In other words, even when the lowest CAPEX solution is chosen, with a very small change in the value of driving voltage, the quality of the transmission can significantly improve. On the other hand, the choice of combining DCF in the transmitter (OLT) and EDC in the receiver (ONU) gives a very constant behaviour for all different lengths, therefore it can be easily suggested when the standardization of a PON is the main target. Finally, the combined use of EDC and DCF can help improve the transmission by a range of 10dB of ROSNR which is translated into cost savings.

Finally, the combination of all the techniques used throughout this thesis, for the optimization of a WDM/TDM PON, was realized in the framework of an experimental

study. The remotely pumped EDFAs providinig in-line amplification were combined with C + L band operation of the WDM/TDM PON. A special C + L band remote node was designed and mounted. Raman amplification was used for the upstream signals and the use of equalization was studied in the downstream signals. The ideas that have been examined throughout this thesis were combined in an experimental set-up and an experimental study, achieving to reach by means of in-line amplification and C+L-band utilization, 106km in a WDM/TDM ring PON architecture, adding this way 6km to previous studies. The special RN design has helped the realization of this goal. The use of equalization has been examined and it does increase the performance of the network especially in the case of a larger ER in a scale of 4-6dB. Nevertheless, even the 3dB ER without the use of equalizer can offer an acceptable performance, so the cost of an equalizer at least at the ONU part, can be avoided. The C+L band use can offer both an increase on the number of end customers as well as the possibility in infrastructure proprietors to lease one fiber to more than one operator. The suggested design can render the network much more competitive, giving this way an impetus to the whole technology.

10.2 Future work

As far as the financial assessment of FTTH optical networks is concerned, in the future, the focus should be on the OFDM and high splitting ratio technologies. Future research has to take place on the techno-economics of such networks, both in terms of OSP cost, as well as active equipment cost. A comparison with metro-access WDM/TDM PON technologies could be very enlightening. Furthermore, research should take place on the OPEX of a WDM/TDM PON so as to have a complete image of such a network's cost.

As mentioned in chapter 9, the capacity of the network with the use of the C + L band and the proper design in the sense of wavelength allocation can theoretically be doubled. This is a subject for further investigation. Further studies should also take place for the examination of the equalizer at the OLT part for the network design presented in the same chapter. Raman amplification in the upstream part has been investigated and the results are processed to be presented. When the aforementioned study is complete, the financial assessment of a WDM/TDM PON functioning in both C and L bands could provide us with some very useful insight.

A. List of Acronyms

A	**AON**	Active Optical Network
	APON	ATM PON
	APD	Avalanche Photo Diode
	ASE	Amplified Spontaneous Emission
	ATM	Asynchronous Transfer Mode
	AWG	Arrayed Waveguide Grating
B	**BER**	Bit Error Ratio
	BPON	Broadband PON
C	**C/L**	C- / L- *Waveband*
	CAPEX	Capital Expenditures
	CO	Central Office
	CPE	Customer Premises Equipment
	CR	Coupler
	CWDM	Coarse Wavelength Division Multiplexing
	CW	Continuous Wave
D	**DBWA**	Dynamic Bandwidth and Wavelength Allocation
	DC	Directed Current
	DCF	Dispersion Compensating Fiber
	DCM	Dispersion Compensation Modules
	DFE	Decision-Feedback Equalizer
	DFB	Distributed Feedback
	DS	Downstream
	DWDM	Dense wavelength division multiplexing
E	**EAM**	Electro-Absorption Modulator
	ECE	Electrical Channel Equalizer
	EDC	Electronic Dispersion Compensation
	EDF	Erbium-Doped Fiber
	EDFA	EDF Amplifier
	EP2P	Ethernet-Point-to-Point
	EPON	Ethernet PON
	EQ	Equalizer
	ER	Extinction Ratio
F	**FDI**	Feeder Distribution Interface
	FEC	Forward Error Correction
	FFE	Feed-Forward Equalizer
	FIR	Finite-Impulse-Response
	FSAN	Full Service Access Network
	FTTB	Fiber-to-the-Building
	FTTC	Fiber-to-the-Curb

	FTTH	Fiber-to-the-Home
	FTTN	Fiber-to-the-Node
	FTTX	Fiber-to-the-X
	FWM	Four-Wave Mixing
G	**GEPON**	Gigabit EPON
	G.Fast	Fast Access to Subscriber Terminals
	GPON	Gigabit PON
H	**HH**	Household
I	**IBS**	Inter Building Spacing
	IEEE	Institute of Electrical and Electronics Engineers
	ISI	Inter Symbol Interference
	ITU-T	International Telecommunication Unit
L	**LD**	Laser Diode
	LMS	Least Mean Squares
	LS	Least Squares
M	**MAC**	Medium Access Control
	MAN	Metropolitan Area Network
	MDU	Multi-Dwelling unit
	MLD/MLSD	Maximum-Likelihood (Sequence) Detector
	MSE	Mean Squared Error
	MMSE	Minimum Mean Squared Error
	MZI	Mach-Zehnder Interferometer
	MZM	Mach-Zehnder Modulator
N	**NG-PON**	Next-Generation PON
	NL-DFE	Nonlinear Decision-Feedback Equalizer
O	**OADM**	Optical Add Drop Multiplexers
	OLT	Optical Line Terminal
	ONU	Optical Network Unit
	OPEX	Operating Expenditures
	OSA	Optical Spectrum Analyzer
	OSNR	Optical SNR
	OSP	Outside Plant
	OSRR	Optical Signal-to-RB Ratio
P	**P2MP**	Point-to-Multipoint
	P2P	Point-to-Point
	PCP	Primary Fiber Concentration Point
	PIN	P-I-N Photodiode
	PON	Passive Optical Network
	POP	Point of Presence
	PRBS	Pseudo-Random Bit Sequence
R	**RB**	Rayleigh Backscattering
	REAM	Reflective EAM
	RN	Remote Node

	ROSNR	Required OSNR
	RSOA	Reflective SOA
	RX	Receiver
S	**SBS**	Stimulated Brillouin Scattering
	SDU	Single Dwelling Unit
	SCP	Secondary Fiber Concentration Point
	SMF	Standard single Mode Fiber
	SNR	Signal-to-Noise Ratio
	SOA	Semiconductor Optical Amplifier
	SPM	Self Phase Modulation
	SRS	Stimulated Raman Scattering
T	**TDM**	Time Division Multiplexing
	TIA	Trans-Impendence Amplifier
	TX	Transmitter
U	**UAE**	United Arabic Emirates
	US	Upstream
	USA	United States of America
V	**VDSL**	Very-high-bit-rate digital subscriber line
	VDSL2	Very-high-bit-rate digital subscriber line 2
	VOA	Variable Optical Attenuator
W	**WDM**	Wavelength Division Multiplexing
	WiMAX	Worldwide Interoperability for Microwave Access
X	**XGPON**	10Gb/s PON
Z	**ZF**	Zero-Forcing

B. Research Publications

B.1 Publications in International, Peer-Reviewed Journals

1) S.Chatzi, J.A.Lazaro, J. Prat and I.Tomkos, "*A Techno-economic study on the outside plant cost of current and next generation FTTx deployments*", Fiber and Integrated Optics, vol.32, pp.12-27, Feb. 2013.
2) S.Chatzi, C.P. Tsekrekos, D. Klonidis, J.A.Lazaro, and I.Tomkos*,"Experimental evaluation and improvement methods for low cost transmitters in long reach PONs",* Optical Fiber Technology, Elsevier.
3) B. Schrenk, S. Chatzi, F. Bonada, J.A. Lazaro, I. Tomkos, and J. Prat, "*Dual Waveband Remote Node for Extended Reach Full-Duplex 10Gb/s Hybrid PONs*", IEEE/OSA J. Lightwave Technol., vol. 28, pp. 1503-1509, May 2010.
4) J. Girão; B. Neto; Rocha, Ana M.; Reis, C.; Dionísio, R.P.; S. Chatzi; F Bonada; J. Lazaro; Teixeira, A.T.; André, P.S; *"C+L band extended reach amplified next generation access networks",* Microwave and Optical Tech. Letters, Vol. 53, No. 10, pp. 2414 - 2418, October, 2011.
5) B. Schrenk, J.A.Lazaro, D. Klonidis, F. Bonada, F. Saliou, E.Lopez, Q.T. Le, P. Chanchlou, L. Costa, A. Texeira, S. Chatzi, I. Tomkos, G.Tosi Beleffi, D. Leino, S.Spirou, G. de Valicourt, R. Brenot, C. Kazmierski and J. Prat*, "Demonstration of a remotely Dual-Pumped Long reach PON for flexible deployment",* J. Lightwave Technol., vol. 30, pp. 953-961, Apr. 2012.

B.2 Publications in Scientific Congresses

1) S. Chatzi, D. Klonidis, J. A. Lazaro, J. Prat and I. Tomkos, *"Design of in-line remote amplification for an extended WDM-PON ring architecture"*, in Proc. NOC, 12.4, Valladolid, Spain, Jun. 2009.
2) S. Chatzi, I. Tomkos, J. A. Lazaro and J. Prat, *"L-band in-line remote amplification for an extended WDM-PON ring architecture"*, in Proc. ICTON, Tu.D5.5, Azores Portugal, Jul. 2009.
3) S. Chatzi, J. A. Lazaro, J. Prat and I. Tomkos, *"Techno-economic comparison of current and next generation long reach optical access networks"*, in Proc. CTTE, Ghent, Belgium, Jun. 2010.

4) S. Chatzi, J. A. Lazaro, J. Prat and I. Tomkos, *"A quantitative techno-economic comparison of current and next generation metro/access converged optical networks"*, in Proc. ECOC, We.8.B.2., Torino, Italy, Sep. 2010.

5) S. Chatzi, C. Tsekrekos, D. Klonidis, and I. Tomkos, *"Performance evaluation and improvement methods for low-driving voltage transmitters in long reach PONs",* in Proc. OSA / OFC/ NFOEC, L.A., (CA), USA, March 2012.

6) S. Chatzi, I. Tomkos, *"Techno-economic study of high–splitting ratio PONs and comparison with conventional FTTH-PONs/FTTH-P2P/ FTTB and FTTC deployments",* in Proc. OSA / OFC/ NFOEC, L.A., (CA), USA, March 2012.

7) J. A. Lazaro, J. Prat, V. Polo, M. Omella, F. Bonada, B. Schrenk, D. Klonidis, S. Chatzi, I. Tomkos, P. Chanclou, "*Scalable WDM/TDM extended reach access network architecture",* in Proc. OPTOEL, Malaga, Spain, 2009.

8) B. Schrenk, S. Chatzi, F. Bonada, J.A. Lazaro, D. Klonidis, I. Tomkos, and J. Prat, "*C+L Band Remote Node for Amplification in Extended Reach Full-Duplex 10Gb/s WDM/TDM Passive Optical Networks*", in Proc. ECOC, We.P6.19, Vienna, Austria, Sept. 2009.

9) B. Neto, R. P. Dionísio, A. M. Rocha, C. Reis, S. Chatzi, F. Bonada, J. A. Lazaro, A. L. J. Teixeira, and P. S. André*, "C+L band extended reach next generation access networks through raman amplification: assessment in rural scenario,"* in OptoElectronics and Communications Conference, 2010. OECC 2010. 15th, 5-9 2010, pp. 1 –2*.*

10) B. Neto, A.M. Rocha, J.P. Girao, R.P. Dionisio, C. Reis, S. Chatzi F. Bonada, J. A. Lazaro, A. L.J. Texeira, P.S.Andre,. *"C+L band gain equalization for extended reach WDM-ring PON using hybrid Raman/in-line EDFA amplification"*, in Proc. ICTON, We.P.18, Munich, Germany, Jun. 2010.

11) J. Bauwelinck, C. Antony, F. Bonada, A. Caballero, S. Chatzi, A.M. Clarke, L.N. Costa, M. Forzati, J.A. Lazaro, A. Maziotis, M. Mestre, I.T. Monroy, P. Ossieur, V. Polo, J. Prat, X.Z. Qiu, P.J. Rigole, B. Schrenk, R. Soila, A. Teixeira, I. Tomkos, P.D. Townsend, X. Yin, and H. Avramopoulos, *"Optical Line Terminal and Remote Node Sub-Systems of Next-Generation Access Networks"*, in Proc. OSA Advanced Photonics Congress / ANIC, AWA5, Karlsruhe, Germany, Jun. 2010.

12) F.Bonada, B.Schrenk, L.Costa, A.Teixeira, S.Chatzi, D.Klonidis, I.Tomkos, J.Prat and J.A.Lazaro, *"Wavelength-tuneable remote node for enhanced resilience and optimization of WDM access networks",* in Proc. ICTON, Tu.B.6.5., Stockholm, Sweden, Jun. 2011.

13) J.Prat, J.A.Lazaro, S.Chatzi and I.Tomkos, *"Techno-economics of resilient extended FTTH PONs"* (Invited)*,* in Proc. ICTON, Tu.A.6.2, Stockholm, Sweden, Jun. 2011.

14) B. Neto, A. Rocha, J. P. Girão, R. P. Dionísio, C. Reis, S. Chatzi, F. Bonada, J. Lazaro, J. A. and, and A. L. J. Teixeira, and P. S. André,

"Comparative analysis of hybrid in line edfa/raman with simple Raman amplification in WDM ring PON for C+L band," in Networks and Optical Communications, 2010. NOC '10. 15th European Conference on, vol. 1, June 2010, pp.

15) B. Schrenk, J.A. Lazaro, D. Klonidis, F. Bonada, F. Saliou, E. Lopez, C. Trung, P. Chanclou, L. Costa, A. Teixeira, S. Chatzi, I. Tomkos, G. Tosi Beleffi, D. Leino, R. Soila, S. Spirou, G. de Valicourt, R. Brenot, C. Kazmierski, and J. Prat*, "Demonstration of a Remotely Pumped Long-Reach WDM/TDM 10 Gb/s PON with Reflective User Terminals",* Proc. ECOC Technical Digest © 2011 OSA, Geneva, Switzerland, Sept. 2011.

B.3 Non-peer reviewed publications In international magazines

- I. Tomkos, S. Chatzi, *"Techno-economic Comparison of Next Generation Access Fiber-to-the-X Network Architectures",* Total Telecom magazine, Dec/Jan 2011.

  http://headley.co.uk/headturner/TTP1210 pp.11-13

B.4 Workshop presentations

- S.Chatzi, I.Tomkos, *''Hybrid WDM/TDM scablabe ring based PON with in-line remote amplification",* Workshop on "Activities and perspectives of EURO-FOS concept", paper P16, 28 March 2011.

C. Bibliography

[1] J.A. Lazaro *et al*, "Remotely amplified SARDANA: Single-fibre tree Advanced Ring-based Dense Access Network Architecture", *Proc. ECOC'06,* Cannes, France, Sept. 2006.

[2] FTTH Council Europe, Press conference, Munich, Germany, 15 February 2012.

[3] FTTH Council Europe, "Winners and losers emerge in Europe's race to a fibre future", London, UK, 20 February 2013.

[4] FTTH Council Europe, "The FTTH Council Europe welcomes French ultra-fast broadband infrastructure investment plan", 25 February 2013, London, UK.

[5] A. Vegara *et al,* "COSTA, a model to analyze next generation broadband access platform competition", 14th International Telecommunications Network Strategy and Planning Symposium (NETWORKS), pp. 1-6, Warsaw, Poland, Sep. 2010.

[6] T. Rokkas *et al.*, "Techno-economic Evaluation of FTTC/VDSL and FTTH Roll-Out Scenarios: Discounted Cash Flows and Real Option Valuation", *IEEE/OSA J. Optical Communication Networks,* vol. 2, pp. 760-772, Sept. 2010.

[7] R. Zhao *et al.*, "Dynamic Migration Planning towards FTTH", in *Proc. NETWORKS'10,* Warsaw, Poland, Sept. 2010.

[8] C.P. Larsen *et al*, "Comparison of Active and Passive Optical Access Networks", *Proc. CTTE'10,* Ghent, Belgium, Jun. 2010.

[9] S. Chatzi *et al.,* "A quantitative techno-economic comparison, of current and next generation metro/access converged optical networks", *Proc. ECOC'10,* We.8.B.2, Torino, Italy, Sep. 2010.

[10] T. Rokkas *et al.,* "Economics of Time and Wavelength Domain Multiplexed Passive Optical Networks", *IEEE/OSA Journal of Optical Communications and Networking*, vol.2, no.12, pp.1042-1051, Dec.2010.

[11] B. Lannoo *et al.*, "Techno-economic feasibility study of different WDM/TDM PON architectures", *Proc. ICTON'10*, Mo.C4.3, Munich, Germany, Jun. - Jul. 2010.

[12] www.ist-pieman.org

[13] www.ist-muse.org

[14] A. Geha *et al*., "HARMONICS, an IP based service network over hybrid fibre-access network supporting QoS", *Proc ICT'03*, Tahiti, France, Feb. - Mar. 2003.

[15] F.T. An *et al*., "SUCCESS-HPON: A next-generation optical access architecture for smooth migration from TDM-PON to WDM-POM", *IEEE Communications Magazine,* vol.43, no.11, Nov. 2005.

[16] www.e-photon-one.org

[17] Y. Cao *et al*. "A novel architecture of reconfigurable WDM/TDM PON", *Proc. WOCC'10*, Shanghai, China, May 2010.

[18] Y. Qian *et al*., "RSOA-based distributed access long reach Hybrid WDM-TDM PON with OADMs", *OSA Chinese Optical letters*, vol.8, no.9, pp.899-901, Sep. 2010.

[19] S.J. Park *et al*., "Hybrid WDM/TDM PON Using Remotely Pumped Optical Amplifier", *Proc. ECOC'07,* Dresden, Germany, 2007.

[20] J. M. Oh *et al*., "Enhanced system performance of an RSOA based Hybrid WDM/TDM –PON system using a remotely pumped erbium doped fiber amplifier", *Proc OSA/NFOEC,* PDP9, Anaheim (CA), USA, Mar.2007

[21] J. Chen *et al*., "Performance Analysis of Protection Schemes Compatible with Smooth Migration from TDM-PON to Hybrid WDM/TDM-PON", *Proc OSA/NFOEC*, JWA85, Anaheim (CA), USA, Mar.2007.

[22] J. Chen *et al*., "Cost vs. Reliability performance study of fiber access network architectures", *IEEE Communications Magazine,* vol.48, no.12, Feb. 2010.

[23] D. J. Shin *et al.* "Hybrid WDM/TDM PON With Wavelength Selection Free Transmitters", *IEEE Journal of Lightwave Technology,* vol.23, no.1, pp. 187-195. Jan.2005

[24] S. Ahsan *et al.* "Migration to the next generation optical access networks using hybrid WDM/TDM PON", *IEEE Journal of Networks*, vol.6, no.1, pp.18-25, Jan.2011.

[25] P.J. Urban *et al.* "Experimental demonstration of a 10Gbit/s wavelength 27km reach WDM/TDM PON based on reconfigurable OADM and colourless ONU", *Proc ECOC'09,* 7.5.2, Vienna, Austria, Sep. 2009.

[26] S. Kimura *et al.* "A 10Gbit/s CMOS burst mode clock and data recovery IC for a WDM/TDM PON access network", *Proc LEOS'04,* TuR1, Rio Grande, Puerto Rico, Nov. 2004.

[27] C. J. Chae *et al*,, "Multi-wavelength PON as a Cost-effective and Power efficient alternative to WDM/TDM PON for extended reach-applications", *Proc LEOS'10,* Denver, Colorado, 2010.

[28] D.M. Seol *et al*,"Passive Protection in a Long Reach WDM /TDM PON", *Proc COIN'10,* The Shila Jeju, Korea, Jul. 2010.

[29] J. H. Lee *et al*,"First commercial deployment of a colorless Gigabit WDM/TDM Hybrid PON system using remote protocol terminator", *IEEE Journal of Lightwave Technology*, vol.28, no.4, pp. 344-351. Feb. 2010.

[30] R. Inohara *et al*, "Reconfigurable WDM/TDM –PON ring architecture by using all-optical wavelength converter and injection-locked FP-LD", *Proc OSA/OFC/NFOEC'10,* OWG5, San Diego (CA), USA Mar. 2010.

[31] X. Cheng *et al*, "Hybrid WDM/TDM PON with dynamic virtual PON (VPON) capability" *Proc ECOC'10,* P6.07, Torino, Italy, Sep. 2010.

[32] F. Khan *et al*, "NUST hybrid (WDM/TDM) EPON based Access network with triple play support", *Proc HONET'07,* Dubai, UAE, Nov. 2007.

[33] J. D. Downie *et al*, "An 11.1 Gb/s WDM/TDM PON system with 100km reach using ultra low loss fiber and duobinary downstream signals", *Proc LEOS'08,* WEE3, Newport Beach (CA), USA, Nov. 2008.

[34] C.H. Chen *et al*, "A Delay sensitive Multicast Mechanism for differentiated services in WDM/TDM PON", *Proc COIN'08,* Tokyo, Japan, Oct. 2008.

[35] L. Shi *et al*, "Behavior-aware user-assignment in Hybrid PON planning", *Proc OSA/OFC/NFOEC'09,* JThA72, San Diego (CA), USA, Mar. 2009.

[36] M. Kassir, "Current and future broadband bandwidth demand, promises and Challenges", Published Capstone, University of Denver, 2006.

[37] S. Kulkarni, *et al*, "FTTH-Based Broadband Access Technologies: Key Parameters for Cost Optimized Network Planning", *Bell Labs Technical Journal*, vol.14, pp.297-309, 2010.

[38] A. Banerjee, M. Sirbu, "Towards technologically and competitively neutral fiber to the home (FTTH) infrastructure," in Broadband services: business models and technologies for community networks, *John Wiley & Sons*, 2005.

[39] T. Koonen, "Fiber to the Home/Fiber to the Premises: What, Where and When?", *Proc. of the IEEE*, vol. 94 no. 5, pp. 547–588, Jun. 2006.

[40] D. Nesset *et al*, "Economic Study Comparing Raman Extended GPON and Mid-span GPON Reach Extenders', *Proc .OSA/OFC/NFOEC'10*, pp.1-3, March 2010.

[41] R.P. Davey *et al*, "The future of optical transmission in access and metro networks-an operator's view", *Proc ECOC'05*, vol. 5, pp. 53-56, Sept. 2005.

[42] B.T. Olsen *et al*, "Models for forecasting cost evolution of components and technologies", in Telectronik, vol. 100, no. 4, 2004.

[43] D. Rokkas, *et al*, "Techno-economic Evaluation of FTTC/VDSL and FTTH Roll-Out Scenarios: Discounted Cash Flows and Real Option Valuation", *IEEE/OSA Journal of Optical Communications and Networking*, vol. 2 no. 9, pp.760-772, Nov. 2010.

[44] http://en.wikipedia.org/wiki/Fiber_to_the_x

[45] ITU-T G.983.2

[46] ITU-T G.984.1

[47] IEEE 802.3

[48] IEEE P802.3av 2009 (9/2009)

[49] ITU-T G.987

[50] L. Wosinska *et al*, "How much to pay for protection in fiber access networks: Cost and reliability tradeoff", *Proc. ANTS'09*, pp. 1-3, Dec 2009.

[51] J.A.Lazaro *et al*, "Scalable Extended Reach PON", *Proc .OSA/OFC/NFOEC'08*, pp. 1-3, Feb. 2008.

[52] J. Aweya, "IP Router Architecture", in Journal of Systems Architecture 46 (2000) pp.483-511, 1999.

[53] IEEE 802.3-2008, "Part 3: Carrier sense multiple access with collision detection (CSMA/CD) access method and physical layer specifications" section 5, clause 58.

[54] FTTH Council, Network committee, "FTTH Infrastructure Components and Deployment Methods", (2007).

[55] S. Azodolmolky *et al*, "A techno-economic study for active Ethernet FTTH deployments", in Journal of Telecommunications Management, vol.1, no.3, 294-310, (2008).

[56] P. Chanclou *et al*, "Overview of the Optical Broadband Access Evolution: A Joint Article by Operators in the IST Network of Excellence e-Photon/One", in Communications Magazine, IEEE, vol. 44, no.8, 29-35, Aug. 2006.

[57] D. Breuer *et al*, "Architectural options and challenges for next generation optical access", in Proc .of 36th European Conference on Optical Communication, 2010 (ECOC 2010), pp. 1-5, Sept. 2010.

[58] S. Chatzi *et al*, "Techno-economic comparison of current and next generation long reach optical access networks", Proc .of 9th Conference on Telecommunications Internet and Media Techno-economics(CTTE) 2010, pp. 1-6, May 2010.

[59] S. Chatzi *et al*, "A Quantitative Techno-economic Comparison of Current and Next Generation Metro/Access Converged Optical Networks", Proc .of 36th European Conference on Optical Communication, 2010 (ECOC 2010), pp. 1-3, Sept. 2010.

[60] S. Chatzi *et al*, "Techno-economic study of high splitting ratio PONs and comparison with conventional FTTH-PONs/FTTH –P2P/FTTB and FTTC deployments", Optical Fiber Communication (OFC), collocated National Fiber Optic Engineers Conference 2011 Conference on (OFC/NFOEC), JWA15.

[61] Optical fiber Communications Gerd Keiser / Mc Graw Hill International editions 2000, pp.92

[62] Optical Networks A practical perspective, Rajiv Ramaswami, Kumar N. Sivarajam, Morgan Kaufman publishers 2002 pp.68

[63] Optical Networks A practical perspective, Rajiv Ramaswami, Kumar N. Sivarajam, Morgan Kaufman publishers 2002 pp. 76

[64] Optical fiber Communications Gerd Keiser / Mc Graw Hill International editions 2000, pp.431

[65] Optical Networks A practical perspective, Rajiv Ramaswami, Kumar N. Sivarajam, Morgan Kaufman publishers 2002

[66] F. Buchali *et al*, "Reduction of the Chromatic Dispersion Penalty at 10Gbls by integrated Electronic Equalisers ", OFC 2000, ThSl-1, vol.3, pp.268-270

[67] S. Otte *et al*, "A decision feedback equalizer for dispersion compensation in high speed optical transmission systems", ICTON 1999, We.B.2, pp.19-22

[68] C.R.S Fludger *et al*, "Electronic Equalisation for Low Cost 10 Gbit/s Directly Modulated Systems", OFC 2004, WM7, vol.1, pp.234-236

[70] C. Xia *et al*, "Performance enhancement for duobinary modulation through nonlinear electrical equalization", ECOC 2005, Tu.4.2.3, vol.2, pp.257-258

[71] P.C. Becker *et al*, "Erbium-Doped Fiber Amplifiers", 1st ed. Ed.USA, Academic Press, 1999, pp. 131-138.

[72] J.A. Lazaro *et al*, "Extended Black-Box Model for Fiber Length Variation of Erbium-Doped Fiber Amplifiers", *IEEE Photon. Technol. Lett,*. vol.20, pp.2063-2065, 2008

[73] J. Burgmeier *et al*, "A black box model of EDFAs operating in WDM systems", *J. Lightw. Technology*, vol.16, no.7, pp.1271-1275, Jul. 1998

[74] R. Marz, *Integrated Optics: Design and Modelling*. Boston, MA: Artech House, 1995.

[75] A. Texeira *et al.*, "Black box model of erbium doped fiber amplifiers in C and L bands," *Telecommunications and Networking (ICT 2004)*, Springer Berlin, 2004, pp. 267-271

[76] X.Zhang *et al.*, "A simple black box model for erbium doped fiber amplifiers," *IEEE Photon. Technol. Lett,.* vol.12, no.1, pp.28-30, Jan. 2000

[77] G. Jacobsen *et al,* "Pump power dependent black box EDFA model", *J. Optic Commun*. vol. 21, pp. 675-681, 2000

[78] G.P. Agrawal, "Fiber Optic Communication Systems", 2nd Ed. John Wiley and Sons, Inc., 2002

[79] P.S. André, "Optoelectronic components for high speed photonic networks", Ph.D. thesis, University of Aveiro, Portugal, 2002

[80] V. Polo *et al,* "Rayleigh scattering reduction by means of optical frequency dithering in passive optical networks with remotely seeded ONUs", *IEEE Photon. Technol. Lett,.* vol.19, no.2, 2007

[81] R. Ramaswami *et al.*, "Optical Networks", 2nd ed., Ed. USA: Morgan Kauffmann publishers, 2002, pp.158-159.

[82] S. Padwal *et al.*, "Modelling of gain in EDFA and its behavior in C and L band", *Intern. Journal of Advanced electrical and electronic engineering,* vol.1, pp. 25-29, 2012

[83] Y. Sugaya *et al.,* "1.58 μm band Er^{3+} doped fiber amplifiactaion with a 1.55 μm-band light injection," *in OECC'98 Tech. Dig*. 1998, pp. 498-499, paper 16C2-4.

[84] J. F. Massicott *et al.,* "Low noise operation of Er^{3+} doped silica fiber amplifier around 1.6μm", *Electron. Lett.*, vol.28, no.20, pp.1924-1925, 1992

[85] Y. Sun *et al.,* "80nm ultra-wideband erbium doped silica fiber amplifier," *Electron. Lett*., vol. 34, no15, pp.1509-1510, 1998

[86] J. Lee *et al.,* "Enhancement of Power conversion efficiency for L-band EDFA with a secondary Pumping effect in the unpumped EDF section", *IEEE Photon. Technol. Lett,.* vol.11, no.1, pp.42-44, 1999

[87] B. H. Choi *et al.*, "New pump wavelength of 1540nm band for long wavelength band erbium doped fiber amplifier (L band EDFA)", *IEEE Journal of Quantum electronics,* vol.39, no.10, 2003

[88] S. Chatzi *et al.,* "L-Band in-line remote amplification for an extended WDM/PON ring architecture" *in ICTON 2009,* Tu.D5.5, pp.1-4, 2009

[89] G. Keiser, "Optical fiber Communications", 3rd ed. , Ed. Singapore: McGraw –Hill, 2000, pp.491-492.

[90] B. Neto *et al,* "C+L Band Gain Equalization for Extended Reach WDM-Ring PON Using Hybrid Raman / in Line EDFA Amplification", in *Proc. ICTON'10,* We.P.18, Munich, Germany, Jun.-Jul. 2010.

[91] X. Liu , "Powerful solution for simulating nonlinear coupled equations describing bidirectionally pumped broadband Raman amplifiers", *Optics express*, vol.12, no.4, pp.545-550, Feb. 2004.

[92] A. A. M. Saleh *et al*, "Modelling of gain in erbium doped fiber amplifiers", *IEEE Photon. Technol. Lett.* vol.2, no10, pp. 714-717, Oct. 1990.

[93] B. Min *et al*, "Efficient formulation of Raman amplifier propagation equation with average power analysis", *IEEE Photon. Technol. Lett.* vol.11, no10, pp. 1486-1488, Nov. 2000.

[94] T. G. Hodgkinson "Improved average power analysis technique for erbium-doped fiber amplifiers" *IEEE Photon. Technol. Lett.* vol.4, no11, pp. 1273-1275, Nov. 1992

[95] M. C. Fugihara *et al*, "Low cost Raman amplifier for CWDM systems", *Microwave. Opt. Technol. Lett.*, vol.50, no2, pp.297-301, 2008.

[96] Y. Sun et al., "80 nm ultra-wideband erbium-doped silica fibre amplifier," El. Lett. 33, 1965 (1997).

[97] R.E. Neuhauser et al, "New remote pump scheme enabling high-capacity (3.2 Tb/s) unrepeatered C + L band transmission over 220 km," Proc. OFC'02, TuR2 (2002).

[98] J. A. Lazaro et al., "Power Budget Improvement for Passive Outside Plant Long Reach High Density Access Network using High Bit Rate RSOA-ONUs", Proc. ECOC'07, We6.4.3 (2007).

[99] F. Bonada, et al, "Remotely Pumped Erbium Doped Fibre Bidirectional Amplifier for Gain Transient Mitigation", Proc. ICTON'09, Tu.D5.4 (2009).

[100] G. Keiser "Optical fiber Communications", 3rd ed., Ed. Singapore: McGraw –Hill, 2000, pp.104.

[101] R. Ramaswami *et al.*, "Optical Networks", 2nd ed., Ed. USA: Morgan Kauffmann publishers, 2002, pp.188.

[102] Z.B. Hao *et al*., "Theoretical analysis of lnGaAsP/lnGaAsP multiple quantum wells electroabsorption modulators for the application of high speed low driving voltage integrated light source" *Journal of Korean Physical Society*, vol.43 April 1999, pp S105-S108.

[103] J.A. Lazaro, *et al*, "Remotely amplified combined ring-tree dense access network architecture using reflective RSOA-based ONU", *IEEE/OSA J. of Optical Networking*, vol. 6, no. 6, pp.801-807, June 2007.

[104] C. Antony *et al*., "Demonstration of a carrier distributed, 8192-split hybrid DWDM-TDMA PON over 124km field installed fibers", *in proc. OFC/NFOEC'10*, PDPD8, San Diego, USA, March 2010.

[105] I. Papagiannakis *et al*., "Design characteristics for a full duplex IM/IM bidirectional transmission at 10Gb/s using low bandwidth RSOA", JLT vol. 28, no. 7, 1094-1101 (2010).

[106] W. Liu *et al*., "The research on 10Gbps optical communication dispersion compensation systems without electric regenerator", *in proc. CISP*, 2010

[107] I. Papagiannakis *et al*., "Performance improvement of low-cost 2.5 Gb/s rated DML sources operated at 10 Gb/s", *IEEE Photonics Technology Letters*, vol. 20, no. 23, pp. 1983-1985, Dec. 2008

[108] N. Iiyama *et al*., "Co-Existent Downstream Scheme Between OOK and QAM Signals in an Optical Access Network Using Software-Defined Technology", *OFC'12, OSA Technical Digest*, paper JTh2A.53, 2012

[109] E. Kehayas *et al*., "All-optical carrier recovery with periodic optical filtering for wavelength reuse in RSOA-based colorless optical network units in full-duplex 10Gbps WDM-PONs", *in proc. OFC/NFOEC*, OWG4, San Diego, USA, March 2010.

[110] B. Schrenk *et al*, "Employing feed-forward downstream cancellation in optical network units for 2.5G/1.25G RSOA-based and 10G/10G REAM-based Passive Optical Networks for efficient wavelength reuse", *in proc. ICTON'09*, Th.B3.4, Azores, Portugal Jul. 2009.

[111] D. Bailey, E. Wright, *Practical Fiber Optics* , 1st ed. Elsevier Ltd, 2003

[112] K. Fröjdh, "Extinction ratio and dispersion penalty effect on 10Gb/s single channels", *Optronic, IEEE 802.3 Ethernet Higher Speed Study Group*, online available at: www.ieee802.org/3/10G_study/public/

[113] B. Schrenk, *et al*, "C+L Band Remote Node for Amplification in Extended Reach Full-Duplex 10Gb/s WDM/TDM Passive Optical Networks" *ECOC 2009*, 20-24 September, 2009, Vienna, Austria

[114] Atalla E. El-Taher, *et al*, "High efficiency supercontinuum generation using ultra-long Raman fiber cavities", Optics Express, Vol. 17, Issue 20, pp. 17909-17915, 2009

[115] W. Liu *et al*., "The research on 10Gbps optical communication dispersion compensation systems without electric regenerator", in proc. *CISP, 2010*

[116] B. Schrenk *et al*., "Employing feed-forward downstream cancellation in optical network units for 2.5G/1.25G RSOA-based and 10G/10G REAM-based Passive Optical Networks for efficient wavelength reuse", in proc. *ICTON*, Th.B3.4, 2009

[117] J. Piprek *et al*., "Analysis of Multi-Quantum Well Electroabsorption Modulators," SPIE Proceedings 4646-77, Physics and Simulation of Optoelectronic Devices X, Photonics West, San Jose, USA, Jan. 2002.

UNIVERSITAT POLITÈCNICA DE CATALUNYA
BARCELONATECH
Escola de Doctorat

Acta de qualificació de tesi doctoral

Curs acadèmic:

Nom i cognoms

Programa de doctorat

Unitat estructural responsable del programa

Resolució del Tribunal

Reunit el Tribunal designat a l'efecte, el doctorand / la doctoranda exposa el tema de la seva tesi doctoral titulada

_____

_____.

Acabada la lectura i després de donar resposta a les qüestions formulades pels membres titulars del tribunal, aquest atorga la qualificació:

☐ NO APTE ☐ APROVAT ☐ NOTABLE ☐ EXCEL·LENT

(Nom, cognoms i signatura) President/a	(Nom, cognoms i signatura) Secretari/ària	
(Nom, cognoms i signatura) Vocal	(Nom, cognoms i signatura) Vocal	(Nom, cognoms i signatura) Vocal

_____, _____ d'/de _____ de _____

El resultat de l'escrutini dels vots emesos pels membres titulars del tribunal, efectuat per l'Escola de Doctorat, a instància de la Comissió de Doctorat de la UPC, atorga la MENCIÓ CUM LAUDE:

☐ SÍ ☐ NO

(Nom, cognoms i signatura) Presidenta de la Comissió de Doctorat	(Nom, cognoms i signatura) Secretària de la Comissió de Doctorat

Barcelona, _____ d'/de _____ de _____